VOL. 10 NO. 2 AUGUST 1965
PUBLISHED MONTHLY

Journal of

ELECTROANALYTICAL CHEMISTRY

International Journal Dealing with all Aspects of Electroanalytical Chemistry, Including Fundamental Electrochemistry

ELSEVIER

GENERAL INFORMATION

See also Suggestions and Instructions to Authors which will be sent free, on request to the Publishers.

Types of contributions

(a) Original research work not previously published in other periodicals.
(b) Reviews on recent developments in various fields.
(c) Short communications.
(d) Bibliographical notes and book reviews.

Languages

Papers will be published in English, French or German.

Submission of papers

Papers should be sent to one of the following Editors:

Professor J. O'M. Bockris, John Harrison Laboratory of Chemistry, University of Pennsylvania, Philadelphia 4, Pa., U.S.A.
Dr. R. Parsons, Department of Chemistry, The University, Bristol 8, England.
Professor C. N. Reilley, Department of Chemistry, University of North Carolina, Chapel Hill, N.C., U.S.A.

Authors should preferably submit two copies in double-spaced typing on pages of uniform size. Legends for figures should be typed on a separate page. The figures should be in a form suitable for reproduction, drawn in Indian ink on drawing paper or tracing paper, with lettering etc. in thin pencil. The sheets of drawing or tracing paper should preferably be of the same dimensions as those on which the article is typed. Photographs should be submitted as clear black and white prints on glossy paper.
All references should be given at the end of the paper. They should be numbered and the numbers should appear in the text at the appropriate places.
A summary of 50 to 200 words should be included.

Reprints

Twenty-five reprints will be supplied free of charge. Additional reprints can be ordered at quoted prices. They must be ordered on order forms which are sent together with the proofs.

Publication

The *Journal of Electroanalytical Chemistry* appears monthly and has six issues per volume and two volumes per year, each of approx. 500 pages.

Subscription price (post free): £ 12.12.0 or $ 35.00 or Dfl. 126.00 per year; £ 6.6.0 or $ 17.50 or Dfl. 63.00 per volume.
Additional cost for copies by air mail available on request.
For advertising rates apply to the publishers.

Subscriptions

Subscriptions should be sent to:

ELSEVIER PUBLISHING COMPANY, P.O. Box 211, Amsterdam, The Netherlands.

SUMMARIES OF PAPERS PUBLISHED IN JOURNAL OF ELECTROANALYTICAL CHEMISTRY

Vol. 10, No. 2, August 1965

THE ELECTROCHEMICAL REDUCTION OF THE TETRAPHENYLSTIBONIUM ION

The electrochemical reduction of tetraphenylstibonium ion has been investigated. A mechanism is proposed for the two-step reduction based on polarographic, controlled-potential electrolysis and cyclic voltammetric data. There is evidence that the strong adsorption of the ion at the electrode surface plays an important role in determining the overall reaction scheme.

M. D. Morris, P. S. McKinney and E. C. Woodbury,
J. Electroanal. Chem., 10 (1965) 85–94

ELECTROCHEMICAL STUDIES OF ORGANIC COMPOUNDS DISSOLVED IN CARBON-PASTE ELECTRODES

The application of the DO–CPE appears to be a promising technique for study of organic compounds normally insoluble in aqueous solutions. The behavior of DO–CPE is very much analogous to the stripping of metal from a mercury-amalgam electrode to an ion in solution. The wave characteristics are similarly affected by adsorption on the electrode surface and by the extent of solubility of neutral species in the electrode material. There seems to be no reason why the DO–CPE cannot be extended to analytical use by taking advantage of preferential liquid–liquid extraction by the CPE of electrochemically-active molecules.

F. A. Schultz and T. Kuwana,

J. Electroanal. Chem., 10 (1965) 95–103

ELECTROLUMINESCENCE IN NON-AQUEOUS SOLUTIONS

J. M. Bader and T. Kuwana,
J. Electroanal. Chem., 10 (1965) 104–109

REDUCTION FROM A PRE-ENRICHED SOLUTION OF AMALGAM-FORMING METALS; A NEW ELECTROANALYTICAL METHOD

A new electroanalytical method, based on pre-enrichment in a mercury drop by constant potential electrolysis, constant potential oxidation and linear cathodic voltage-scan voltammetry, has been developed; it provides an alternative approach to cases where anodic stripping methods are difficult to apply and may be a novel tool for the investigation of electrode kinetics.

CH. YARNITSKY AND M. ARIEL,

J. Electroanal. Chem., 10 (1965) 110–118

THE RETARDATION OF ELECTROCHEMICAL REACTIONS BY ADSORBED ORGANIC MOLECULES; A QUANTITATIVE TREATMENT INVOLVING THE THEORY OF IRREVERSIBLE POLAROGRAPHIC WAVES

The inhibition of the cathodic discharge of Cu^{2+}, Cd^{2+} and Zn^{2+} by adsorbed *n*-butanol has been studied by polarographic and differential capacity measurements under similar conditions of adsorption and inhibition. By a superposition of coverage and current data, new "polarographic waves at constant coverage" are derived. The latter are analysed with the theory of irreversible polarographic waves in order to calculate the standard rate constant ($K_{s,\theta}$) and the cathodic energy transfer coefficient as a function of the degree of coverage θ. For the Zn^{2+} discharge reaction, $K_{s,\theta}$ depends on θ linearly only for θ values less than 0.5. For higher values of θ, a lateral interaction term is necessary. The equation $K_{s,\theta}=K_{s,0}\ (1-\theta)^b$ where b is a constant (> 1) is in quantitative agreement with the results for Zn^{2+} discharge inhibited by *n*-butanol over a wide range of coverage ($0 \leqslant \theta \leqslant 0.85$). The lateral interaction term b is also specific for the nature of the reducible ion. For the reactions of Cd^{2+}- and Cu^{2+}-discharge, when the experimental values of $K_{s,\theta}$ are extrapolated to $\theta = 0$ using the above equation, the standard rate constants in the absence of inhibition ($K_{s,0}$) that are obtained are of the correct order. It is concluded that the mechanism of retardation of the electrochemical reactions by adsorbed *n*-butanol may be due to a "crowding effect". The cathodic transfer coefficient is, in general, independent of θ except at limiting high values of the latter, indicating that the nature of the rate-determining step for the electrode reactions is changed only at coverages approaching that of a monolayer.

S. SATHYANARAYANA,
J. Electroanal. Chem., 10 (1965) 119–139

THEORETICAL ELECTROMOTIVE FORCES FOR CELLS CONTAINING A SINGLE SOLID OR MOLTEN OXIDE

W. J. HAMER,

J. Electroanal. Chem., 10 (1965) 140–150

CATHODIC REDUCTION OF FOUR-VALENT GERMANIUM

An investigation of solutions containing germanium established that in all the systems explored and under all the conditions applied, germanium takes part in electrode reactions. In cathodic reactions an important part is played by (i) the different forms in which Ge(IV) is present in the solution (pentamer, monomer, anions), (ii) the equilibria between them and (iii) the rate of transition from one form to the other. When a decrease of hydrogen overvoltage was observed, some special features of the mechanism of this phenomenon have been noted. It has been firmly established that in all systems examined, cathodic reduction gives rise to a more-or-less stable intermediate product. Its form, as a rule, increasingly approaches the defined Ge(II) when the alkalinity of solution is increased. Bivalent germanium, prepared by reduction of Ge(IV) in alkaline medium, is relatively stable even when the solution is made acid. Evidence has also been adduced that with germanium thus prepared, the form in which it is present in the solution plays an important part.

B. LOVREČEK AND LJ. DUIĆ,

J. Electroanal. Chem., 10 (1965) 151–163

THE ELECTROCHEMICAL REDUCTION OF THE TETRAPHENYLSTIBONIUM ION

M. D. MORRIS*, P. S. MCKINNEY AND E. C. WOODBURY
Department of Chemistry, Harvard University, Cambridge (U.S.A.)
(Received March 15th, 1965)

The polarographic activity of the tetraphenylstibonium ion, $(C_6H_5)_4Sb^+$, was reported several years ago by SHINAGAWA and co-workers[1]. More recently, AFFSPRUNG AND GAINER[2] described the polarographic behavior of the tetratolylstibonium ion. The analogous compounds of arsenic and phosphorus are also reported to be reducible at the dropping electrode in aqueous solution[3]. The electrochemistry of these "onium" compounds is of interest, not only because they represent an interesting group of organometallics, but also because of their possible use as amperometric titrants for various inorganic anions[4–6]. Also, the electrochemical reduction of the tetraphenylstibonium ion, and other tetraaryl antimony compounds, appears to be unique among the "onium" compounds of the group V elements in that a two-step reduction is involved. Both tetraphenylarsonium and tetraphenylphosphonium ions are reported to exhibit single, two-electron polarographic waves[3]. The different behavior of the antimony and arsenic compounds, in particular, is quite interesting in view of their typically common chemistry.

The purpose of this paper will be to elucidate the mechanism for the electrochemical reduction of the tetraphenylstibonium ion and to propose an explanation for the unique electrochemical behavior of the stibonium compounds.

The polarographic wave

Figure 1 shows a typical undamped polarogram of millimolar tetraphenylstibonium ion in an HCl–KCl supporting electrolyte of pH 1.5. The solution contains approximately 0.02% Triton-X-100 as a maximum suppressor. In the absence of any maximum suppressor, the waves are badly distorted with an acute maximum at the potential of the first wave and violent current fluctuations at potentials just prior to the second wave. 0.01% Triton X-100 reduces the maximum to a sufficiently low level to allow the measurement of the diffusion current, but 0.02% is necessary to eliminate the maximum entirely, when an undamped polarogram is recorded. Even in the presence of this large amount of suppressor, the current–time curves for individual drops remain badly distorted by adsorption. This was particularly true during the early stages of drop growth. For this reason, undamped polarograms were recorded and maximum rather than average currents were measured throughout the study.

* Present address: Department of Chemistry, The Pennsylvania State University, University Park, Pennsylvania.

Tetraphenylstibonium ions and their reduction products are strongly adsorbed at a mercury surface. The potential range over which adsorption occurs is indicated by the electrocapillary curve shown in Fig. 2. In this figure the drop-time, which is closely related to the mercury–solution interfacial tension[7], is plotted as a function of applied potential for solutions of millimolar tetraphenylstibonium ion in 0.1 *F* KCl, with and without 0.01% Triton X-100. Similar plots of the supporting electrolyte alone are shown for comparison. It is clear that strong adsorption occurs at potentials more negative than +0.05 V *vs.* S.C.E. Desorption of the surface active material takes

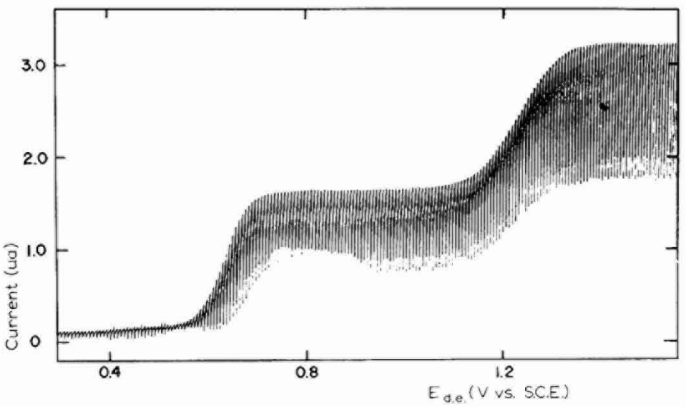

Fig. 1. A polarogram of $1.03 \cdot 10^{-3}$ *F* tetraphenylstibonium ion in a supporting electrolyte of pH 6.5. Triton X-100 has been added to suppress maxima.

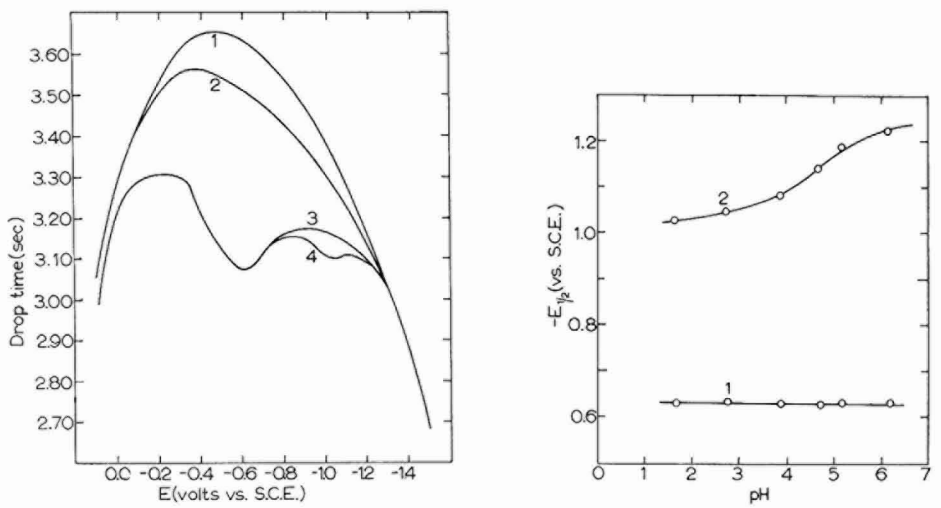

Fig. 2. Electrocapillary curves at 25.0° of solns. used in this study. (1), 0.1 *F* KCl; (2), 0.1 *F* KCl containing 0.01% Triton X-100; (3), $1 \cdot 10^{-3}$ *F* tetraphenylstibonium ion in 0.1 *F* KCl; (4) $1 \cdot 10^{-3}$ *F* tetraphenylstibonium ion in 0.1 *F* KCl containing 0.01% Triton X-100. All measurements were made at a capillary flow rate of 2.16 mg/sec.

Fig. 3. The dependence of half-wave potential on pH for $1 \cdot 10^{-3}$ *F* solns. of tetraphenylstibonium ion. (1), first wave; (2), second wave. All measurements were made at a capillary flow of 2.16 mg/sec.

place at about -1.3 V. The presence of Triton X-100 has little apparent effect on the adsorption picture at the electrode. The adsorption behavior is essentially the same at pH values from 1.5–6.5.

The dependence of the half-wave potentials on several factors is relevant to the elucidation of the mechanism involved. As indicated in Fig. 3, the first half-wave potential is independent of pH over the range 1.5–6.5. The value is -0.635 ± 0.005 V *vs.* S.C.E. which is about 0.07 V more positive than the value reported by SHINAGAWA[1]. The reason for this discrepancy is not known. There appears to be a slight dependence of the $E_{\frac{1}{2}}$ on drop time for the first wave. Because of the difficulty of making precise half-wave potential measurements in the presence of large amounts of Triton X-100, an accurate drop-time dependence could not be determined. The first half-wave potential is independent of concentration. The second $E_{\frac{1}{2}}$ is strongly dependent on pH, but the dependency cannot be described by any simple relationship. The potential appears to be independent of drop-time, but is strongly dependent upon the concentration of tetraphenylstibonium ion. The dependency is described approximately by the relationship $\Delta E_{\frac{1}{2}}/\Delta \log C = -0.050$ V.

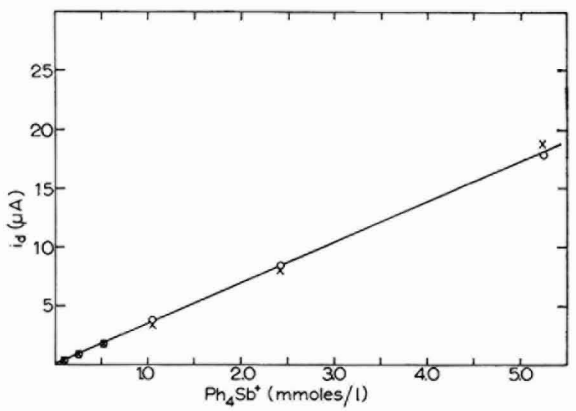

Fig. 4. The dependence of limiting current on concn. of tetraphenylstibonium ion. All measurements were made in a buffer of pH 6.5 at a capillary flow rate of 2.16 mg/sec. The first limiting current was measured at -0.9 V *vs.* S.C.E. The second limiting current was measured at -1.4 V *vs.* S.C.E. (○), 1st wave; (×), 2nd wave.

The slope of a plot of $\log i/(i_d - i)$ *vs.* E for the first wave is 0.059 V, suggesting polarographic reversibility for the electron transfer process involved. AFFSPRUNG AND GAINER[2] find, by the same criterion, that the first wave for the reduction of tetratolylstibonium ion is also due to a reversible, one-electron process. The slope of the log plot for the second wave is greater than 0.059 V and is dependent on pH, becoming smaller with increasing acidity. This is interpreted as evidence for the irreversibility of the second electron transfer.

In buffered solutions, both limiting currents are proportional to tetraphenylstibonium ion concentration over the range $1 \cdot 10^{-4}$–$5 \cdot 10^{-3}$ F. The first and second limiting currents are equal, within experimental error and with appropriate corrections for changes in drop time, at all pH values and concentrations studied. Figure 4 illustrates the relationship in a buffer of pH 6.5. It is not possible to prepare solutions

greater than $5.25 \cdot 10^{-3}$ F in this buffer because of the precipitation of the electroactive material presumably as a phosphate-containing species. The linear relation of the second limiting current with concentration contradicts the findings of SHINAGAWA and coworkers[1]. They report that in 0.1 F KCl the height of the second wave is described by a function of the form, $i_l = aC/(b-C)$, where i_l is the limiting current, C the bulk concentration of tetraphenylstibonium ion and a and b are constants. Hence, they attribute this non-linearity to adsorption of the ion at the electrode surface. However, Fig. 2 indicates that desorption occurs at -1.3 V *vs.* S.C.E., or about 0.1 V more positive than the potential at which limiting current measurements are made on the second wave. An explanation for the discrepancy can be found in the fact that the earlier workers used a neutral, unbuffered solution for the concentration studies. As indicated in Fig. 3, the potential of the second wave is dependent on hydrogen ion concentration. Furthermore, as indicated in a later section of this paper, an increase in pH during the course of controlled-potential electrolysis in an unbuffered, originally neutral solution, demonstrates that hydrogen ions are consumed by the reaction occurring at potentials on the second wave. This means that in such solutions the diffusion layer rapidly becomes alkaline. The solubility product of tetraphenylstibonium hydroxide[8] is about $1.2 \cdot 10^{-8}$. Hence, in an unbuffered, originally neutral solution, some of the tetraphenylstibonium ion will be precipitated by the generated hydroxide ion and will never reach the electrode surface. The limiting current in such cases will be less than the true diffusion current whenever the concentration exceeds a certain value. Based upon the data of SHINAGAWA[1], this limiting concentration appears to be approximately $2 \cdot 10^{-3}$ M tetraphenylstibonium ion.

The equivalent conductance of tetraphenylstibonium bromide was measured at 25°. The conductance varies linearly with the square root of salt concentration below $1 \cdot 10^{-3}$ F and extrapolation to infinite dilution gives $\Lambda_0 = 107 \pm 1$ cm^2 ohm^{-1} equiv.$^{-1}$. Because the infinite dilution equivalent conductance of the bromide ion is 78.1 at this temperature[9], the value for the tetraphenylstibonium ion becomes 29 ± 1. This equivalent conductance value leads, through the Nernst–Hartley relation[10], to a diffusion coefficient of $(0.78 \pm 0.03) \cdot 10^{-5}$ cm^2/sec for the tetraphenylstibonium ion at 25°.

The use of this diffusion coefficient in the Ilkovic equation for maximum current (constant equal to 706) indicates that both polarographic steps involve the transfer of one electron.

Controlled-potential electrolysis

In addition to the polarographic data detailed above, controlled-potential electrolysis provides further information concerning the reduction process. Large-scale electrolysis at a mercury pool cathode carried out at potentials on the diffusion current plateau of the first wave produced a white, water-insoluble precipitate. Integration of the current required for exhaustive electrolysis at this potential indicated that one faraday of electricity is consumed per mole of tetraphenylstibonium ion. The ultraviolet spectrum of the aqueous cell solution following electrolysis was identical with that for a supporting electrolyte solution alone. In particular, though special precautions were taken to carry out the electrolysis in a sealed cell, no trace of benzene was found as a product of the electrolysis at potentials on the first wave.

Thin-layer chromatography of the precipitate, dissolved in carbon tetrachloride, indicated the presence of two materials. Attempts to separate the two compounds by column chromatography were not successful. It was noted however that a clean separation could be affected by fractional crystallization from *n*-pentane. Although this procedure did not allow a quantitative recovery of the two products, enough of both materials was obtained to permit characterization. The compounds were identified as triphenylstibine, $(C_6H_5)_3Sb$, and diphenylmercury, $(C_6H_5)_2Hg$. Identification was made on the basis of a comparison of infrared spectra and thin-layer chromatographic R_F values, with those of authentic samples of the compounds. Mixed melting points were sharp and in agreement with literature values for the compounds. No biphenyl was detected as a constituent of the precipitate.

TABLE 1

WEIGHT OF PRECIPITATE RECOVERED FROM ELECTROLYSIS AT POTENTIALS PRIOR TO THE SECOND POLAROGRAPHIC WAVE IN A SOLUTION AT pH 6.5

Wt. of $(Ph)_4SbBr$ *(mg)*	*Wt. ppt. recovered (mg)*	*% of theoretical*[a]
51.9	52.5	98[b]
51.9	52.8	99[c]
51.9	51.9	97[d]

[a] Based on expected yield of diphenylmercury and triphenylstibine.
[b] Potential equal −0.90 V *vs.* S.C.E.
[c] Potential equal −0.75 V *vs.* S.C.E., 0.02% Triton X-100 present.
[d] Potential equal −0.75 V *vs.* S.C.E.

To demonstrate further that only two products are formed by this electrolysis, a gravimetric analysis was made of the precipitate. The results of several of these determinations are outlined in Table 1. It is clear that $(C_6H_5)_4Sb^+$ is converted quantitatively to $(C_6H_5)_2Hg$ and $(C_6H_5)_3Sb$. Furthermore, the presence of Triton X-100 as a maximum suppressor has no significant effect on the results, nor does the control potential, so long as it is not more negative than potentials on the second wave.

The products of electrolysis carried out at potentials on the plateau of the second wave were identified as $(C_6H_5)_3Sb$ and benzene. The benzene was identified by its u.v. spectrum. No other products were found. The weight of the triphenylstibine recovered was within about 2% of the theoretical yield based on a stoichiometric conversion of the tetraphenylstibonium ion. Finally, the apparent coulometric *n* value, measured at −1.40 V *vs.* S.C.E., was 2.0.

Because the conditions of a large-scale electrolysis differ substantially from those encountered polarographically, an electrolysis was performed at potentials on each wave under polarographic conditions in a micro-cell. Thin-layer chromatograms of carbon tetrachloride extracts from the micro-cell indicated formation of the same products as in the large scale electrolysis experiments.

Reaction scheme for tetraphenylstibonium ion reduction

In agreement with the data detailed above, the following reaction scheme is proposed to account for the electrochemical reduction of the tetraphenylstibonium ion. The first wave is accounted for by the reaction

$$(C_6H_5)_4Sb^+ \text{ ----- } Hg + e^- \rightarrow (C_6H_5)_3Sb + [C_6H_5Hg\cdot] \quad (1)$$

The radical then decays rapidly *via* the disproportionation reaction

$$2[C_6H_5Hg\cdot] \rightarrow (C_6H_5)_2Hg + Hg \quad (2)$$

The second electron transfer corresponds to

$$[C_6H_5Hg\cdot] + H^+ + e^- \rightarrow C_6H_6 + Hg \quad (3)$$

or to the overall reaction

$$(C_6H_5)_4Sb^+ \text{ --- } Hg + 2\,e^- + H^+ \rightarrow (C_6H_5)_3Sb + C_6H_6 + Hg \quad (3a)$$

To emphasize the strong adsorption of the tetraphenylstibonium ion at the mercury electrode, and the subsequent involvement of mercury in the overall reaction, it seemed logical to include mercury as a constituent of the species reacting at the electrode. It is not meant to imply chemical bond formation necessarily, although as will be discussed later, this appears to be a possible interpretation of the reaction sequence.

Because polarographic and coulometric evidence indicates a one-electron process for the first step, a radical must at least formally be considered as the first product. The lifetime of this radical must be very short as evidenced by the results of rapid scan cyclic voltammetry at a hanging mercury drop. Such a polarogram is shown in Fig. 5. Two features are of particular importance. First, the absence of

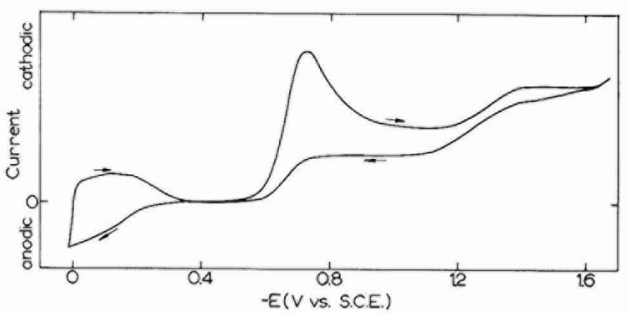

Fig. 5. A cyclic polarogram of $1 \cdot 10^{-3}$ *F* tetraphenylstibonium ion in a buffer soln. of pH 6.5. Triton X-100 has been added to suppress maxima. Scan rate equals 0.05 c/sec.

anodic waves on the positive-going sweep indicates that there is no reoxidation of any of the products of the preceding cathodic sweep. Hence, the radical product of the first wave, which would be expected to produce an anodic wave if stable, must decay rapidly to the electro-inactive products, triphenylstibine and diphenylmercury. This is further substantiated by the flat appearance of the second wave. If the product of the first electron transfer, or an electro-active decay product were stable and further reduced to produce the second wave, the concentration of this substance in the vicinity of the electrode would build up during the plateau of the first wave and produce a maximum in the second wave similar to that observed in the first. If however, the product of the first wave decays rapidly to form inactive materials, then there would be no build up of electro-active material prior to the second wave, and hence no current

maximum. The reaction is similar in this regard to the reduction of benzaldehyde which exhibits a similar cyclic voltammetric behavior[11].

The rapid disappearance of the radical helps explain some of the observed polarographic data. The first wave is reversible, but the half-wave potential appears to be dependent upon the drop-time. It has been reported that this behavior can be expected when the product of the reversible reaction is inactivated by a fast chemical reaction[12].

Support for reaction (2), the disproportionation of the phenylmercuric radical, comes from several pieces of data. First, of course, the formation of diphenylmercury as a product indicates that such a reaction must take place. However, the reaction also helps to explain the concentration dependence of the second half-wave potential. If the rate of the second electron transfer is of the same order of magnitude as that of the disproportionation, then any factor which would tend to increase the rate of disproportionation would require that the applied potential be more negative before the second electron transfer reaction could be competitive with reaction (2). It is expected that the rate of reaction (2) should be proportional to the square of the concentration of the radical and hence an increase in tetraphenylstibonium ion concentration should shift the second half-wave potential to more negative values. This is in agreement with the observed data.

The second electron transfer, as represented by reaction (3) or (3a), seems quite straightforward and the involvement of hydrogen ion in the reaction explains the pH-dependency of the second wave. If the reaction were reversible it would be expected that the half-wave potential would shift 0.059 V with each unit increase in pH. The fact that the shift is irregular is not unusual in cases where the reaction is irreversible as it is here.

Some comment seems necessary on the proposed nature of the radical product of the first electron transfer. It could well be argued that the product should be a species like [Ph_4Sb --- Hg·] which then undergoes disproportionation to form triphenylstibine, diphenylmercury and mercury. There is some precedent for this type of a "radical-amalgam" intermediate[13], and certainly such a scheme would satisfy the experimental evidence presented thus far. However, there is considerable circumstantial evidence to support the contention that the phenylmercury radical is involved in this case. Such radicals are well known, the methyl compound having been first prepared by the reduction of methylmercuric compounds at $-33°$ in liquid ammonia[14]. More recently a series of analogous alkyl and aryl compounds has been prepared[15]. COATES prefers to call these compounds "organic metals" since they do not display many of the properties usually associated with free radicals[16]. In the present case, the choice of [RHg·] as the form of the "radical" intermediate is based largely on the similar polarographic behavior of $(C_6H_5)_4Sb^+$ to that of phenylmercuric compounds as reported by BENESCH AND BENESCH[17]. In particular, the dependence of the second half-wave potential on concentration and pH is almost identical for both compounds, implying that the same reaction is involved. To emphasize further this point, a polarogram was recorded for a mixture of tetraphenylstibonium bromide and phenylmercuric acetate. Figure 6 shows that there are only three waves. The first is due to the first step in the reduction of phenylmercuric acetate. The second wave is, of course, the first reduction step of the tetraphenylstibonium ion. The third wave, the height of which is equal to the sum of the first two, is the second reduction step for both

compounds. The third wave appears to be smooth and uniform, as does a derivative polarogram of the same solution, and there is no indication of its being a combination of two waves. Cyclic voltammetric studies of the mixture show again only three waves on the cathodic sweep and no anodic waves on the reverse sweep.

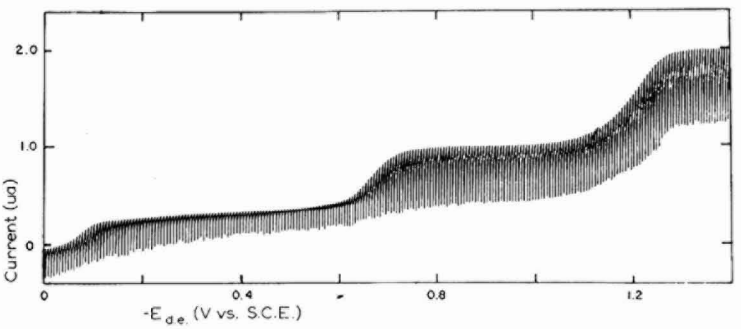

Fig. 6. A polarogram of a mixture of $5 \cdot 10^{-4}$ *F* tetraphenylstibonium and $5 \cdot 10^{-4}$ *F* phenylmercuric acetate in a buffer of pH 6.5.

It is interesting to note that the same type of "organic metal" compound has been proposed as the product of the first reduction step in polarographic studies of iodonium salts, $R_2I^+X^-$ [18] and allyl and benzyl iodides[19].

Comparison of the polarographic behavior of group V tetraphenyl-"onium" compounds

The polarographic reduction of tetraphenylarsonium and tetraphenylphosphonium ions appears to proceed *via* a single two-electron step in aqueous solution[3]. The dissimilar behavior of the arsenic and antimony compounds seems particularly interesting in view of their very similar general chemistry. A clue to the different polarographic behavior may be found in their adsorption behavior at a mercury electrode. As indicated in Fig. 2, the tetraphenylantimony compound is strongly adsorbed at mercury prior to the first reduction step. The electro-capillary curve for the tetraphenylarsonium ion under identical conditions indicates no adsorption, although there is a slight deviation from the supporting electrolyte curve at -1.5 V *vs.* S.C.E., perhaps due to the formation of insoluble triphenylarsine. It seems possible that the antimony compound, being more covalent and having a larger central atom may be able to distort readily from a tetrahedral configuration to adopt a distorted trigonal bi-pyramid with mercury at one of the apices. This is believed to be the geometry of the triphenyldichloro compound of antimony[20]. In this arrangement, an electron could be transferred to the antimony and the compound could then, with little rearrangement, form triphenylstibine, and a phenylmercury radical which remains at the electrode for the formation of diphenylmercury. This would help to explain also why the radical reacts with the electrode material rather than with the solvent to form benzene or with itself to form biphenyl. It is of interest to note in this regard that triphenylsulfonium ion, which also exhibits a two-step polarographic reduction wave[3], is adsorbed strongly at the D.M.E.[21] This particular reaction is under further study at the present time.

EXPERIMENTAL

Tetraphenylstibonium bromide was prepared according to the method of WILLARD *et al.*[22] Eastman White-Label triphenylstibine was first reacted with chlorine and then the resulting dichloride was reacted with phenylmagnesium bromide. The final product had a melting point of 214–215°. Eastman, practical grade, phenylmercuric acetate was used without further purification.

All polarographic supporting electrolytes contained 0.1 *F* potassium chloride and a buffer of the desired composition when necessary. Clark and Lubs buffers were used to maintain pH 6.5 and 5.2, acetate buffers for pH 5.0 and 3.5 and a KCl–HCl mixture for a pH of 1.5.

All polarograms were run with a controlled potential and derivative polarograph[23] manufactured by the Indiana Instrument and Chemical Co. The waves were recorded without filtering on a Sargent Model MR recording potentiometer with a full-scale response of less than one second. All polarograms were recorded at $25 \pm 0.2°$.

The D.M.E. capillary had a flow rate of 2.16 mg/sec at a mercury column height of 53.9 cm, corrected for back pressure. The open-circuit drop time in a 0.1 *F* KCl solution was 3.30 sec.

The micro-cell used for small scale electrolysis at a D.M.E. was constructed from a piece of Corning, #7930 porous-glass tubing 4 cm in length and 9 mm in diameter. The porous-glass tube was inserted through a rubber stopper in the bottom of a 6-cm length of 40-mm pyrex-glass tubing. A mercury reservoir was attached to the bottom of the porous-glass tube so that the solution level in the small tube could be adjusted. The outer pyrex tube was filled with supporting electrolyte to a level just below the top of the inner porous-glass tube and the mercury reservoir adjusted so that mercury completely filled the porous glass. The supporting electrolyte solution was deaerated. The mercury reservoir was lowered and a deaerated 0.1-ml portion of the test solution placed in the porous-glass tube. The D.M.E. was then positioned in the porous tube in contact with the test solution. The reference and auxiliary electrodes were positioned in the outer tube containing supporting electrolyte and the electrolysis was performed by adjusting the initial potential of the polarograph to the desired value. It was possible to perform electrolyses on even smaller samples by using 6-mm porous-glass tubing and a D.M.E. constructed from 1-mm capillary tubing drawn down to a fine tip.

Conductance measurements were made with an Industrial Instruments type IR-II bridge and a dip-type cell.

Controlled-potential electrolysis was performed using a Lingane–Jones potentiostat[24]. The electrolysis current was measured with the Sargent recorder and the amount of electricity consumed was determined by gravimetric integration of the current–time trace.

Cyclic polarograms were displayed on a Moseley Model X-Y recorder[20], with a full-scale response of less than one second. The triangular wave was obtained from a Hewlett Packard Model 202A low frequency function generator. The electrode used in these studies was a slow dropping mercury electrode constructed by constricting a Sargent 6–12 sec capillary. The drop time of this electrode was about 200 sec and the cyclic polarograms were recorded 100 sec into the drop life.

The precipitates produced by large-scale electrolysis were separated from the

mercury cathode either by washing into a sintered-glass filter crucible or by extraction with carbon tetrachloride. Both methods allowed the quantitative recovery of triphenylstibine and diphenylmercury.

Thin-layer chromatography was carried out on microscope slides. Silica gel H was used as the adsorbent and a mixed solvent of 70% *n*-pentane and 30% dichloromethane used as the developing system. Visualization was effected with iodine. Eastman White-Label triphenylstibine and diphenylmercury were used as reference standards for comparison.

ACKNOWLEDGEMENT

The authors gratefully acknowledge the financial assistance of the Milton Fund of Harvard University.

SUMMARY

The electrochemical reduction of tetraphenylstibonium ion has been investigated. A mechanism is proposed for the two-step reduction based on polarographic, controlled-potential electrolysis and cyclic voltammetric data. There is evidence that the strong adsorption of the ion at the electrode surface plays an important role in determining the overall reaction scheme.

REFERENCES

1 M. SHINAGAWA, H. MATSUO AND H. OKASHITA, *Bunseki Kagaku (Japan Analyst)*, 7 (1958) 219.
2 H. E. AFFSPRUNG AND A. B. GAINER, *Anal. Chim. Acta*, 27 (1962) 578.
3 H. MATSUO, *J. Sci. Hiroshima Univ., Sec. A.*, 22 (1958) 281.
4 M. SHINAGAWA, *Progress in Polarography*, Vol. 2, edited by P. ZUMAN AND I. M. KOLTHOFF, Interscience Publishers, Inc., New York, 1962, ch. 31.
5 H. NEZU, *Bunseki Kagaku (Japan Analyst)*, 10 (1961) 571.
6 H. E. AFFSPRUNG AND V. S. ARCHER, *Anal. Chem.*, 35 (1963) 976.
7 I. M. KOLTHOFF AND J. J. LINGANE, *Polarography*, Interscience Publishers, Inc., New York, 2nd ed., 1952, ch. 8.
8 K. D. MOFFETT, J. A. SIMMLER AND H. A. POTRATZ, *Anal. Chem.*, 28 (1956) 1356.
9 R. A. ROBINSON AND R. H. STOKES, *Electrolyte Solutions*, Butterworths Publications, Ltd., London, 1959, 2nd ed., appendix 6.1.
10 See, for example, ref. 7, ch. 3.
11 Unpublished results of P.S.M.
12 P. ZUMAN, *Organic Polarographic Analysis*, The MacMillan Company, New York, 1964, ch. 1.
13 B. C. SOUTHWORTH, R. OSTERYOUNG, K. D. FLEISCHER AND F. C. NACHOD, *Anal. Chem.*, 33 (1961) 208.
14 C. A. KRAUS, *J. Am. Chem. Soc.*, 35 (1923) 1732.
15 B. C. GOWENLOCK AND J. TROTMAN, *J. Chem. Soc.*, 2114 (1957).
16 G. E. COATES, *Organo-Metallic Compounds*, John Wiley and Sons., Inc., New York, 1960, ch. II.
17 R. BENESCH AND R. E. BENESCH, *J. Am. Chem. Soc.*, 73 (1951) 3391.
18 E. I. COLICHMAN AND G. P. MAFFEI, *J. Am. Chem. Soc.*, 74 (1952) 2744.
19 N. S. HUSH AND K. B. OLDHAM, *J. Electroanal. Chem.*, 6 (1963) 34.
20 E. G. ROCHOW, D. T. HARD AND R. N. LEWIS, *The Chemistry of Organo-Metallic Compounds*, John Wiley and Sons Inc., New York, 1957, ch. 8.
21 Unpublished results of P.S.M.
22 H. H. WILLARD, L. R. PERKINS AND F. F. BLICKE, *J. Am. Chem. Soc.*, 70 (1948) 737.
23 M. T. KELLEY, H. C. JONES AND D. J. FISHER, *Anal. Chem.*, 31 (1959) 1475; *ibid*, 32 (1960) 1262.
24 J. J. LINGANE AND S. L. JONES, *Anal. Chem.*, 22 (1950) 1169.

ELECTROCHEMICAL STUDIES OF ORGANIC COMPOUNDS DISSOLVED IN CARBON-PASTE ELECTRODES

FRANKLIN A. SCHULTZ AND THEODORE KUWANA
Department of Chemistry, University of California, Riverside (U.S.A.)
(Received March 1st, 1965)

INTRODUCTION

The carbon-paste electrode (CPE) developed by ADAMS[1] has been used for electro-oxidation and reduction studies of both inorganic and organic substances[2-10]. Since the conducting graphite particles are mixed with a viscous organic liquid, use of the CPE has been limited to aqueous solutions. This limitation, as applied to water-insoluble, electroactive organic compounds, may be circumvented by dissolving these organics in the electrode itself. A preliminary communication[11] reported the application of such a technique to the electrolysis of certain organic compounds.

The purpose of this paper is to present the results of a quantitative investigation of the parameters which affect the overall electrochemical and physical characteristics of the dissolved organics–CPE (DO–CPE). Ferrocene was the compound most extensively used since the ferrocene–ferricinium couple behaved the most reversibly and also exhibited desirable solubility properties. Data for other compounds are also discussed.

EXPERIMENTAL

The chronopotentiometric circuit was conventional in all respects. Potential–time patterns were recorded using either a Leeds and Northrup Model H or a Sargent Model SR strip chart recorder. The cyclic voltammetry unit was constructed following the circuit of ALDEN, CHAMBERS AND ADAMS[12] and used with a Moseley Model S-22 X-Y recorder. All recorders used a cathode-follower input.

A conventional H-type cell was used with the working electrode (DO–CPE) and a saturated calomel reference electrode located in the main compartment. All potentials reported are referred to this electrode. A large platinum-gauze electrode served as auxiliary electrode in the other compartment. The cavity for the DO–CPE was constructed by machining a cylindrical hole, 6 mm in diameter and 10 mm deep, in a Teflon rod which was 20 mm in length and 10 mm in diameter. A platinum wire, which passed through the central axis of the glass tubing and the Teflon rod, made electrical contact to the DO–CPE.

Commercially-obtained ferrocene was further purified chromatographically on an alumina column with redistilled *n*-hexane as eluent, and then recrystallized from spectroscopic-quality methanol. The melting point of the ferrocene was 174–

175°. Substituted ferrocenes were purified chromatographically. Benzophenone was recrystallized three times from ethanol. The following compounds were used as received: lithium perchlorate, anhydrous (reagent-grade, G. F. Smith Chemical Co.); perchloric acid (60%, reagent-grade, Baker and Adamson); 1-bromonaphthalene and 1-chloronaphthalene (reagent-grade, Matheson, Coleman and Bell); 1-methylnaphthalene (reagent-grade, Eastman Organic Chemicals); 2-ethylnaphthalene (reagent-grade, Aldrich Chemical Co.); *n*-undecane (pure grade, 99% minimum, Phillips Petroleum Co.); iodine, potassium carbonate and sodium hydroxide were reagent-grade stock chemicals. The carbon was Grade 38 graphite powder from the National Carbon Co. Water was redistilled from alkaline permanganate. Pre-purified-grade nitrogen was used for degassing purposes.

PROCEDURE

Homogeneous pastes of uniform composition were prepared by dissolving a weighed quantity of ferrocene (or other organic) in a known volume of pasting liquid. A weighed amount of graphite was then added and mixed in an agate mortar until the carbon appeared uniformly wetted. The paste was stored under water in a small vial; reproducible transition times could be obtained with stored pastes for a period of 3–4 days.

The electrode was prepared by packing the Teflon cavity with the paste, smoothing the surface with a stainless-steel spatula, and removing excess paste from the edge surface of the Teflon with tissue paper. After each chronopotentiometric run, it was necessary to remove a thin surface-layer of paste in which the concentration of electroactive material had been changed by electrolysis. The measured geometric area of the electrode surface was 0.28 cm^2; evaluation of the electrode area by chronopotentiometric reduction of ferricyanide in 0.1 *F* KCl gave a value of 0.32 cm^2 using 0.76×10^{-5} cm^2/sec as the value of the diffusion coefficient[13] for ferricyanide ion.

The choice of electrolytes for the aqueous solutions was based on the stability of the organic ion formed in the electrolysis. For example, ions which would complex with ferric ion were avoided since such ions appeared to accelerate the decomposition of ferricinium ion. All solutions were degassed with nitrogen.

RESULTS AND DISCUSSION

The chronopotentiometric waves for oxidation of ferrocene from DO–CPE were well-defined in pastes prepared from substituted naphthalenes and pure, long-chain hydrocarbons (*e.g.*, *n*-undecane), but Nujol, used by ADAMS in some pastes, gave poorly-developed waves. Values of quarter-wave potential, $E_{\frac{1}{4}}$, and of $E_{0.22}$ (for reverse wave) evaluated for ferrocene with DO–CPE are compared in Table 1 with those obtained for ferrocene in various other systems. The agreement is surprising in view of the marked difference in the systems; it undoubtedly reflects the low solvation energy and the symmetrical structure of ferrocene and ferricinium ion. The reversibility of the electrode reaction and the internal resistance of the DO–CPE (and consequently the $E_{\frac{1}{4}}$ values) were affected by the ratio of carbon to pasting liquid and the viscosity of the pasting liquid.

TABLE 1

CHRONOPOTENTIOMETRIC $E_{1/4}$ AND $E_{0.22}$ VALUES FOR FERROCENE

$E_{1/4}$ (V)	$E_{0.22}$ (V)	System	Ref.
+0.38[a]	+0.33	DO–CPE, 0.1 *F* $LiClO_4$ and 0.1 *F* $HClO_4$–aqueous	
+0.307	+0.300	Pt, 0.2 *F* $LiClO_4$ in acetonitrile	14
+0.341	+0.335	Pt, 0.2 *F* $LiClO_4$ in acetonitrile	15
+0.315	—	Pt, 0.2 *F* $LiClO_4$ in acetonitrile	16
+0.31[b]	—	DME, 90% ethanol, $NaClO_4$–$HClO_4$	17

[a] The value depends on the components of the CPE as well as the current density and temperature. Value is uncorrected for potential drop due to internal resistance.
[b] Polarographic $E_{1/2}$ value.

Current density

Effects of current density on $E_{\frac{1}{4}}$ values and transition times at constant paste composition were examined in order to evaluate the degree of reversibility and to determine the mode of mass transfer. In Table 2 the average value of $i\tau^{\frac{1}{2}}$ is 868 ± 19 μA sec$^{\frac{1}{2}}$ over a current range of 90–302 μA. Mild stirring of the solution during the

TABLE 2

CHRONOPOTENTIOMETRIC DATA FOR FERROCENE OXIDATION, DO–CPE

i (μA)	$\tau^{\frac{1}{2}}$ (sec$^{\frac{1}{2}}$)	$i\tau^{\frac{1}{2}}$ (μA sec$^{\frac{1}{2}}$)[a]	$E_{1/4}$ (V)	Slope[b]
90	10.19	917±30	+0.356	0.074
118	7.34	867±34	0.358	0.074
157	5.47	859± 7	0.370	0.082
200	4.39	878±27	0.366	0.088
236	3.54	835±24	0.380	0.089
302	2.83	855±16	0.371	0.108

[a] Average of 4 or more trials.
[b] Reciprocal slope of plot of E *vs.* log $[(\tau^{\frac{1}{2}}-t^{\frac{1}{2}})/t^{\frac{1}{2}}]$.

forward chronopotentiogram did not affect the transition time, indicating that mass transfer of ferrocene is from the paste. Absence of convective currents in the paste makes it possible to obtain reliable transition times of much greater duration than with ordinary electrode systems. There was no reverse wave for reduction of ferricinium ion if the solution was stirred. Plots of $\tau^{\frac{1}{2}}$ *vs.* $1/i$ for varying concentrations were linear and extrapolated to the origin (Fig. 1) as did plots of $i\tau^{\frac{1}{2}}$ *vs.* concentration (Fig. 2). The constancy of $i\tau^{\frac{1}{2}}$ with varying current indicates quite conclusively that the mass transfer rate of ferrocene is governed by diffusion from the paste. There is little doubt that the electrode reaction is the oxidation of ferrocene as follows:

ferrocene (organic liquid–paste) $\rightarrow$ ferricinium ion (aqueous) $+ e^-$

The $E_{\frac{1}{4}}$ values and the reciprocal slopes of the plot of E *vs.* log $[(\tau^{\frac{1}{2}}-t^{\frac{1}{2}})/t^{\frac{1}{2}}]$ increase with current (Table 2). Although both values reflect a degree of irreversibility of the electrode reaction, the shift in $E_{\frac{1}{4}}$ with current density appears to be

largely due to internal resistance of the DO–CPE. This shift is approximately linear with current and gives a resistance of 170 Ω for a typical bromonaphthalene paste of 1.70 (g C to cm³ bromonaphthalene).

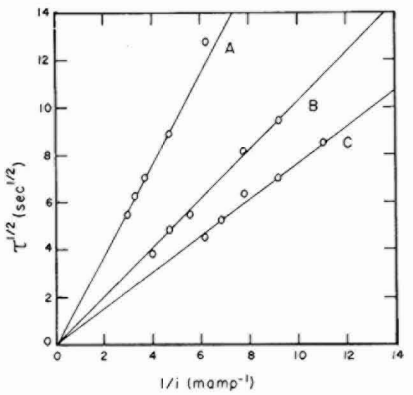

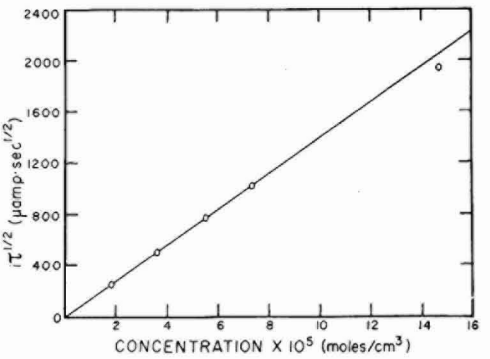

Fig. 1. $\tau^{\frac{1}{2}}$ plotted *vs.* $1/i$ for various concns. of ferrocene in bromonaphthalene paste. Concn. expressed as moles ferrocene/cm³ bromonaphthalene: (A), 1.47 × 10⁻⁴; (B), 7.35 × 10⁻⁵; (C), 5.51 × 10⁻⁵.

Fig. 2. $i\tau^{\frac{1}{2}}$ *vs.* concn. for ferrocene dissolved in bromonaphthalene paste.

Paste composition

The relative weight ratio of carbon to pasting liquid influenced the values of transition time and quarter-wave potential. In order to retain units used in the Sand equation[18], the concentration of electroactive species was always expressed as moles per cm³ of pasting liquid; the ratio of graphite to pasting liquid must also be specified. In Table 3 the effect of changing the weight of graphite per volume of pasting liquid is shown for a constant concentration of ferrocene in bromonaphthalene. Transition time decreased as carbon content increased since the carbon acted as a diluent. In the limiting case, where ferrocene is present only on the surface of the carbon, the transition time would be the total time required to oxidize ferrocene coulometrically.

TABLE 3

EFFECT OF GRAPHITE:LIQUID RATIO ON TRANSITION TIME AND REVERSIBILITY

Grams graphite/cm³ bromonaphthalene	$i\tau^{\frac{1}{2}}$ *(μA sec$^{\frac{1}{2}}$)*	$E_{1/4}$ *(V)*	*Slope*[a]
1.33[b]	1144 ± 26[c]	+0.63	0.187
1.40	1056 ± 7	0.63	0.211
1.50	1060 ± 20	0.42	0.149
1.60	960 ± 39	0.40	0.151
1.70	930 ± 35	0.38	0.108
1.80	852 ± 10	0.36	0.122
1.90	880 ± 11	0.36	0.087
2.00	806 ± 22	0.35	0.128

[a] Reciprocal slope of E *vs.* log $[(\tau^{\frac{1}{2}}-t^{\frac{1}{2}})/t^{\frac{1}{2}}]$.
[b] Ferrocene concn., 7.35 × 10⁻⁵ moles/cm³ bromonaphthalene.
[c] Average value of 4 or more runs.

This is similar to the case where electroactive substances are adsorbed on carbon, as reported by VOORHIES AND DAVIS[19].

The general increase in the values of the reciprocal slope of E *vs.* $\log [(\tau^{\frac{1}{2}} - t^{\frac{1}{2}})/t^{\frac{1}{2}}]$ plots indicated greater irreversibility with decreased carbon content. The increase in the $E_{\frac{1}{4}}$ value was in accord with irreversibility trends, and reflected the increased internal resistance of the DO–CPE with lower carbon content. Pastes with low carbon content (below 1.50) tended to be somewhat fluid, while pastes with high carbon content (above 1.80) were "dry". Neither extreme was amenable to easy filling of the electrode cavity, so a paste with the ratio of 1.70 was selected as a compromise between the most desirable consistency and the maximum reversibility of the electrode reaction. It should be noted that this value is higher than the 1.50 ratio recommended by ADAMS[3].

Effect of temperature and viscosity

If mass transfer rate is governed by diffusion, the viscosity of the pasting liquid should affect this rate and consequently the transition time. The Stokes–Einstein relation[20]:

$$D = kT/6\eta\pi r$$

(where D is the diffusion coefficient in $cm^2\ sec^{-1}$, T the temperature in absolute degrees, k the Boltzmann constant, r the radius of the diffusing molecule or ion, and η the viscosity in centipoise units) predicts a linear relationship between D and the reciprocal of viscosity. ADAMS has verified the above relationship for several organic molecules dissolved in non-aqueous solvents using radiotracer techniques[21]. In this paper, relative diffusion coefficients of ferrocene were calculated from chronopotentiometric data using pasting liquids of different viscosities in the DO–CPE. The plot of D *vs.* $1/\eta$, shown in Fig. 3, is linear and extrapolates to the origin. Since the actual, effective concentration in the pasting liquid is not known, the calculated values of the

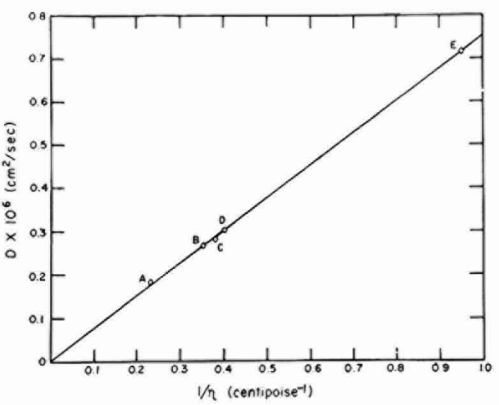

Fig. 3. Apparent diffusion coefficient *vs.* reciprocal viscosity for ferrocene in pastes prepared from liquids of various viscosities. Viscosity determined as described in footnote b, Table 4. (A), 1-bromonaphthalene[22]; (B), 1-chloronaphthalene[22]; (C), 1-methylnaphthalene[23]; (D), 2-ethylnaphthalene[24]; (E), *n*-undecane[25]. Superscript on compound gives ref. for viscosity values. Temp. = 27°.

diffusion coefficient must be considered as apparent values whose importance is their relative magnitude.

Substitution into the Sand equation for the value of D from the Stokes–Einstein relation results in the following:

$$i\tau^{\frac{1}{2}} = 1/2\ nFAC(kT/6\eta\pi r)^{\frac{1}{2}}$$

where n is the number of electrons transferred per molecule, F the Faraday, A the electrode area in cm^2, C the concentration in moles per cm^3, and all other terms have their usual significance. The dependence of transition time, τ, on temperature and viscosity, with all other factors held constant, is given by:

$$\tau = \frac{T}{\eta} K$$

where K is a constant equal to $(nFAC)^2k/24\pi ri^2$. The constancy of the values of $\tau\eta/T$ (last column, Table 4) for 1-bromonaphthalene and 1-chloronaphthalene is in good agreement with theoretical expectations.

TABLE 4

RELATIONSHIP BETWEEN TRANSITION TIME, VISCOSITY AND TEMPERATURE[a]

Liquid	*T* (°K)	*τ* (sec)	*η* (cp)[b]	*τη/T*
1-bromonaphthalene	300	19.4 ± 1.0	4.28	0.277
	307	24.6 ± 0.4	3.67	0.294
	314	29.8 ± 0.9	3.12	0.298
	321	35.2	2.67	0.296
				av. 0.291 ± 0.007
1-chloronaphthalene	275	12.7 ± 1.0	5.45	0.252
	300	28.1 ± 2.7	2.83	0.265
	307	32.4 ± 1.7	2.45	0.258
	315	40.4 ± 2.3	2.06	0.264
	323	46.5 ± 1.1	1.76	0.253
				av. 0.258 ± 0.005

[a] Ferrocene concn., 7.35×10^{-5} moles/cm^3 pasting liquid; ratio of g C/cm^3 pasting liquid, 1.70; area of electrode, 0.32 cm^2; const. current of 197 μA.
[b] Values for η were determined by plotting literature values *vs.* temp. and selecting from the graph the viscosity at the given temp. 1-Bromonaphthalene and 1-chloronaphthalene, ref. 22.

The least viscous liquid, *n*-undecane, gave a more well-defined wave and lower $E_{\frac{1}{4}}$ value for ferrocene than any of the naphthalene pastes. The $E_{\frac{1}{4}}$ values were 0.328 V, 0.374 V, 0.371 V, 0.363 V and 0.378 V for *n*-undecane, 1-bromo-, 1-chloro-, 1-methyl-, and 2-ethyl-naphthalene, respectively. A higher activity for a given concentration is indicated by the data for ferrocene in *n*-undecane and solubility and diffusion data also support this.

Comments on mechanism for ferrocene

A preliminary study[11] of ferrocene with DO–CPE gave for the ratio of forward to reverse transition times, τ_f/τ_r, a value of 3:1 in agreement with predictions for a diffusion-controlled electrode reaction[26]. It now appears that this was a fortuitous

observation since it has been found that the ratio depends on current density and temperature.

Since $i\tau_f^{\frac{1}{2}}$ is independent of i, and τ_f shows the predicted dependence on T, the deviation of τ_f/τ_r must be from the reverse step of ferricinium reduction. A value for τ_f/τ_r of less than 3 indicates that ferricinium ion in excess of that from diffusion is supplied, perhaps, by adsorption on the electrode surface; a value greater than 3 indicates depletion of the ion other than by diffusion from the electrode surface. Since transition times were sufficiently short to eliminate convection as a major factor, the most logical explanation of this observation would be the kinetic decomposition of ferricinium ion. An overall (ferrocene oxidation–reduction) scheme consistent with the above findings would be:

$$Fe(C_5H_5)_2 \xrightarrow{-e^-} Fe(C_5H_5)_2^+(\text{adsorbed}) \xrightarrow{k_1} Fe(C_5H_5)_2^+ \xrightarrow{k_2} \rightarrow \text{non-electroactive product}$$

This scheme predicts that the τ_f/τ_r ratio would decrease with an increase in current density, and correspondingly increase with an increase in temperature. The data

TABLE 5

EFFECT OF CURRENT DENSITY AND TEMPERATURE ON THE RATIO, τ_f/τ_r[a]

Variation with i[b]		*Variation with T*[c]	
i (μA)	τ_f/τ_r	T (°)	τ_f/τ_r
115	3.58	2	2.41
151	3.20	27	3.04
192	3.03	34	3.21
232	3.06	41	3.80
292	2.73	48	5.67

[a] Pasting liquid, 1-bromonaphthalene; ferrocene concn., 7.35×10^{-5} moles/cm^3 pasting liquid; ratio of g C/cm^3 pasting liquid, 1.70.
[b] $T = 24°$.
[c] Current = 197 μA.

presented in Table 5 are in agreement with the above contention. Coulometric studies[27] of ferrocene oxidation in acetonitrile, alcohol and alcohol–water solutions have also indicated a slow decomposition of ferricinium ion.

Electrochemical studies of other compounds

In the study of other compounds, iodine and benzophenone gave well-developed cyclic voltammetric waves but poorly-defined chronopotentiometric waves; the converse was true for the phenazine derivatives. The best results were obtained with a series of substituted ferrocenes. The data are summarized in Tables 6 and 7. The alkyl-phenyl groups on ferrocene were chosen with expectations that these would remain adsorbed on the surface of the electrode, but the ratio of τ_f/τ_r given in Table 6 indicates otherwise.

An interesting result was observed in the cyclic voltammetric study of iodine

TABLE 6

CHRONOPOTENTIOMETRIC STUDIES OF COMPOUNDS DISSOLVED IN THE DO–CPE

Substituted ferrocenes[a]

Substituent group	$i\tau^{\frac{1}{2}}$ *(μA sec$^{\frac{1}{2}}$)*	$E_{1/4}$ *(V)*	$E_{0.22}$ *(V)*	τ_f/τ_r
$-CH=CHPh$	370	+0.46	+0.45	2.35
$-CH_2CH_2Ph$	394	0.43	0.42	2.66
$-C(OH)(Ph)CH_2Ph$	339	0.48	0.47	2.64
$-CH(OH)CH_2Ph$	368	0.42	0.41	2.73
$-C(Ph)=CHPh$	357	0.48	0.47	2.95
$-COCH_3$	431	0.57	0.55	4.7

Other compounds

Compound	*Pasting liquid*	*Supporting electrolyte*	$E_{1/4}$ *(V)*	$E_{0.22}$ *(V)*
Acid phenazine derivative[b]	1-bromonaphthalene	0.1 *F* NaOH	−0.75	−0.68
Basic phenazine derivative	1-bromonaphthalene	0.1 *F* K_2CO_3	−0.43	—

[a] Ferrocene concn., 3.67×10^{-5} moles/cm^3 pasting liquid; ratio g C/cm^3 pasting liquid, 1.70; pasting liquid, 1-bromonaphthalene; supporting electrolyte, 0.1 *F* $LiClO_4$, 0.1 *F* $HClO_4$.
[b] Both the forward and reverse waves were better defined for the acidic derivative than for the basic derivative.

TABLE 7

CYCLIC VOLTAMMETRIC STUDIES OF COMPOUNDS IN THE DO–CPE

Compound	*Pasting liquid*	*Supporting electrolyte*	$E_{p/2}$ *(V)*
Benzophenone	*n*-undecane	0.1 *F* K_2CO_3	−0.39
Iodine	1-methylnaphthalene	1 *F* H_2SO_4	+0.34
Iodine	*n*-undecane	1 *F* H_2SO_4	+0.45

dissolved in *n*-undecane paste. On the first scan there was observed, in addition to the expected wave for reduction of iodine, a smaller less well-defined second wave. A sharp drop in current was also noted between the first and second waves. Evidence for a double anodic wave was much less pronounced than for the cathodic wave. These double waves (observed only with *n*-undecane, and not with other pasting liquids) could possibly be due to the formation of I· radicals similar to the case discussed by DAVIS[9] for bromine. The stability of these radicals would be much greater in a paraffinic solvent such as *n*-undecane than in the naphthalenes, where the radicals would be quenched by the aromatic system.

ACKNOWLEDGEMENT

Preliminary experimental work performed by Mr. DEAN CARTER and the samples of substituted ferrocenes provided by Dr. DONALD BUBLITZ are greatly appreciated. The authors gratefully acknowledge the support of this work by grant No. GM 11670 from the Public Health Service. Portions of this work were presented

before 127th meeting of Electrochemical Society, San Francisco, May 1965, and release for publication in this journal is appreciated.

SUMMARY

The application of the DO–CPE appears to be a promising technique for study of organic compounds normally insoluble in aqueous solutions. The behavior of DO–CPE is very much analogous to the stripping of metal from a mercury-amalgam electrode to an ion in solution. The wave characteristics are similarly affected by adsorption on the electrode surface and by the extent of solubility of neutral species in the electrode material. There seems to be no reason why the DO–CPE cannot be extended to analytical use by taking advantage of preferential liquid–liquid extraction by the CPE of electrochemically-active molecules.

REFERENCES

1 R. N. ADAMS, *Anal. Chem.*, 30 (1958) 1576.
2 R. N. ADAMS, *Rev. Polarog. (Kyoto)*, 11 (1963) 71.
3 C. OLSEN AND R. N. ADAMS, *Anal. Chim. Acta*, 22 (1960) 582.
4 T. R. MUELLER, C. OLSEN AND R. N. ADAMS, *Advances in Polarography*, Vol. 1, Pergamon Press, Oxford, 1960, p. 198.
5 Z. GALUS AND R. N. ADAMS, *J. Am. Chem. Soc.*, 84 (1962) 2061.
6 C. OLSEN, H. Y. LEE AND R. N. ADAMS, *J. Electroanal. Chem.*, 2 (1961) 396.
7 Z. GALUS, C. OLSEN, H. Y. LEE AND R. N. ADAMS, *Anal. Chem.*, 34 (1962) 164.
8 Z. GALUS AND R. N. ADAMS, *J. Am. Chem. Soc.*, 86 (1964) 1666.
9 D. G. DAVIS AND M. E. EVERHART, *Anal. Chem.*, 36 (1964) 38.
10 H. JEHRING AND W. STOLLE, *Z. Chem.*, 4 (1964) 309.
11 T. KUWANA AND W. G. FRENCH, *Anal. Chem.*, 36 (1964) 241.
12 J. R. ALDEN, J. Q. CHAMBERS AND R. N. ADAMS, *J. Electroanal. Chem.*, 5 (1963) 152.
13 M. VON STACKLEBERG, M. PILGRAM AND V. TOOME, *Z. Elektrochem.*, 57 (1953) 342.
14 T. KUWANA, D. E. BUBLITZ AND G. HOH, *J. Am. Chem. Soc.*, 82 (1960) 5811.
15 G. L. K. HOH, W. E. MCEWEN AND J. KLEINBERG, *J. Am. Chem. Soc.*, 83 (1961) 3949.
16 W. F. LITTLE, C. N. REILLEY, J. D. JOHNSON AND A. P. SANDERS, *J. Am. Chem. Soc.*, 86 (1964) 1382.
17 J. A. PAGE AND G. WILKINSON, *J. Am. Chem. Soc.*, 74 (1952) 6149.
18 H. J. S. SAND, *Phil. Mag.*, 1 (1901) 45.
19 J. D. VOORHIES AND S. M. DAVIS, *J. Phys. Chem.*, 67 (1963) 332.
20 R. A. ROBINSON AND R. H. STOKES, *Electrolyte Solutions*, Academic Press, New York, 1959.
21 T. A. MILLER, B. PRATER, J. K. LEE AND R. N. ADAMS, *J. Am. Chem. Soc.*, 87 (1965) 121.
22 W. M. HESTON, JR., E. J. HENNELLY AND C. P. SMYTH, *J. Am. Chem. Soc.*, 72 (1950) 2071.
23 R. W. RAMPOLLA AND C. P. SMYTH, *J. Am. Chem. Soc.*, 80 (1958) 1057.
24 H. KÖLBEL, *Brenstoff-Chem.*, 30 (1949) 73.
25 *Selected Values of Physical and Thermodynamic Properties of Hydrocarbons and Related Compounds*, Carnegie Press, Pittsburgh, Pa., 1953.
26 T. BERZINS AND P. DELAHAY, *J. Am. Chem. Soc.*, 75 (1953) 4205.
27 T. KUWANA AND F. C. ANSON, unpublished data.

ELECTROLUMINESCENCE IN NON-AQUEOUS SOLUTIONS

J. M. BADER AND T. KUWANA
Department of Chemistry, University of California, Riverside (U.S.A.)
(Received March 1st, 1965)

INTRODUCTION

Chemiluminescence, at least for low levels of light emission, appears to be a widespread phenomenon. Electrochemical processes seem a likely source for luminescence since they produce products or intermediates similar to those already suggested as sources of chemiluminescence or as precursors of chemiluminescent reactions.

This paper deals with the low-level light emission from the cyclic potential scans of a platinum electrode immersed in acetonitrile or dimethylsulfoxide (DMSO) with 0.2 F $LiClO_4$ as supporting electrolyte. These solvents were studied in the presence and absence of dissolved oxygen and/or anthracene.

Previous[1,2] reports of electroluminescence from our laboratory have been concerned with the electro-oxidation of luminol (5-aminophthalhydrazide) at a platinum electrode. VOJIR[3] earlier reported the observation of light emission from the cathodic polarization of an alkaline luminol solution and attributed this to the reaction of electro-generated hydrogen peroxide with luminol. We[4] have found that light emission also occurred in this system when the potential was sufficiently cathodic to electro-reduce alkali-metal ions at a mercury electrode. Recently, HICKLING and co-workers[5-7] have reported electroluminescence from the high voltage, anodic electrolysis of alkaline aqueous solutions or of liquid ammonia solutions.

SHLYAPINTOKH *et al.*[8] have observed chemiluminescence in the electrolysis of 0.1 N NaOH in the presence of fluorescein or eosin at smooth platinum electrodes. HERCULES[9] has reported electroluminescence from the alternating polarization of a platinum electrode in acetonitrile or dimethylformamide solutions that contained polycyclic aromatics. He suggested that the luminescence, which was characteristic of the fluorescent color of the particular aromatic, was a consequence of a reaction between the positive (perhaps associated or dimeric) and negative radical ions. CHANDROSS AND SONNTAG[10], and CHANDROSS AND VISCO[11] have made similar observations and suggested that the luminescence resulted from the positive radical ion or another oxidant removing an electron from the more stable bonding orbital of the negative radical anion. This would leave an electron in the higher-energy antibonding orbital to undergo transition to the lower-bonding orbital with the emission of a photon.

There have also been several interesting reports[12-14] of chemiluminescence from a hydrogen peroxide–sodium hypochlorite solution which emits in the near infrared region. The spectrum has been assigned to the spin-forbidden transitions from the excited singlet to the ground triplet state of oxygen. Decomposition of

hydroperoxides[15,16] also exhibit chemiluminescence and VASIL'EV AND VICHUTINSKII[17] have attributed the light emission to the following:

$$ROO\cdot + ROO\cdot = \text{products} + O_2 + h\nu \qquad (1)$$

where ROO· is a peroxy radical.

EXPERIMENTAL

The general cell configuration with appropriate electrodes and circuitry for cyclic voltammetry has been previously described[2]. Emitted light was monitored by a 1 ½ in. diameter, head-on Dumont K-1953 photomultiplier tube. Two channels of a Sanborn recorder Model 154-100 were used for simultaneous recording of photomultiplier output current and current flowing through the electrochemical cell; current–potential patterns from cyclic voltammetry were recorded simultaneously by an Electro-Instruments Model 101TB X-Y recorder. Matheson, Coleman and Bell spectroquality acetonitrile and reagent-grade DMSO were used with portions of the DMSO dried with Linde 4A molecular sieve. Anhydrous lithium perchlorate was obtained from the G. F. Smith Co. Commercially-obtained anthracene was zone-refined. Solution degassing was discussed previously[18].

RESULTS

The current–potential patterns for the cyclic scans of a platinum electrode in DMSO containing 0.2 *F* lithium perchlorate and dissolved oxygen are given in Fig. 1. If the potential is scanned cathodically from 0.0 V (all potentials will be referred

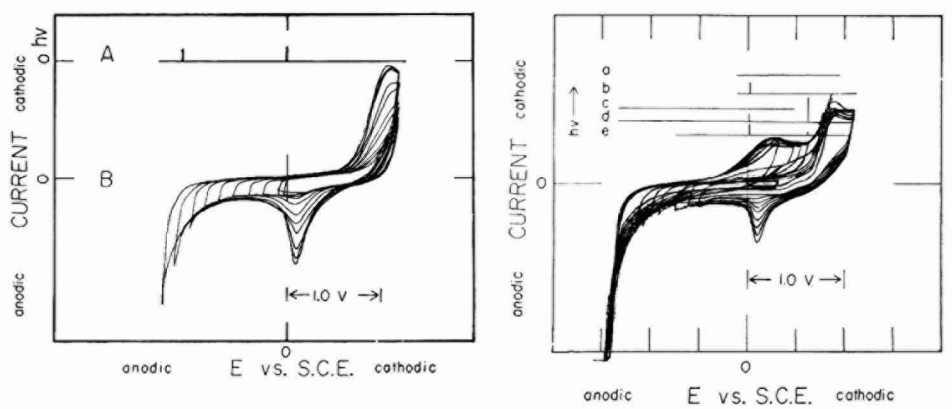

Fig. 1. Cyclic scans in un-degassed DMSO. (A), The potential at which electroluminescence occurs is indicated by the horizontal lines; (B), cathodic potential limit −1.2 V with anodic limit increasing on successive scans to +1.4 V.

Fig. 2. Cyclic scans in un-degassed DMSO with potential limits and electroluminescence shown by horizontal and vertical lines above the current–voltage patterns. (a), no electroluminescence between +0.1 and −0.9 V; (b), electroluminescence at 0.0 V from anodic wave if potential limits between +0.1 and −1.2 V; (c) no electroluminescence between potential limits of −0.5 and +1.4 V although additional cathodic wave observed; (d), electroluminescence observed at foot of oxygen reduction wave if potential limits between −1.2 and +1.4 V; (e), electroluminescence at foot of oxygen reduction wave decreases as anodic limit decreases.

to a saturated calomel electrode) to −0.9 V, a cathodic current is observed due to reduction of oxygen to hydrogen peroxide[19]. No light emission results from this oxygen reduction. In thoroughly degassed solutions, this wave is absent. If, however, the potential is scanned further cathodically to −1.2 V and then reversed to the anodic direction, an anodic wave with a peak potential of −0.2 V develops. While scanning through this anodic wave, light emission occurs at *ca.* 0.0 V which corresponds to the descending current portions following the peak of this wave. If the cathodic limit of the electrode is maintained at −1.2 V and the anodic limit is progressively increased, oxidation of the background solution (presumably of DMSO) begins with a decomposition potential of *ca.* +1.1 V. Low-level light emission is found concurrently with this oxidation. However, if the cathodic limit of the electrode is maintained at −0.5 V, (less than the potential required to reduce oxygen) and the anodic limit is allowed to increase on successive scans to +1.4 V, a cathodic wave develops with a peak potential of −0.2 to −0.3 V (Fig. 2). No light emission is observed within these limits. If the cathodic limit is now allowed to increase, light emission is observed at the foot of the wave for reduction of oxygen. This light emission may be due to a reaction between the oxidized product of DMSO and the product of the reduction of oxygen. In DMSO dried over a molecular sieve or distilled at 38° under vacuum, results are similar with slight shifts in the potentials of various waves. The potential limits of the scans are shown graphically by horizontal lines on the upper portion of Fig. 2. The vertical lines indicate potentials at which light is observed.

Figures 3 and 4 show similar data for acetonitrile. In well-degassed solutions, moderate light emission results at −2.9 V where lithium ion is being reduced to

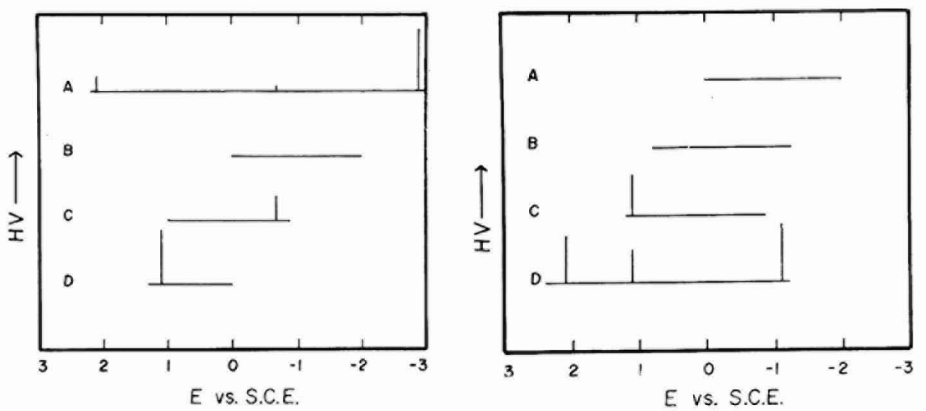

Fig. 3. Potential limits and potentials at which electroluminescence observed in cyclic scans of acetonitrile. (A), background electroluminescence pattern in un-degassed acetonitrile; (B), no electroluminescence between potential limits of 0.0 and −2 V in un-degassed acetonitrile; (C), with 10^{-3} *M* anthracene, electroluminescence at potential corresponding to reduction of anthracene when anodic limit is +0.9 V; (D), electroluminescence at +1.0 V from oxidation of anthracene

Fig. 4. Potential limits and electroluminescence in degassed acetonitrile containing anthracene. (A), no electroluminescence between potential limits of 0.0 and −2 V; (B), no electroluminescence between the potential limits of +0.9 and −1.2 V; (C), electroluminescence at potential of anthracene oxidation if cathodic limit is −0.9 V; (D), electroluminescence at potentials for oxidation and reduction of anthracene and oxidation of solvent if potential limits are +2.4 and −1.2 V.

lithium metal[20]. Undoubtedly, reduction of lithium is concurrent with reduction of small amounts of water which are always present in solvents such as acetonitrile. If the potential is scanned in an anodic direction, light emission is observed at a potential corresponding to oxidation of the solvent and/or perchlorate ion at *ca.* +2.1 V (see Fig. 3A). The product of this oxidation is dinitrile succinimide[20] with good evidence[20,21] that the mechanism is through oxidation of the perchlorate anion to the neutral free radical. Again, water present in trace quantities is undoubtedly undergoing concurrent oxidation.

If anthracene (AN) is added and oxygen is not removed from the solution. two successive cathodic waves are found with decomposition potentials (E_d) of −0.7 V and *ca.* −1.1 V due to reduction of oxygen and AN, respectively. No electroluminescence results from these two waves. If the cathodic limit is set at *ca.* −0.9 V, (*i.e.*, reduction of oxygen but not AN occurs) light emission is observed on each cycle at E_d of −0.7 to −0.8 V (at the foot of the oxygen reduction wave) when the anodic limit is between +0.7 and +0.9 V. If the anodic limit is allowed to progress further, an anodic wave corresponding to the oxidation of AN develops with an E_d of +1.05 V. Light emission results from this oxidation.

In well-degassed solutions of AN in acetonitrile, light emission is not observed if the electrode is cycled between the potentials of 0.0 and −2.0 V, or between +0.9 and −1.2 V. However, if the electrode is scanned anodically to +1.2 V, where AN is oxidized, light emission occurs. If the electrode is scanned cyclically between the potentials of +1.2 and −1.1 V (AN is reduced at −1.1 V), light emission is found at both +1.2 and −1.1 V. This result is in agreement with earlier observations of HERCULES[9] and of CHANDROSS AND VISCO[11]. It should be pointed out, however, contrary to conclusions in the literature[22] suggestive of an one-electron oxidation of AN in acetonitrile, that if the potential is sufficiently positive to reach the limiting current value for oxidation of AN, the value of n (the number of electrons transferred per molecule of AN) is between 3 and 4. Recent tracer diffusion studies by ADAMS[23] have verified earlier conclusions[24] about the value of the diffusion coefficient of AN in acetonitrile. Thus, for AN, the positive ion that oxidizes the negative anion radical may be $(AN)_2^+$ or $(AN)_2^{2+}$, where $(AN)_2$ is a dimeric species coupled through the 9-position of AN. Such an oxidizing species would circumvent the necessity of postulating an oxidation involving AN^+ which, as HERCULES pointed out, is known to be a short-lived species. The source of the chemiluminescence may be the negative anion radical as in the mechanism suggested by CHANDROSS AND SONNTAG[10]. If the electrode is cycled between +2.2 and −1.2 V, an additional light peak which corresponds to the oxidation of the background solution is found at +2.1 V.

DISCUSSION

Chemiluminescence appears to be a general phenomenon for oxidative processes involving oxygen or hydrogen peroxide in alkaline solutions[25,26]. Electroluminescence from oxidation of certain organic and inorganic substances in the presence of oxygen or hydrogen peroxide also seems fairly widespread[27,2].

In the present experiment, recombination of the radicals formed from the electro-oxidation reaction:

$$RH = R\cdot + H^+ + e^- \qquad (2)$$

where RH represents an organic substance, should furnish sufficient energy for light in the visible region of the spectrum. In solutions, energy loss through vibrational–collisional processes is certainly favored, particularly for aliphatic compounds. It is, however, possible that the following reactions occur to some extent in the presence of oxygen:

$$R\cdot + O_2 = ROO\cdot \quad (3)$$

$$ROO\cdot + ROO\cdot = ROOR + O_2 + h\nu \quad (4)$$

Reaction (4) is in accord with a previously proposed mechanism[17]. Even in degassed solutions at anodic potentials where the background solution is being oxidized, oxygen is undoubtedly being formed from the concurrent oxidation of traces of water present in the solvent. The necessity of oxygen for chemiluminescence in a special electro-oxidation process[1,2] has been previously demonstrated.

If reaction (4) is a source of chemiluminescence, the appearance of light during reduction of oxygen is possibly due to the following reactions:

$$O_2 + e^- = O_2^- \quad (5)$$

$$O_2^- + RH = R\cdot + HO_2^- \quad (6)$$

with the radical, R·, now reacting through the sequence of reactions (3) and (4) for chemiluminescence. Annihilation of the radical, R·, may proceed through several alternate routes (such as: $R\cdot + R\cdot = R\text{-}R$) and reaction (3) is undoubtedly of secondary importance.

In a few instances, electroluminescence was obtained at the potential for oxygen reduction only if the potential was first cycled anodically to +0.7 or +0.9 V. Whether the anodic pre-scan involves oxidation of traces of dissolved species or a change in the nature and role of the electrode surface is not at present clear.

Chemiluminescence from reduction of lithium ion in degassed acetonitrile solutions probably results from radical recombination reactions similar to processes described by HICKLING and co-workers[5–7]. Lithium metal can reduce both acetonitrile and traces of water as follows:

Primary process: $Li^+ + e^- = Li^\circ$ (7)

Secondary processes: $Li^\circ + H_2O = H\cdot + OH^- + Li^+$ (8)

$$Li^\circ + H_2O = e_{H_2O}^- + Li^+ \quad (9)$$

$$e_{H_2O}^- + H_2O = H\cdot + OH^- + H_2O \quad (10)$$

$$H\cdot + H\cdot = H_2 \quad (11)$$

$$\text{or, } Li^\circ + CH_3CN = Li^+ + H{:}^- + \cdot CH_2CN \quad (12)$$

$$H{:}^- + H_2O = H_2 + OH^- \quad (13)$$

$$2\cdot CH_2CN = CN—CH_2—CH_2—CN \quad (14)$$

Reactions (9) and (10) suggest the possibility of hydrated electrons participating in the reduction of water. Reactions (11), (13) and (14) are sufficiently energetic to produce light in the visible region. Energy produced by radical recombinations may be lost not by a collisional process, but rather through emission of a photon due to recombinations within a reaction "cage" formed in the solvent. Recombinations may also be occurring within micro-gas pockets formed by hydrogen gas from reaction (11).

Electroluminescence from alternating electro-oxidation and reduction of AN is in agreement with previous[9,11] experimental observations. However, as BARD[28] has observed in the case of 9,10-diphenylanthracene (DPA), the DPA^+ ion is not necessarily the oxidant that reacts with DPA^- to produce chemiluminescence. The same appears to be true in the case of AN. Apparently, an oxidizing species formed electrochemically may oxidize the anion radical (formed cathodically) to produce the excited, fluorescent state.

The suggested possibility[2] that a direct heterogeneous electron-transfer reaction may produce an excited state has been reported recently for rubrene[29]. The evidence is not conclusive, and further progress must await determination of spectral distribution, quantum yield and fluorescent yield (in solvent used), and identification of species generated electrochemically.

ACKNOWLEDGEMENT

The assistance of Mr. AL GOOLSBY in this work is greatly appreciated. The authors gratefully acknowledge the support of this work by grant no. GM 11670 from the Public Health Service and a NDEA graduate fellowship (J.M.B.).

REFERENCES

1 T. KUWANA, B. EPSTEIN AND E. T. SEO, *J. Phys. Chem.*, 67 (1963) 2243.
2 T. KUWANA, *J. Electroanal. Chem.*, 6 (1963) 164.
3 V. VOJIR, *Collection Czech. Chem. Commun.*, 19 (1954) 862.
4 E. T. SEO AND T. KUWANA, unpublished data. Results can be duplicated by the use of a dropping sodium–mercury amalgam electrode.
5 A. HICKLING AND G. R. NEWNS, *J. Chem. Soc. (London)*, (1961) 5186.
6 A. HICKLING AND M. D. INGRAM, *Trans. Faraday Soc.*, 60 (1964) 783.
7 A. HICKLING AND M. D. INGRAM, *J. Electroanal. Chem.*, 8 (1964) 65.
8 V. YA. SHLYAPINTOKH, J. M. POSTNIKOV, O. N. KARPUKHIN AND A. YA. VERETIL'NYI, *Zh. Fiz. Khim.*, 37 (1963) 2374.
9 D. M. HERCULES, *Science*, 145 (1964) 808.
10 E. A. CHANDROSS AND F. I. SONNTAG, *J. Am. Chem. Soc.*, 86 (1964) 3179; *Chem. Eng. News*, 31 (1964) 32.
11 E. A. CHANDROSS AND R. VISCO, *J. Am. Chem. Soc.*, 86 (1964) 5350.
12 H. SELIGER, *Anal. Biochem.*, 1 (1960) 60. *J. Chem. Phys.*, 40 (1964) 3133.
13 A. U. KHAN AND M. KASHA, *J. Chem. Phys.*, 39 (1963) 2105.
14 R. J. BROWNE AND E. A. OGRYZLO, *Proc. Chem. Soc.*, (1964) 117.
15 I. V. ZAKHAROV AND V. YA SHLYAPINTOKH, *Dokl. Akad. Nauk SSSR*, 150 (1963) 1069.
16 E. J. BOWEN AND R. A. LLOYD, *Proc. Roy. Soc. London, Ser A*, 275 (1963) 465, and references therein.
17 R. F. VASIL'EV AND A. A. VICHUTINSKII, *Dokl. Akad. Nauk SSSR*, 142 (1962) 615.
18 T. KUWANA, *Anal. Chem.*, 35 (1963) 1398.
19 D. T. SAWYER AND J. ROBERTS, unpublished data. The first reduction wave of oxygen in DMSO corresponds to the production of either HO_2^- or H_2O_2, depending on the water level in DMSO.
20 J. P. BILLON, *Bull. Soc. Chim. (France)*, (1962) 863.
21 A. H. MAKI AND D. H. GESKE, *J. Chem. Phys.*, 30 (1959) 1356.
22 J. O. VOORHIES AND N. H. FURMAN, *Anal. Chem.*, 31 (1959) 381.
23 T. A. MILLER, B. PRATER, J. K. LEE AND R. N. ADAMS, *J. Am. Chem. Soc.*, 87 (1965) 121.
24 T. KUWANA, Ph. D. Thesis, University of Kansas, 1959, pp. 109–112.
25 R. AUDUBERT, *Trans. Faraday Soc.*, 35 (1939) 197.
26 J. STAUFF, H. SCHMIDKUNZ AND G. HARTMANN, *Nature*, 198 (1963) 281.
27 W. D. BANCROFT AND H. B. WEISER, *J. Phys. Chem.*, 18 (1914) 762.
28 K. S. V. SANTHANAM AND A. J. BARD, *J. Am. Chem. Soc.*, 87 (1965) 121.
29 American Cyanamid Company, *Chemiluminescent Materials*, Technical Report No. 5, Contract Nonr 4200(00); AD606989 U. S. Department of Commerce, Office of Technical Services.

REDUCTION FROM A PRE-ENRICHED SOLUTION OF AMALGAM-FORMING METALS; A NEW ELECTROANALYTICAL METHOD

CH. YARNITSKY* AND M. ARIEL

Laboratory of Analytical Chemistry, Department of Chemistry, TECHNION-Israel Institute of Technology, Haifa (Israel)

(Received February 7th, 1965)

PRINCIPLE AND SCOPE OF THE METHOD

A new electroanalytical trace method[1], based on pre-enrichment in a mercury drop by constant potential electrolysis, constant potential oxidation and linear cathodic voltage-scan voltammetry, promises improved sensitivity and resolution for the analysis of certain ion mixtures, where proximate half-wave potentials or adverse relative concentrations render electroanalysis difficult. The new method has also potentialities as a tool for the study of the kinetics of electrochemical reactions at the mercury-drop electrode.

The metallic ion, present in low concentration (10^{-6} M or less) in the sample solution, is initially concentrated in a hanging mercury-drop electrode (HMDE) by applying constant potential electrolysis, with agitation of the sample solution, in complete analogy to anodic stripping voltammetry (a.s.v.) (including a final waiting period, during which the solution is allowed to come to rest). The electrode potential is now switched to a more positive value, at which the amalgam, formed in the electrolysis step, is partially re-oxidized. In contrast to a.s.v., this step is not recorded; the oxidation current is governed by the current–time function derived for constant potential voltammetry[2].

During this step, metallic ions are reformed at the drop–solution interface and diffuse away from it; ion concentration is maximum at the interface and decreases gradually with increased distance, until the limiting concentration of the original sample solution is reached. The vicinity of the electrode may be regarded as a region in which the concentration of the ion in question is considerably higher than the original sample concentration (although not homogeneously distributed).

After a controlled oxidation interval (of the order of a few seconds) a linear voltage scan, rising towards cathodic values, is applied and the voltagram recorded; this is identical with the curves obtained in single sweep methods. The direct connection between the reduction peak current obtained and the preliminary concentration and oxidation steps is easily demonstrated: no useful reduction peaks are obtained by applying the linear voltage scan directly to sample solutions more dilute

* Part of a M.Sc. thesis presented by CH. YARNITSKY to the Senate of the Technion.

than 10^{-7} M; in the case of more concentrated samples, the reduction peaks obtained after pre-enrichment are immeasurably higher. This increased sensitivity should be of the order achieved by a.s.v.; assuming similar diffusion coefficients for the metal in mercury and its ions in solution, and assuming that the metal ion concentration, at the interface, during the oxidation step, does not exceed its concentration inside the HMDE at the beginning of this step, one would expect the reduction current peak, obtained from pre-enriched solution, and the oxidation current peak, obtained by a.s.v., to have similar heights.

However, as is well known, the applicability of a.s.v. is often limited by background effects of condenser and parasitic faradaic currents; in complex samples, oxidation currents of additional depolarizers, present in solution and reacting electrochemically at potentials proximate to that of the ion question, may interfere (*e.g.*, the case of an a.s.v. peak coalescing with the mercury oxidation current).

Quantitative evaluation of a.s.v. peaks may be interfered with or prevented entirely; in some cases, the method of medium exchange[3] offers a solution.

By applying the new method and choosing the oxidation potential selectively, so that mainly the desired depolarizer is re-oxidized, some of the above difficulties may be surmounted; the solution near the HMDE will not be enriched either by the interfering depolarizer or mercury and the subsequent reduction wave will be undistorted. The method can be applied to the analysis of solutions with a concentration range similar to those suitable for a.s.v. (down to 10^{-9} M).

The application of this method to kinetic investigations seems promising. Being derived from a.s.v., the method has some of the limitations inherent in that method, such as its applicability to amalgam-forming metals only and its requirement of strict control of electrolysis conditions, etc. Additional experimental parameters requiring control are: duration and potential of oxidation step. It is also essential to differentiate between simple and kinetically-complicated cases.

The practical exploitation of the method involves preliminary tests for ascertaining its applicability in a wide concentration range, setting up of calibration

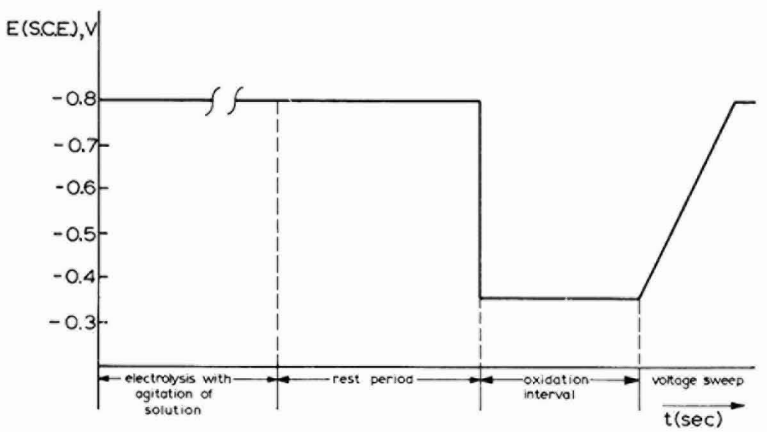

Fig. 1. Potential of working electrode (*vs.* S.C.E.) during the various steps in the determination of cadmium by the new method.

curves and investigating the dependence of reduction current peak height on the rate of voltage scan and duration of oxidation. As is the case in other trace analytical methods, numerous factors affect the shape and height of the final voltagrams; their evaluation and control may often prove difficult.

A schematic curve depicting the electrode potential–time changes occurring in the course of a determination by the new method is given in Fig. 1.

EXPERIMENTAL

Apparatus and reagents

The electrolysis cell and electrode have been previously described[4]. A polarizing unit, constructed for this investigation and similar to the instrument described by DAVIS AND SEABORN[5] is employed; triggering is manual, instead of being activated by drop detachment. The unit supplies all the potentials (constant and scan) required in the course of the experiments; it contains a linear voltage scan source, a compensating circuit and a timer for switching the potential from the cathodic values, required for electrodeposition, to anodic values required for re-oxidation, keeping the potential constant for a pre-determined time interval and finally initiating the linear cathodic voltage scan. The values of pre-electrolysis potential, oxidation potential, duration of oxidation step and the rate of linear voltage scan are adjustable as desired; the compensating circuit is designed to correct deviations from linearity of the voltage scan, resulting from the in-series connection of the measuring resistor.

A Tektronix type-502 Dual-Beam oscilloscope, with camera, served as recording instrument.

All reagents were of reagent grade; deionised distilled water was employed throughout.

Procedure

The deaerated sample solution, containing the ion to be determined and a suitable supporting electrolyte, is introduced into the electrolysis cell. The solution is stirred magnetically, nitrogen gas is passed over its surface and the ion electrodeposited in the HMDE by applying to the electrode a potential more negative than the half-wave potential of the particular ion in the chosen medium. Choice of electrolysis duration is arbitrary, being governed by the concentration of the sample solution; at its end, stirring is stopped, the solution allowed to come to rest (during 30 sec); the electrode potential is kept unchanged at the electrodeposition value. The timer switch is now activated, causing the electrode potential to jump to a value exceeding the half-wave potential by 200 mV, stay there for a predetermined oxidation interval and finally change linearly towards negative values, at a chosen rate of voltage scan; the voltagram obtained during the scan is displayed on the screen of the oscilloscope and photographed.

RESULTS AND DISCUSSION

Analytical evaluation

The applicability of the method to quantitative determinations was tested for a number of ions (Cu^{2+}, Pb^{2+}, Tl^{+}, Cd^{2+} and Zn^{2}), all determinable by a.s.v. In

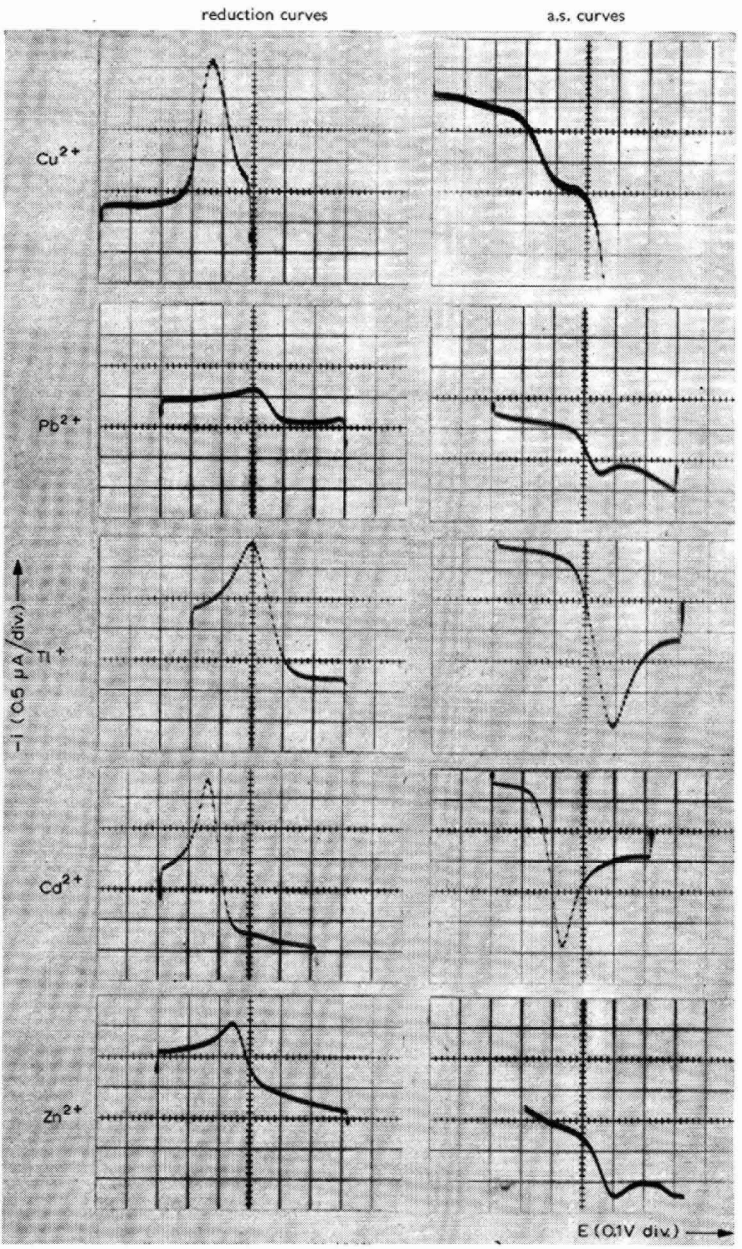

Fig. 2. Comparison of a.s. curves and reduction curves obtained from pre-enriched solution.

order to curtail the large number of experiments required in an evaluation of this kind (and resulting directly from the numerous parameters involved), a single supporting electrolyte was employed throughout. Temperature was kept at 23°–25°;

the effect of temperature variation within these limits was negligible when compared to the experimental error. Mercury drops of approximately 8 mg in weight were used on the HMDE; since reduction currents depend on drop size, a single drop, as a rule, was employed throughout any series of experiments designed to investigate any one particular factor. Electrolysis time, as a rule, was 3 min.

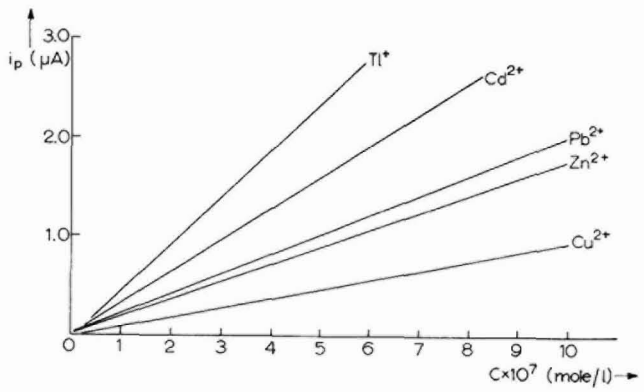

Fig. 3. Height of reduction current peak as function of depolarizer concn.

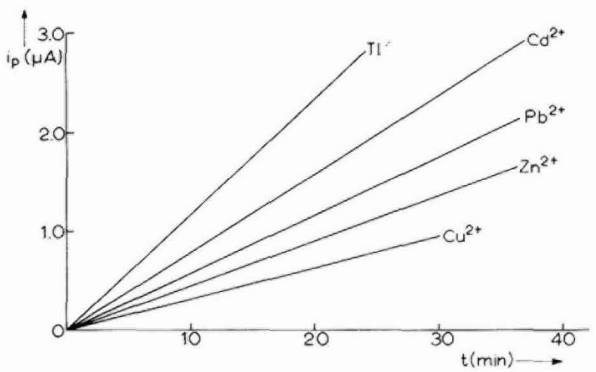

Fig. 4. Height of reduction current peak as function of duration of electrolysis.

A preliminary investigation of the shape of the voltagram, obtained from the sample solution by a.s.v., is generally desirable. Whenever, due to extreme sample dilution, no serviceable voltagram is obtained after 3-min pre-electrolysis, electrolysis must be prolonged to effect higher metal concentration in the HMDE. These a.s.v. voltagrams provide general information regarding the sample, such as half-wave potential values in the particular medium, suitable oxidation potential and interferences due to the presence of other ions, etc.

The reduction wave from a pre-enriched solution was first observed in the case of a single metallic ion (Pb^{2+}); the other four ions (Cd^{2+}, Tl^+, Cu^{2+} and Zn^{2+}) were chosen to test the generality of the phenomena observed. Since all these ions

gave a.s.v. oxidation curves (Fig. 2), the following experiments could be planned to investigate the effect of a number of experimental parameters on the shape and height of the reduction wave from pre-enriched solution:

(a) concentration of depolarizer in sample solution;

(b) duration of pre-electrolysis;

(c) duration of oxidation step.

The first series of experiments was carried out with solutions in the 10^{-6}–10^{-7} *M* concentration range (Fig. 3); in the second series, electrolysis times ranging from 3–30 min and arranged in an ascending arithmetic series were investigated (Fig. 4). The effect of varying the duration of the oxidation step is shown in Fig. 5.

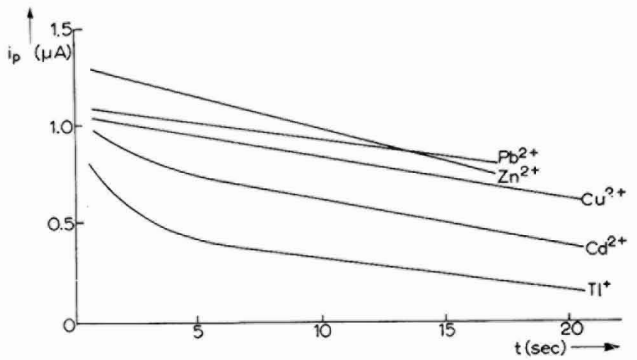

Fig. 5. Height of reduction current peak as function of oxidation interval.

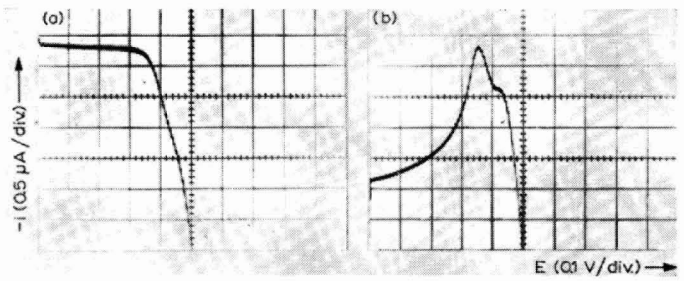

Fig. 6. A.s. and reduction curves of 10^{-6} *M* Cd^{2+} in 0.1 *M* KCl, in the presence of 10^{-5} *M* Tl^{+}: (a), a.s. voltagram; (b), reduction curve from pre-enriched solution. Experimental conditions: duration of electrolysis (for both a and b): 3 min; oxidation interval (for b): 5 sec; rate of voltage sweep (for both a and b): 0.3 V/sec.

In some cases, *e.g.*, with thallium, the height of the reduction peak depends critically on duration of oxidation. Quantitative thallium determinations, therefore, require strict adherence to pre-determined oxidation intervals.

The following determinations were chosen to illustrate the usefulness of the new method:

(a) 10^{-6} *M* Cu^{2+}, in chloride medium, is not easily determined by a.s.v.; the

new method produces a reduction wave which is readily evaluated quantitatively (Fig. 2a).

(b) 10^{-6} *M* Cd^{2+}, in the presence of 10^{-5} *M* Tl^{+}, cannot be determined by a.s.v., due to thallium interference (Fig. 6a); application of the new method solves this problem (Fig. 6b).

LIMITATIONS AND INTERFERENCES

The preliminary concentration step by electrolysis into the HMDE, is a source of non-reproducibility, both in a.s.v. and the new method. Stirring must be initiated and stopped as rapidly as possible; a synchronic magnetic stirrer must be employed, well-centered with regard to the cell to minimize irregular motion. The HMDE should be placed 1–2 cm above the stirrer bar, in the center of the electrolysis cell.

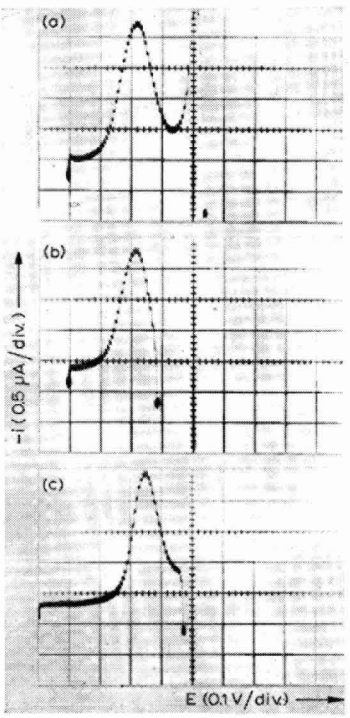

Fig. 7. Proper choice of oxidation potential, allowing evaluation of reduction curve; curves obtained with 10^{-6} *M* Cu^{2+}, at potential values: (a), too positive; (b), too negative; (c), optimal.

Should the HMDE, for some reason, be not placed centrally, care must be taken to remove it sufficiently from the stirring bar, in order to prevent the drop from falling off.

The oxidation potential requires careful choice; too negative values curtail oxidation and result in a cut-off wave (Fig 7).

The various parameters should be adjusted until the resulting voltagram has a base line and current peak which allow easy quantitative interpretation.

The ideal shape of the reduction current peak, as predicted by ŠEVČIK[6] and RANDLES[7], may be distorted through the presence of additional electrode reactions. Traces of dissolved oxygen must be guarded against; fresh mercury drops must be employed; distorted voltagrams are obtained on drops kept in distilled water overnight, possibly due to formation of a passive film; in some cases the voltagram is suppressed entirely.

The adequate coating of the platinum contact on which the HMDE hangs is very important both in a.s.v. and in the new method. Whenever wave distortion resulting from the poor quality of this coating is suspected, the electrode must be cleaned with dilute (1:1) HNO_3, rinsed with water and replated.

KINETIC EFFECTS

The passage of metal from the amalgamated HMDE into the surrounding solution and the transport of metal ions from the interface are governed by a series of steps, some of which may be faster and others slower than pure diffusion. In the simple case described above, diffusion control was assumed; this allowed the HMDE

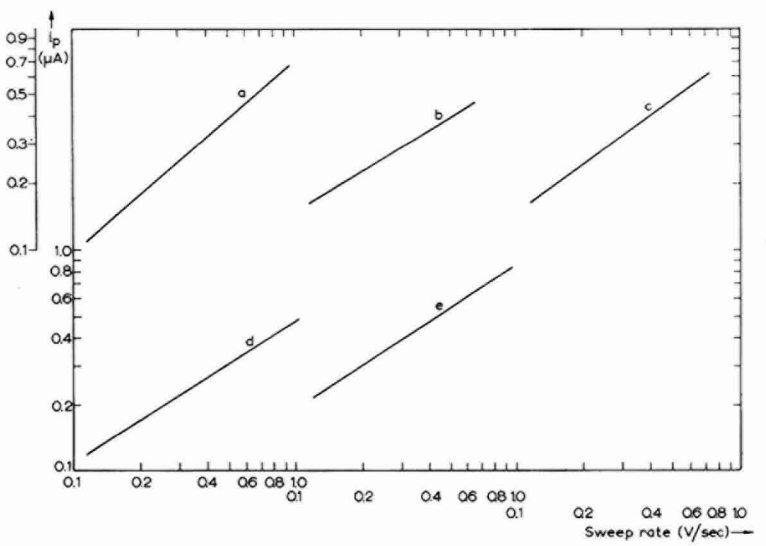

Fig. 8. Height of reduction current peak as function of voltage sweep rate. (a), Cu^{2+}, $i_p \propto v^{0.84\pm0.08}$; (b), Pb^{2+}, $i_p \propto v^{0.58\pm0.06}$; (c), Tl^{+}, $i_p \propto v^{0.77\pm0.08}$; (d), Cd^{2+}, $i_p \propto v^{0.61\pm0.06}$; (e), Zn^{2+}, $i_p \propto v^{0.66\pm0.07}$.

to be regarded as placed in a new solution, more concentrated than the original sample, during the amalgam oxidation step. Carrying this assumption further, the height of the reduction peak (i_p) obtained would be expected to be proportional to the square root of the rate of voltage scan (v)[6,7]. Experimental results show significant deviations from this relation, although the results for lead and cadmium approach it (Fig. 8). This aspect is under continued investigation.

The above relation was also investigated with solutions containing mixtures of

two different ions, one of which had previously been shown to adhere to the $i_p \propto v^{\frac{1}{2}}$ relation, when present singly (this ensured that the determination of the $i_p = f(v)$ was not affected by experimental errors). Results show that each ion behaves as if present singly and its $i_p = f(v)$ relation is unaffected.

SUMMARY

A new electroanalytical method, based on pre-enrichment in a mercury drop by constant potential electrolysis, constant potential oxidation and linear cathodic voltage-scan voltammetry, has been developed; it provides an alternative approach to cases where anodic stripping methods are difficult to apply and may be a novel tool for the investigation of electrode kinetics.

REFERENCES

1 M. ARIEL AND CH. YARNITZKI, *Israel J. Chem.*, 1 (1963) 305.
2 H. A. LAITINEN AND I. M. KOLTHOFF, *J. Am. Chem. Soc.*, 61 (1939) 3344.
3 M. ARIEL, U. EISNER AND S. GOTTESFELD, *J. Electroanal. Chem.*, 7 (1964) 307.
4 M. ARIEL AND U. EISNER, *J. Electroanal. Chem.*, 5 (1963) 362.
5 H. M. DAVIS AND J. E. SEABORN, *Electron. Eng.*, 25 (1953) 314.
6 A. ŠEVČIK, *Collection. Czech. Chem. Commun.*, 13 (1948) 349.
7 J. E. B. RANDLES, *Trans. Faraday Soc.*, 44 (1948) 322.

THE RETARDATION OF ELECTROCHEMICAL REACTIONS BY ADSORBED ORGANIC MOLECULES; A QUANTITATIVE TREATMENT INVOLVING THE THEORY OF IRREVERSIBLE POLAROGRAPHIC WAVES

S. SATHYANARAYANA
Department of Chemistry, Indian Institute of Technology, Powai, Bombay-76 (India)
(Received March 20th, 1965)

INTRODUCTION

The kinetics of electrochemical reactions are profoundly altered when small quantities of electro-inactive organic surface-active substances are present in solution. The subject is of theoretical as well as practical importance in the fields of electrodeposition, corrosion protection, secondary batteries etc. A number of reviews has appeared on this subject in recent years[1-6] and an exhaustive coverage of literature is therefore unnecessary. However, some recent papers not covered by the above reviews are given[7-10] in the reference list.

The effect of adsorption of electro-inactive organic molecules on the kinetics of electrode processes at a dropping mercury electrode (D.M.E.) may be broadly classified into three divisions[8]: (a) adsorption and mass transfer kinetics; (b) adsorption and charge transfer kinetics; (c) non-equilibrium adsorption on the expanding mercury drop. The present paper is concerned with some aspects of the second effect.

The influence of adsorption of neutral organic molecules on the charge transfer kinetics of electrochemical reactions at a D.M.E. is generally to retard the rate of the reaction (decrease the current at a given potential) in the region of adsorption of the surfactant. The resulting polarographic waves are considerably drawn out on the potential scale and thus rendered "irreversible" to a varying extent. However, the theory of irreversible polarographic waves has not been applied for a quantitative interpretation of such inhibited polarographic waves in terms of kinetic parameters because the surface excess of the adsorbate (and hence the degree of inhibition) varies with the electrode potential.

The dependence of the kinetic parameters on the degree of coverage of the electrode surface by adsorbed organic molecules has been studied by earlier workers using three methods: (a) galvanostatic[8] and voltage-step[9] techniques with small excursions of the electrode potential from its equilibrium value; (b) current–time curves for single drops[10-15]; and (c) faradaic impedance technique[9,14]. The results obtained lend support for a linear dependence of the standard rate constant on the degree of coverage according to the equation

$$K_{s,\theta} = K_{s,0}(1-\theta) + K_{s,1}\theta \qquad (1)$$

where $K_{s,\theta}$, $K_{s,0}$ and $K_{s,1}$ are the standard rate constants corresponding to the degree

of coverage θ, 0 and 1, respectively. There is also an indication that the transfer coefficient may either be independent of θ[8], or decrease slightly with an increase in θ[20].

According to FRUMKIN[6] the mode of inhibition may be expected to change when the degree of coverage changes from a low to a high value, due to lateral interaction among the molecules of the adsorbate. In such a case, we may expect that a simple linear relation between $K_{s,\theta}$ and θ may not be valid over the whole range $0 \leqslant \theta \leqslant 1$. A change in the mechanism of inhibition may also be reflected as a change in the magnitude of the transfer coefficient (α) with an increase in θ.

The mechanism of inhibition itself has been attributed to one or more of the following[1-5]: (a) a "blocking effect"—an *apparent* inhibition of the electrochemical reaction due to a reduction in the true area of the electrode surface, at a given potential, on adsorption; (b) a "sieve effect"—inhibition due to an increase in the activation energy for the reactant ion while approaching the reaction site in the pre-electrode layer either through holes or monomolecular pores[16] in the adsorbed layer; (c) an "electrostatic effect"—inhibition due to a change in the effective potential difference between the metal and the plane of closest approach for the reactant ion in the presence of adsorbed molecules in the double layer; (d) a "(chemical) kinetic effect"—inhibition of a preceding chemical reaction that gave rise to the actual reacting ion near the pre-electrode layer.

The determination of the particular mechanism of inhibition in a given case may be facilitated if the kinetic parameters are obtained over a wide range of θ, using alternative methods.

The present investigation is an attempt to develop a new method for a theoretical analysis of irreversible polarographic waves in the presence of adsorbed neutral molecules without introducing any assumptions regarding the mechanism of inhibition, and to verify from experimental results the relation between the kinetic parameters ($K_{s,\theta}$ and α) and the degree of coverage (θ) by the adsorbate.

THEORY

The equation for a single polarographic wave (*e.g.*, purely cathodic) which may be partially or totally irreversible with currents measured at the end of the drop life is[17-19]

$$\frac{i_t}{i_d} = \frac{\varphi(\chi)}{1 + \sqrt{\frac{D_O}{D_R}} \exp\{nf(E - E_f^0)\}} \tag{2}$$

where i_t is the instantaneous value of the current at the end of the drop life, t the drop time, i_d the limiting diffusion current for a reaction $O + n\,e \leftrightarrows R$ which is of the first-order in both directions and for which the formal standard potential is E_f^0, E the electrode potential corresponding to the current i_t and $f = F/RT$, F being the Faraday. From the tabulated values[33] of $\varphi(\chi)$ χ can be obtained for various values of E. Since

$$\chi = \sqrt{\frac{12\,t}{7\,D_O}}\, K_f \left[1 + \sqrt{\frac{D_O}{D_R}} \exp\{nf(E - E_f^0)\}\right] \tag{3}$$

a plot of log K_f against E is drawn and K_s (the standard rate constant) is obtained as the value of K_f when $E = E_f^0$. The other symbols have the usual meaning.

The kinetic parameters obtained by this procedure correspond to a situation where the potential difference across the diffuse double layer is zero or at least constant (which gives a constant error in K_s). This is approximately true when there is a large excess of a capillary inactive supporting electrolyte (for example, 1 M $NaClO_4$) with the electrode potential close to the point of zero charge of mercury or negative to it. On the other hand, if the solution contains a surface-active substance, the double layer is partly diffuse in the region of adsorption. Moreover, the degree of coverage of the electrode by the adsorbate changes, in general, continuously with the electrode potential. The potential at the reaction site in the double layer is therefore not even approximately constant at different potentials of the electrode and eqn. (2) is inapplicable.

This difficulty can be overcome by the following method. Families of curves for the coverage–potential and current–potential characteristics are obtained under similar conditions of adsorption and inhibition, for various concentrations of the surfactant in solution. At the electrode potentials for a given coverage, the corresponding currents are read from the appropriate polarisation curves. This results in a

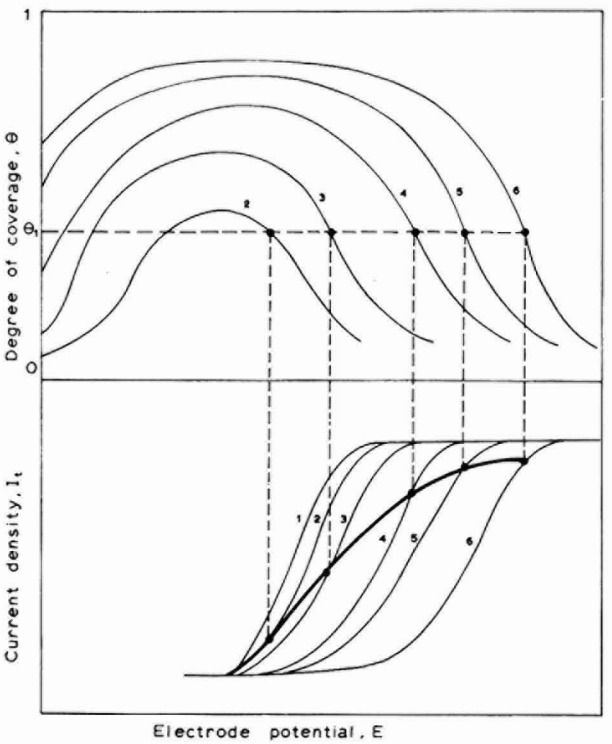

Fig. 1. Schematic illustration of superposition of coverage–potential curves on polarographic waves in order to derive "constant coverage polarographic waves". One such wave for a coverage θ_1 is shown in the lower set of curves (polarographic waves) as a curve with a hard line.

new polarisation curve which would be experimentally observed if the coverage could be artificially held constant when the electrode potential is changed. The procedure is graphically illustrated for clarity in Fig. 1.

In this figure, a polarographic wave corresponding to a coverage θ_1 at all points along the curve is shown as a thick line. By a superposition of coverage and polarographic data for different values of θ, a family of what may be briefly called "constant coverage polarographic waves" is derived.

A constant coverage polarographic wave should satisfy eqn. (2) since the structure of the double layer is essentially constant at different points along the wave. The kinetic parameters may therefore be calculated for a given coverage by the procedure described.

Moreover, the values of both i_t and i_d are obtained from the constant coverage polarographic wave; the ratio $(i_t/i_d)_\theta$ which is the quantity required now for substitution in eqn. (2), becomes therefore independent of any "blocking effect" that may be present since the free surface of the electrode available for the reaction is the same for both values of the current.

A slight decrease in the limiting diffusion current is generally observed with increasing quantities of the surfactant in solution. This decrease is partly or mainly due to a decrease in the drop time and therefore a decrease in the area of the D.M.E. on adsorption. In order to allow for a variation of the electrode area of a D.M.E. with the potential as well as with adsorption, the constant coverage polarographic waves should be constructed using current densities (current/area) and not just currents.

The kinetic parameters obtained from constant coverage polarographic waves, *i.e.*, using $(I_t/I_d)_\theta$ where I_t and I_d are the current densities corresponding to i_t and i_d, respectively, in eqn. (2) are therefore representative of the charge transfer characteristics proper with due corrections applied for mass transfer polarisation, backward reaction rate, "blocking effect", and variation of interfacial adsorption with the electrode potential.

If the potential at the reaction site is known for a given value of θ, the usual double-layer corrections of FRUMKIN may also be applied. The accurate evaluation of this potential in presence of an adsorbed substance is difficult at the present time[4,8,20]. In the present work, kinetic parameters are therefore calculated as a function of θ without applying the double-layer corrections. The potential drop across the diffuse double layer may be expected to be small and not to change rapidly with a change in θ in a 0.5 M Na_2SO_4 solution used as the supporting electrolyte in the present work. The kinetic parameters obtained without the double-layer corrections may therefore be expected to differ from the true values (*i.e.*, with double-layer corrections) by a small, constant value.

EXPERIMENTAL

A D.M.E. has been used in this work for studying both adsorption and inhibition of electrochemical reactions. Complications due to slow adsorption kinetics at the D.M.E. are minimised by choosing *n*-butanol as the surfactant and 9–10 sec for the drop time of the D.M.E. It is well-known[21] that the adsorption–desorption exchange process at the mercury/solution interface is quite fast for the lower aliphatic alcohols. The adsorption of *n*-butanol at the end of the drop life may therefore be

considered as close to its equilibrium value. Since *n*-butanol is only weakly surface active, relatively large concentrations are required in the solution in order to observe any significant inhibition of an electrode reaction. At such large concentrations of butanol in the solution, diffusion of butanol to the D.M.E. may also cease to be a slow step in controlling the adsorption rate.

The retardation of the rate of discharge of Cu^{2+}, Cd^{2+} and Zn^{2+} by adsorbed *n*-butanol was studied by current as well as differential capacity measurements at the D.M.E.

The choice of the reducible species was determined by the fact that while Cd^{2+} discharge takes place not far from the null point of mercury, the discharge of Cu^{2+} and Zn^{2+} takes place at potentials considerably positive and negative, respectively, to the null point. The effect of the double-layer structure may therefore be judged, at least qualitatively, on the three reactions under otherwise identical conditions. Moreover, the discharge of these cations from simple salt solutions on to a D.M.E. is probably uncomplicated by any preceding slow chemical reaction; the interpretation of the results will therefore be simplified.

Instantaneous currents and differential capacities were measured at the end of the drop life using the same D.M.E. with the same drop time and in the same supporting electrolyte containing identical amounts of the surfactant. A complete correspondence was thus achieved between adsorption and reaction-rate measurements, facilitating a quantitative correlation of the two phenomena. The absence of the reducible ions (Cu^{2+}, Cd^{2+} or Zn^{2+}) in the solution used for capacity measurements is assumed to introduce no serious error since the specific adsorption for these ions at the low concentrations used (about 1 mM in each case) may be expected to be too small to affect the double-layer structure in the presence of 0.5 M Na_2SO_4.

Differential capacity measurement

The differential capacities were measured by the bridge method, which is essentially the same as that of GRAHAME[22] in which, as pointed out later by DAMASKIN[23], there is a significant advantage in using the polarising source of e.m.f. not across the cell but across a diagonal of the bridge. The test signal for the bridge was of 400 c/sec frequency and 5-mV amplitude. Necessary shielding and grounding were provided. The bridge was balanced at the end of drop life. The drop time required for the calculation of area of the D.M.E. was registered with a precision of ± 0.01 sec by an electronic-mechanical relay connected across the output of the pre-amplifier of the oscilloscopic null detector. The relay operated as a bi-stable multivibrator triggered by successive pulses from the D.M.E. at the instant of detachment of the drops from the capillary[24]. A precision decade capacity box (Leeds and Northrup Co., Catalogue No. 1091) was used in the variable arm of the bridge. Capacity measurements were precise to 0.5% except near the desorption peaks at positive potentials where it was about 2%. Since the mass rate of flow of mercury through the capillary is known and the drop times determined as above, the area of the mercury drop at the moment of detachment was calculated assuming a spherical shape for the electrode.

Polarographic measurements

The polarising circuit was set up with the smallest resistance possible; the potential of the D.M.E. was thus constant to ± 0.2 mV during a drop life. The relative-

ly long drop times (9–10 sec) used, prevented the occurrence of any polarographic maxima of the second kind. A critically-damped galvanometer with a period of 4 sec and a sensitivity of 1.75×10^{-9} A/mm was used to measure the instantaneous currents at the end of the drop life.

Chemicals

Care was taken to eliminate surface-active impurities. Doubly-distilled water, with the second distillation over alkaline permanganate in an all-glass assembly, was used throughout. The inorganic salts used (sodium sulphate, and sulphates of copper, cadmium and zinc) were recrystallised from A.R. grade salts and ignited in air below the temperatures of decomposition of the corresponding salts. Mercury was purified by prolonged aeration under hot dilute nitric acid and distilled under vacuum. Hydrogen from an all-glass electrolysis unit was used for de-aeration after passing over heated platinum black, alkaline plumbite solution and silica gel, respectively. The de-aeration time was 2 h. The supporting electrolyte used in all the experiments was 0.5 *M* sodium sulphate (relatively capillary inactive) and 0.001 *M* sulphuric acid; the latter is necessary to suppress the hydrolysis of the copper, cadmium or zinc salts in the otherwise neutral solution. Eastman Kodak grade *n*-butanol was distilled in an all-glass unit before use.

Cell

The cell was of all-glass construction with suitable inlets through ungreased ground-glass joints for the D.M.E., reference electrode, and addition of *n*-butanol. The reference electrode for measuring the potential of the D.M.E. was of the mercury–mercurous sulphate type in contact with a solution of 0.5 *M* Na_2SO_4 and 0.001 *M* H_2SO_4. The reference electrode bridge filled with the same solution (thus avoiding liquid junction potentials) was connected to the cell through a closed, ungreased stopcock, which terminated in a Luggin capillary close to the D.M.E. A large platinum cylinder surrounding the D.M.E. was used as the auxiliary electrode. The temperature of the cell was maintained at $25° \pm 0.2°$.

Procedure

The addition of definite quantities of *n*-butanol to the test solution was accomplished so that before and between successive additions of butanol, access of air to the test solution was completely avoided. To a known volume of the de-aerated solution in the cell, butanol was added dropwise through a fine capillary tip. This capillary was fused to a reservoir containing the butanol and attached to the cell by an ungreased ground-glass joint. The dropwise addition of *n*-butanol was effected by compressing the air space above the butanol in the reservoir with a flexible polyethylene cap so that drops were formed and detached slowly from the vertical tip. After the addition of the desired number of drops, hydrogen was bubbled through the solution for one minute to effect mixing. The same schedule of stirring by hydrogen was maintained for both polarographic and capacity measurements. Then measurements of the current or the differential capacity were carried out manually at the end of a drop life at 5–10 mV intervals in the potential range of interest. The electrode potentials were measured accurately to ± 0.5 mV using a Cambridge vernier potentiometer. The capillary characteristics were $m = 1.4$ mg/sec and $t = 9.6$ sec under a 30-cm head

of mercury, at the point of zero charge of mercury in the supporting electrolyte. The cross-section of the capillary bore at the tip was circular and of 90 μ internal diameter.

RESULTS AND DISCUSSION

Adsorption measurements

The differential capacity–potential curves for the supporting electrolyte with such concentrations of *n*-butanol as were found suitable for the study of inhibition are shown in Fig. 2.

The surface charge density on mercury was obtained by a graphical integration of the capacity curves and the coverage was calculated by Frumkin's equation,

$$q_\theta = q_0(1-\theta) + q_1\theta \qquad (4)$$

where q_θ, q_0 are the surface charge densities for the coverages θ, 0 and 1, respectively. The integration constant for the capacity curve with the pure supporting electrolyte was determined from the drop-time curve (measured precisely to ± 0.01 sec during capacity measurements). The value obtained was -0.83 V *vs.* 0.5 *M* sulphate reference electrode which is within 10 mV of GOUY's value[25], and within 5 mV of GRAHAME's value[30]. The potentials of zero charge for solutions containing *n*-butanol could not be directly obtained from electrocapillary (or drop-time) curves since these are too flat in the presence of *n*-butanol to permit an accurate evaluation of maxima on the curves[26]. At first, an integration constant for all the capacity curves with butanol was taken as the common charge density as for the base curve at -2.1 V (*vs.* 0.5 *M* sulphate reference electrode) corresponding to the fusion of all the capacity curves (within about 2%) after desorption. The charge density–potential curves thus obtained did not, however, intersect at a common point (as they should have done according to eqn. (4)) in the adsorption region. This is perhaps because of the use of non-zero-frequency capacities and/or slight errors in capacity measurements. The calculation of θ near this region of intersection, which is also in the important region for studies of inhibition, obviously gives erroneous results using eqn. (4) since all the charge densities, q_θ, q_0 and q_1, are close to one another and minor errors in their determination give too large or too small values of θ.

A better method would be to take for the solution with the highest butanol concentration (least control by slow diffusion of the surfactant) the integration constant as above with the same charge density as for the base solution at -2.1 V (*vs.* reference electrode). The above two charge density–potential curves are found to intersect at a point having co-ordinates -2.6 μCcm^{-2}, -0.93 V. This point is then taken as the integration constant for all other capacity curves. The correctness of this procedure is confirmed by the following facts: (a) by this method, much smoother θ–potential curves are obtained, particularly in the region of maximum adsorption; (b) the coverage, θ, may be directly calculated from the capacity curves in the region of maximum adsorption (away from the capacity peaks) as $\theta = (C_0 - C_\theta)/(C_0 - C_1)$, where C is the differential capacity of the electrode at a given potential and at the coverage shown as the subscript; these values of θ agree well with the θ–E curve obtained above, whereas the agreement is very poor with the θ–E curves obtained by the charge density–potential curves if, for the latter, a common charge density was assumed at -2.1 V (*vs.* reference electrode).

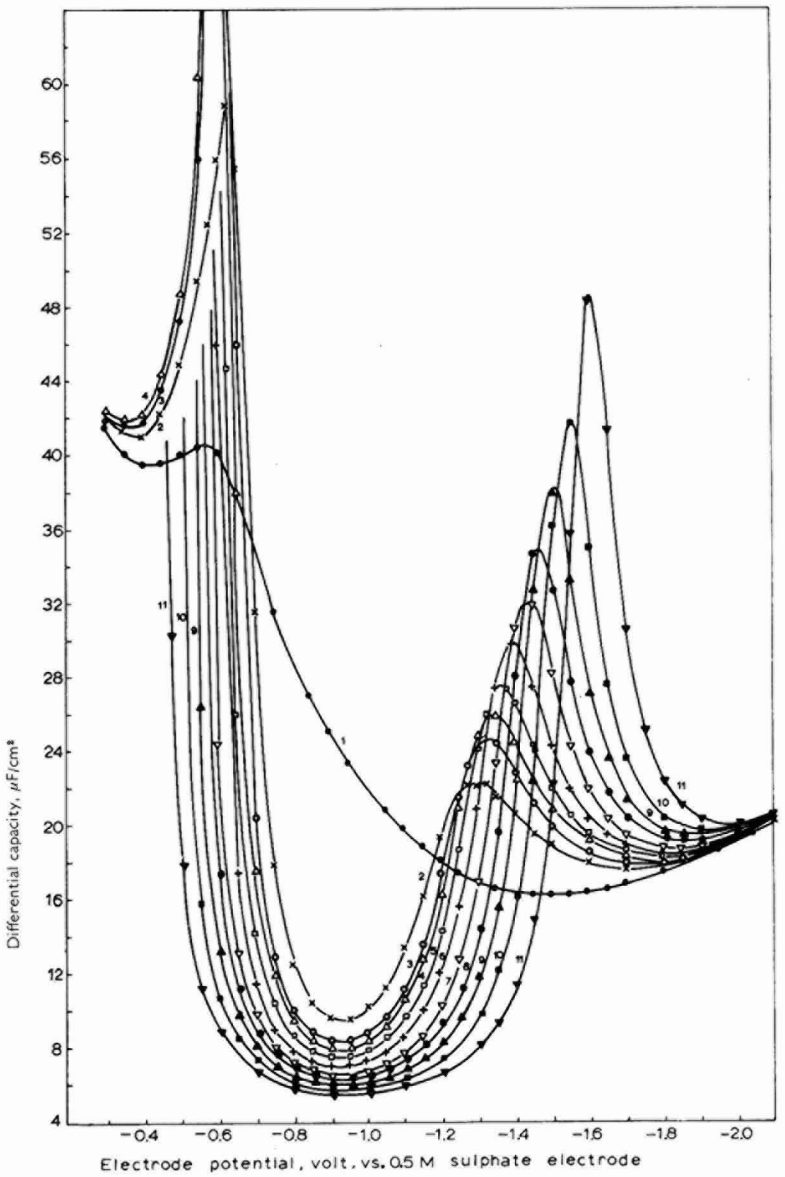

Fig. 2. The dependence of the differential capacity of a D.M.E. on the electrode potential in a solution of 0.5 *M* Na_2SO_4 and with different concns. of *n*-butanol(x) in soln. in m mole/l: (1), 0; (2), 29; (3), 38; (4), 46; (5), 55; (6), 67; (7), 84; (8), 101; (9), 126; (10), 168; (11), 252.

The potentials of zero-charge of mercury in the solution containing various quantities of *n*-butanol are obtained from the charge density–potential curves and shown in Table 1.

TABLE 1

THE DEPENDENCE OF THE POTENTIAL OF ZERO CHARGE E_z (*vs.* 0.5 *M* SULPHATE REFERENCE ELECTRODE) OF MERCURY ON THE CONCENTRATION OF *n*-BUTANOL IN A SOLUTION OF 0.5 *M* Na_2SO_4 AND 0.001 *M* H_2SO_4.

c (*m mole/l*)	E_z (*V*)	*c* (*m mole/l*)	E_z (*V*)
0	−0.830	84	−0.626
29	−0.724	101	−0.611
38	−0.695	126	−0.592
46	−0.685	168	−0.572
55	−0.666	252	−0.550
67	−0.646		

The *relative* accuracy of the θ values (Fig. 3) may be assumed to be of the same order as the mean deviation of experimental points from the smoothed curves and is about 1%. The *absolute* accuracy will not be as good, particularly near the desorption potentials, but this is of no serious consequence in interpreting the dependence of $K_{s,\theta}$ and α on θ.

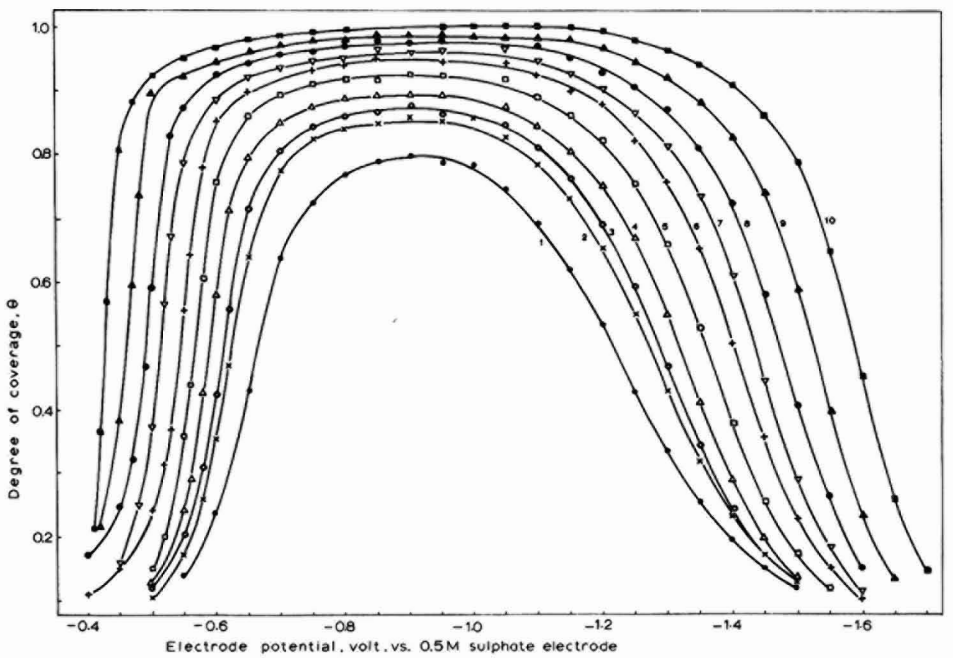

Fig. 3. The dependence of the degree of coverage of the electrode by adsorbed *n*-butanol on the electrode potential and with different concns. of *n*-butanol in soln. in m mole/l: (1), 29; (2), 38; (3), 46; (4), 55; (5), 67; (6), 84; (7), 101; (8), 126; (9), 168; (10), 252.

Polarisation measurements

The polarographic waves for the discharge of Cu^{2+}, Cd^{2+} and Zn^{2+} are shown in Fig. 4–6, for various additions of *n*-butanol. As may be expected, in the region of

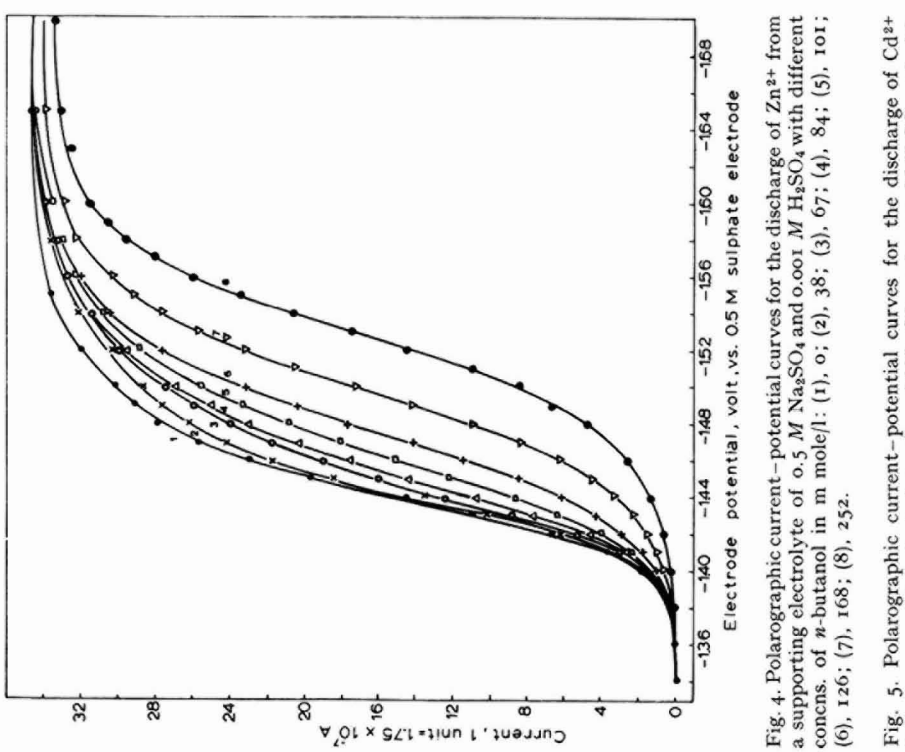

Fig. 4. Polarographic current–potential curves for the discharge of Zn^{2+} from a supporting electrolyte of 0.5 *M* Na_2SO_4 and 0.001 *M* H_2SO_4 with different concns. of *n*-butanol in m mole/l: (1), 0; (2), 38; (3), 67; (4), 84; (5), 101; (6), 126; (7), 168; (8), 252.

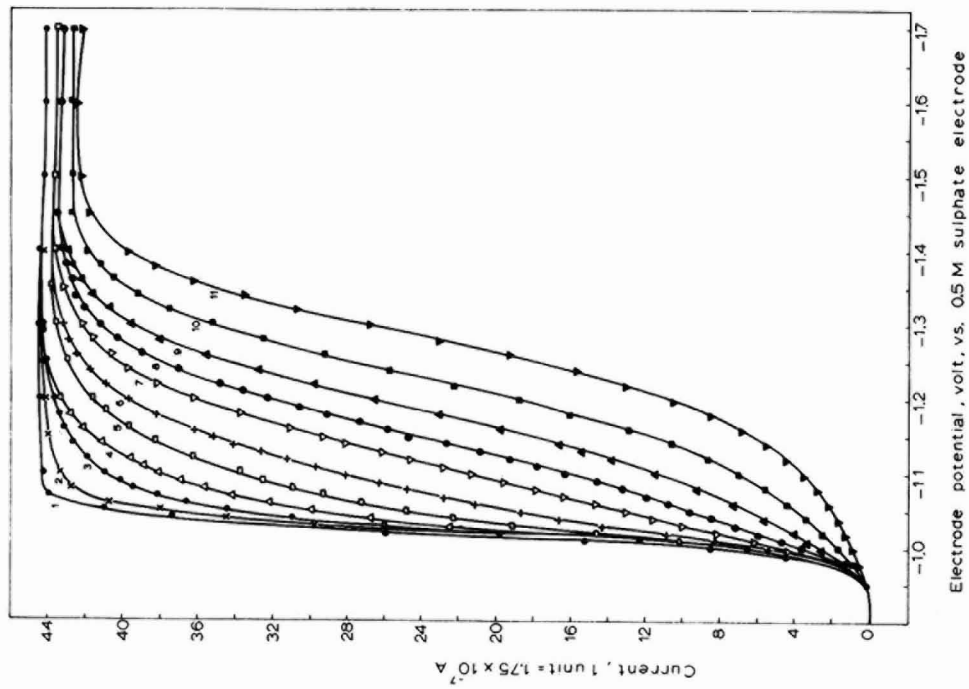

Fig. 5. Polarographic current–potential curves for the discharge of Cd^{2+} from a supporting electrolyte of 0.5 *M* Na_2SO_4 and 0.001 *M* H_2SO_4 and with different concns. of *n*-butanol in m mole/l: (1), 0; (2), 29; (3), 38; (4), 46; (5), 55; (6), 67; (7), 84; (8), 101; (9), 126; (10), 168; (11), 252.

adsorption of *n*-butanol, the waves become progressively irreversible in shape with increasing concentrations of *n*-butanol. The magnitude of the effect is different for the three reactions, being least for Zn^{2+} discharge .This is due to the complex dependence of the current on the overpotential and degree of coverage.

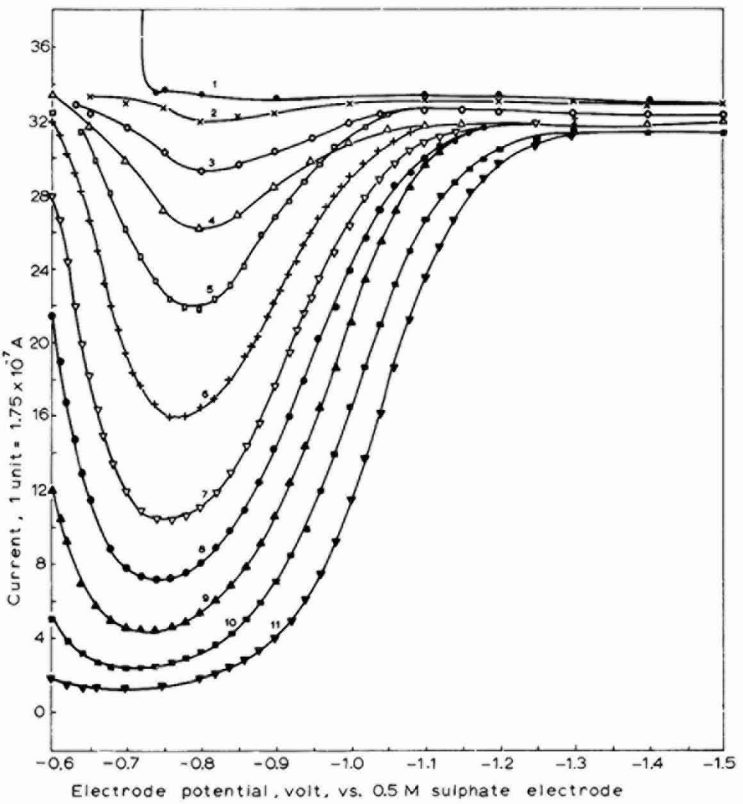

Fig. 6. Polarographic current–potential curves for the discharge of Cu^{2+} from a supporting electrolyte of 0.5 *M* Na_2SO_4 and 0.001 *M* H_2SO_4 with different concns. of *n*-butanol, as in Fig. 5.

Families of "constant polarographic waves" are derived as described earlier by a superposition of the $\theta-E$ curves (Fig. 3) and the polarographic waves (Figs. 4–6). These are shown in Figs. 7–9 for the three reactions. As pointed out above, *current densities* are plotted to get the constant coverage polarographic waves in order to correct for variations in the area of the D.M.E. The area at the end of drop life was calculated for each potential from the drop time ($\pm$0.01 sec) at this potential in the given solution.

By comparing the ordinary polarographic wave without surfactant (*i.e.*, $\theta=0$) with the constant coverage polarographic waves for $\theta>0$ it is seen that for the three reactions the limiting diffusion current density when $\theta>0$ is practically the same as that when $\theta=0$; for larger values of θ however, only this trend is clearly seen since sufficiently negative potentials to observe the limiting values of the current

density are not accessible. We may therefore conclude that there is no 'blocking effect' during the inhibition of these reactions by adsorbed *n*-butanol.

Kinetic parameters

For each value of the current density ,I_t, on a given constant coverage polarographic wave, the ratio $(I_t/I_d)_\theta$ is obtained taking the value of I_d corresponding to

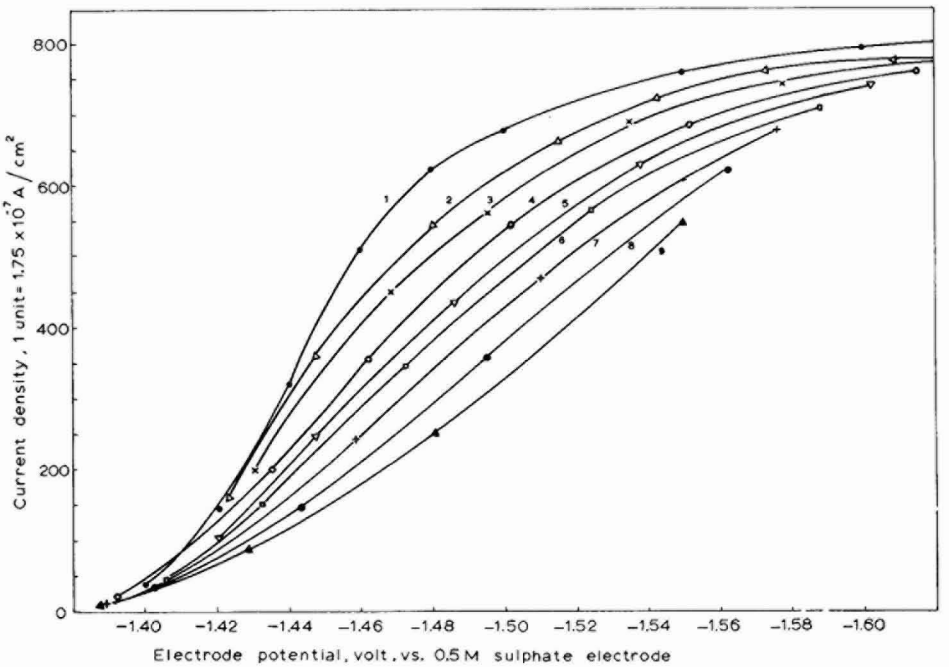

Fig. 7. Constant coverage polarographic waves for the discharge of Zn^{2+} at different degrees of coverage (θ) of the electrode by *n*-butanol: (1), 0; (2), 0.20; (3), 0.30; (4), 0.40; (5), 0.45; (6), 0.50; (7), 0.55; (8), 0.60; (9), 0.65.

$\theta = 0$ since there is no 'blocking effect' and I_d is thus independent of θ. Substituting these values of $(I_t/I_d)_\theta$ in place of (i_t/i_d) in eqn. (2), several plots of log K_f *vs.* $(E - E_f^0)$ corresponding to various values of θ are obtained for the three reactions (Figs. 10–12). The cathodic transfer coefficient is related to the slope of these lines as

$$\frac{\partial \log K_f}{\partial (E - E_f^0)} = -\frac{\alpha nf}{2.303}$$

The value of log $K_{s,\theta}$ is obtained as the value of log K_f when $E = E_f^0$. For the discharge of Zn^{2+} and Cd^{2+} the values of E_f^0 were determined from the polarographic waves without added butanol as[27]

$$\lim_{i \to 0} \left(E - \frac{RT}{nF} \ln \frac{i_d - i}{i} \right) = E_f^0 \qquad (5)$$

For Cu^{2+} discharge, E_f^0 was taken as the half-wave potential of the polarographic wave without added butanol. The values of E_f^0 thus obtained are -1.437, -1.018, and -0.410 (V, *vs.* 0.5 *M* sulphate reference electrode) for the discharge of Zn^{2+}, Cd^{2+} and Cu^{2+}, respectively.

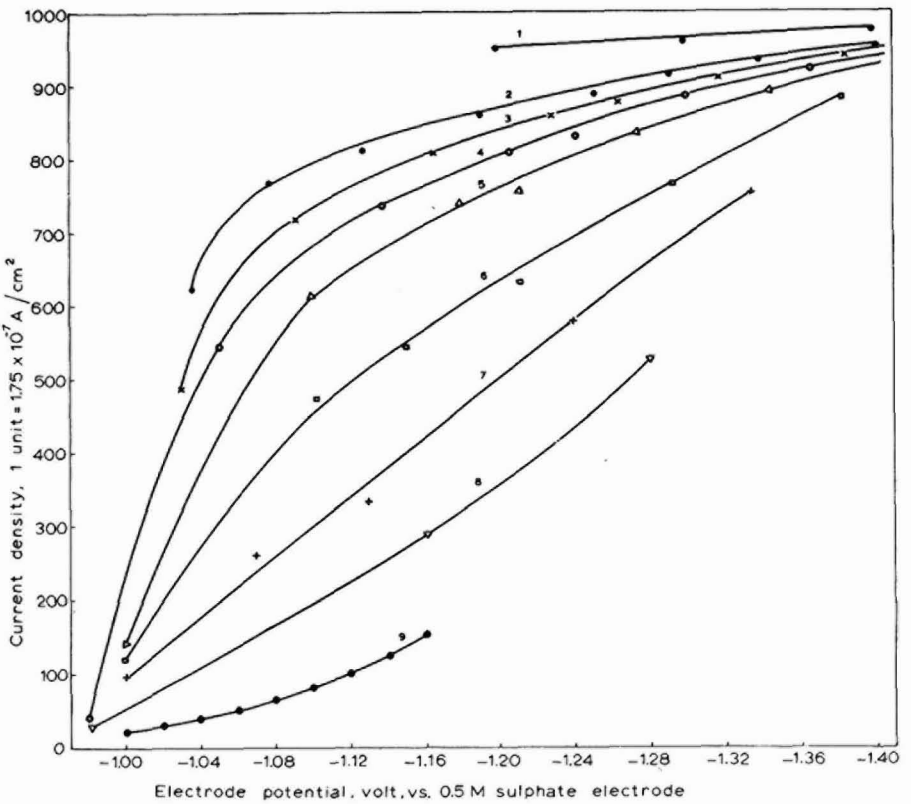

Fig. 8. Constant coverage polarographic waves for the discharge of Cd^{2+} at different degrees of coverage (θ) of the electrode by *n*-butanol: (1), 0; (2), 0.825; (3), 0.85; (4), 0.87; (5), 0.89; (6), 0.925; (7), 0.95; (8), 0.97; (9), ≈ 1.0.

Retardation of Zn^{2+} discharge by adsorbed butanol

It was possible to determine the dependence of K_f for the reaction of discharge of Zn^{2+} on the electrode potential and in a wide range of θ ($0 \leqslant \theta \leqslant 0.65$) (Fig. 10). Since the slopes of the log K_f *vs.* $(E - E_f^0)$ lines are practically identical in this wide interval of coverage, the average value of the slope was used to calculate $K_{s,\theta}$ for θ ranging from 0.70 to 0.89 in which range a few points from constant coverage polarographic waves were still available but not enough to draw a log K_f–E plot. In this way $K_{s,\theta}$ was obtained as a function of θ over the range $0 \leqslant \theta \leqslant 0.89$ (Fig. 13).

It is seen from Fig. 13 that eqn. (1) is valid only for $\theta \leqslant 0.5$. In this range the data correspond to the equation

$$K_{s,\theta} = K_{s,0}\,(1-\theta) \tag{6}$$

since $K_{s,1}$ is practically zero. A better fit with the experimental data in the whole range of θ studied is obtained with the equation,

$$K_{s,\theta} = K_{s,0}\,(1-\theta)^b \qquad (7)$$

where b is a constant. Equation (7) applied to the experimental data has been shown in Fig. 13 as a plot of log $K_{s,\theta}$ against log $(1-\theta)$ with the slope, $b = 1.74$.

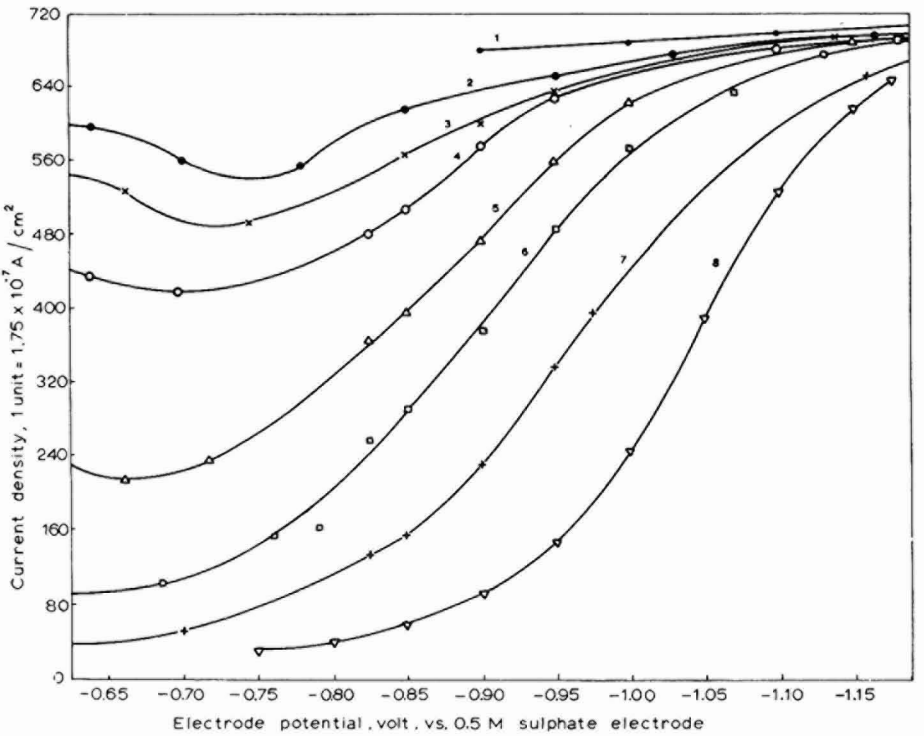

Fig. 9. Constant coverage polarographic waves for the discharge of Cu^{2+} at different degrees of coverage (θ) of the electrode by n-butanol: (1), 0; (2), 0.85; (3), 0.87; (4), 0.89; (5), 0.925; (6), 0.95; (7), 0.97; (8), $\approx$ 1.0.

The mechanism of inhibition expressed by eqns. (6) and (7) cannot be one of a "blocking effect" because this effect has been allowed for using "constant coverage polarographic waves" for the calculation. There is probably no 'kinetic' effect due to the retardation of a preceding slow chemical reaction, since, for the discharge of Zn^{2+} on mercury it is known that the charge transfer reaction is the same as the overall reaction ($Zn^{2+} + 2\,e \rightarrow Zn(Hg)$) and that the stoichiometric number for the rate-determining step of this reaction is unity[28,32]. An "electrostatic effect" may not completely account for eqn. (7) for the following reasons:

(a) The potential of zero charge of mercury in the supporting electrolyte is shifted on adding n-butanol, to more positive values (Table 1). Therefore, the poten-

tial at (or near) the outer Helmholtz plane may be considered as constant in the range of the large negative potentials required for Zn^{2+} discharge.

(b) At these negative potentials, there is no significant specific adsorption of the ions of the supporting electrolyte.

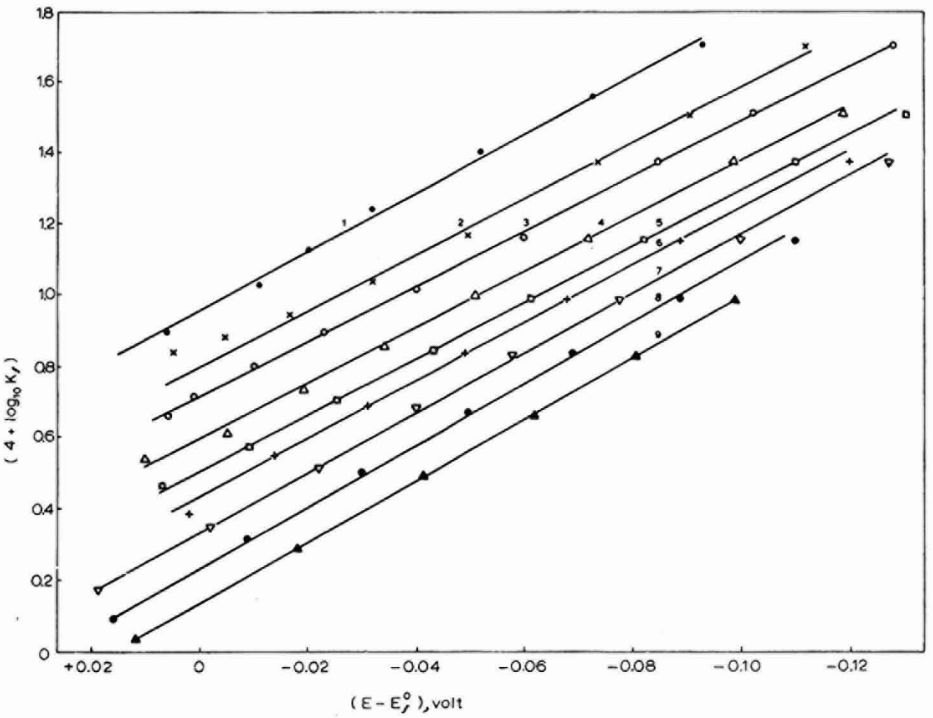

Fig. 10. Rate constant–potential plots for the polarographic reduction of Zn^{2+} at different degrees of coverage (θ) of the electrode by *n*-butanol as in Fig. 7.

The mechanism of retardation of Zn^{2+} discharge by adsorbed *n*-butanol may therefore be attributed to some form of the 'sieve effect'. The standard rate constant may be interpreted[29] as the rate of penetration of the energy barrier at the interface by the reacting ion. This rate is then reduced in presence of adsorbed neutral molecules because of the additional work required to transfer the reacting ions from the solution to the pre-electrode layer[6] crowded partly with the molecules of the surfactant. Such a mechanism may perhaps be termed as the "crowding effect"—a term introduced by GRAHAME[30] in the double-layer theory. A lateral interaction among the adsorbed and oriented dipoles of the surfactant should make the relation between $K_{s,\theta}$ and θ depart from the linearity of eqn. 6. The interaction coefficient, b, in eqn. (7) will be greater than unity if there is a repulsive interaction. Equation (7) with $b = 1.74$, which fits well the experimental results for Zn^{2+} discharge, shows that there is a repulsion among adsorbed *n*-butanol molecules, which at the same time retard the rate of Zn^{2+} discharge.

The measured value of the cathodic transfer coefficient, α, in the range $0 \leqslant \theta \leqslant 0.65$ is remarkably constant, and has the value 0.24 ± 0.01. The rate-determining step for the Zn^{2+} discharge reaction is therefore unchanged by the presence of *n*-butanol in solution, at least up to $\theta = 0.65$.

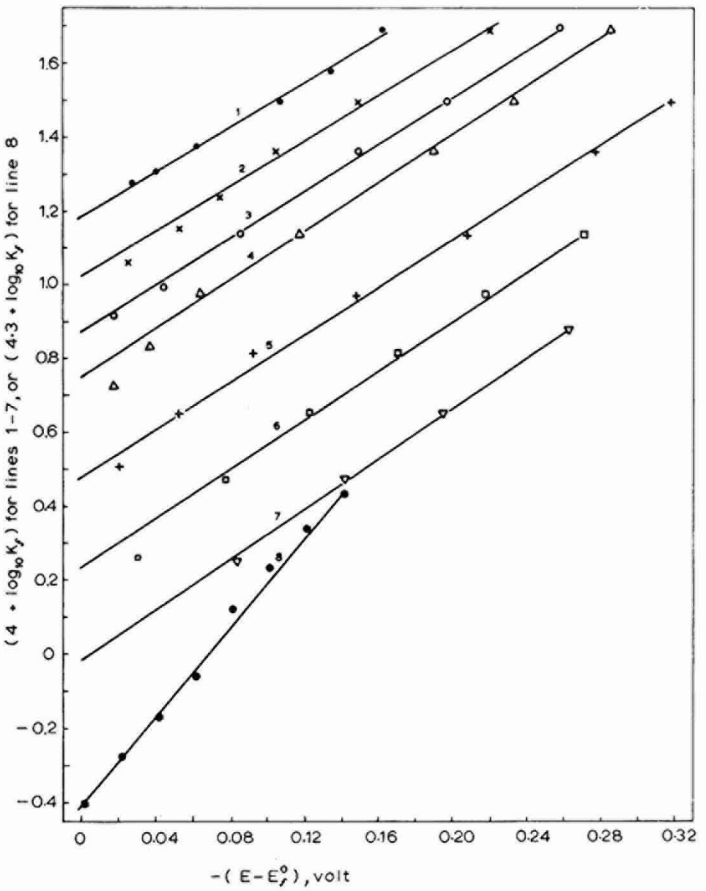

Fig. 11. Rate constant–potential plots for the polarographic reduction of Cd^{2+} at different degrees of coverage (θ) of the electrode by *n*-butanol: (1), 0.825; (2), 0.85; (3), 0.87; (4), 0.89; (5), 0.925; (6), 0.95; (7), 0.97; (8), ≈ 1.

The retardation of the discharge of Cu^{2+} and Cd^{2+} by adsorbed n-butanol

The experimental data for these two reactions did not allow "constant coverage polarographic waves" to be drawn for $\theta < 0.82$. However, the kinetic parameters could be obtained in the range $0.82 < \theta \lesssim 1$ for both reactions and therefore a comparison is possible.

The effect of a specific adsorption of sulphate anions from the supporting electrolyte at large positive potentials in accelerating the reaction of Cu^{2+} discharge is clearly evident from the constant coverage polarographic waves (Fig. 9). Hence, only

the current data at the more negative potentials were used to calculate the log K_f–E plot (Fig. 12) in order to obtain the values for $K_{s,\theta}$ unaffected by SO_4^{2-} adsorption. This difficulty does not arise for Cd^{2+} discharge reaction since the latter takes place at potentials that preclude anion adsorption (Figs. 8 and 11). The plots of $K_{s,\theta}$ *vs.* θ for the two reactions are shown in Fig. 14.

If eqn. (6) were to be correct, the slope of $K_{s,\theta}$ *vs.* θ should be

$$\frac{\partial K_{s,\theta}}{\partial \theta} = -K_{s,0}$$

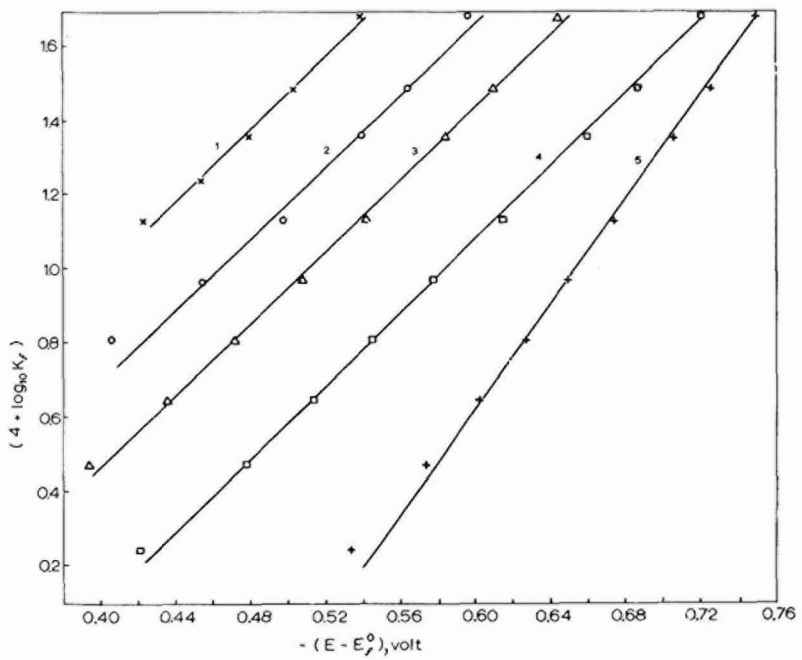

Fig. 12. Rate constant–potential plots for the polarographic reduction of Cu^{2+} at different degrees of coverage (θ) of the electrode by *n*-butanol: (1), 0.89; (2), 0.925; (3), 0.95; (4), 0.97; (5), $\approx$ 1.

Since the standard rate constants, $K_{s,0}$, for both Cd^{2+} and Cu^{2+} discharge on mercury may be expected to be of the same order ($\sim 10^{-2}$ cm/sec)[31] the marked difference in the slopes of the $K_{s,\theta}$ *vs.* θ plots for the two reactions *in the same range of* θ shows a specificity in the degree of retardation of different charge transfer reactions by *n*-butanol.

Assuming the validity of eqn. (7) for these reactions, we may plot log $K_{s,\theta}$ *vs.* log $(1-\theta)$ and extrapolate to get the value of $K_{s,0}$ for the uninhibited 'fast' reactions (Fig. 14). For Cd^{2+} discharge, the result is $K_{s,0} = (4.5 \times 10^{-2} \pm 30\%)$ cm/sec. The value of $K_{s,0}$ obtained by relaxation techniques[34] is about 4.2×10^{-2} cm/sec. Although the good agreement between the two values is perhaps more accidental than real, one may take this at least as an evidence for the correctness of eqn. (7) rather than eqn. (6), or the analogous eqn. (1). For the discharge of Cu^{2+} on mercury from a Na_2SO_4

solution there is no value for $K_{s,0}$ reported in the literature, but from 1 M KNO_3 solution, $K_{s,0}=4.5\times10^{-2}$ cm/sec[31]; an extrapolation of log $K_{s,\theta}$ *vs.* log $(1-\theta)$ for this reaction as in Fig. 14 gives however, $K_{s,0}=(6.5\times10^{-2}\pm50\%)$ cm/sec, which is of the correct order. The interaction coefficients, b, for the discharge of Cd^{2+} and Cu^{2+} are 1.93 and 3.97, respectively, indicating a repulsive interaction in both cases.

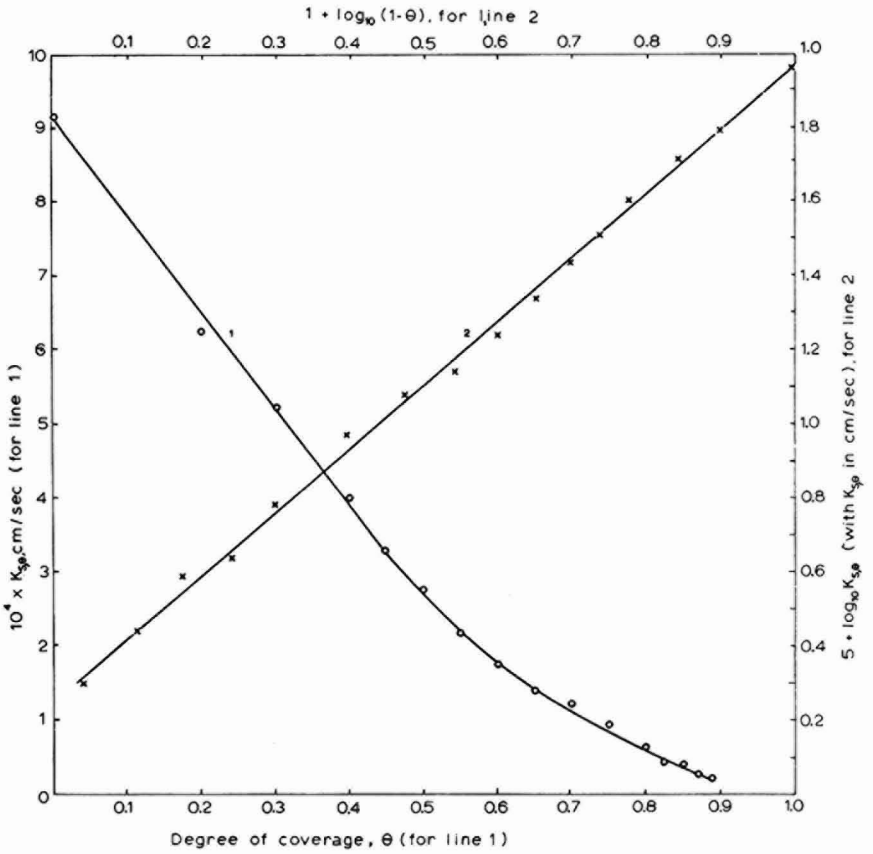

Fig. 13. The dependence of the standard rate constant ($K_{s,\theta}$) for the polarographic reduction of Zn^{2+}, on the degree of coverage θ by *n*-butanol: (1), variation of $K_{s,\theta}$ with θ; (2), variation of log $K_{s,\theta}$ with log $(1-\theta)$.

The value of α for Cd^{2+} discharge is constant in the range $0.83\leqslant\theta\leqslant0.97$ and has the value 0.1, which is less than the value reported in the literature[34] ($\alpha=0.19\pm0.02$) in the absence of any surfactant. For Cu^{2+} discharge, α is again constant, being equal to 0.15 in the range $0.89\leqslant\theta\leqslant0.97$. There is a sudden increase in the value of α, to nearly twice these values, when θ is close to unity for both reactions. This may indicate a new rate-determining step for the electrode reactions when the coverage is nearly that of a monolayer.

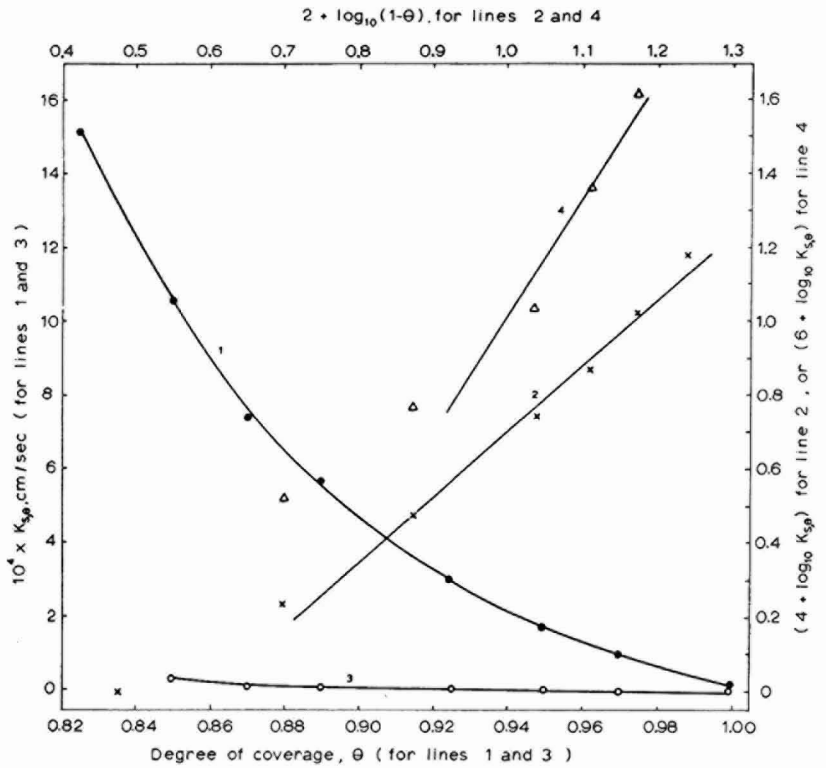

Fig. 14. The dependence of the standard rate constant ($K_{s,\theta}$) for the polarographic reduction of Cd^{2+} (curves 1 and 2) and Cu^{2+} (curves 3 and 4) on the degree of coverage θ by *n*-butanol: (1), variation of $K_{s,\theta}$ with θ, for Cd^{2+} discharge; (2), variation of log $K_{s,\theta}$ with log $(1-\theta)$ for Cd^{2+} discharge; (3), variation of $K_{s,\theta}$ with θ, for Cu^{2+} discharge; (4), variation of log $K_{s,\theta}$ with log $(1-\theta)$, for Cu^{2+} discharge.

CONCLUSIONS

The mechanism of retardation of electrochemical reactions by adsorbed neutral organic molecules such as *n*-butanol seems to be due to a 'crowding effect', the standard rate constant varying with coverage linearly for low coverages and with an allowance for lateral repulsion of adsorbed molecules up to high coverages according to the equation

$$K_{s,\theta} = K_{s,0}\,(1-\theta)^b \qquad (7)$$

where the constant $b(>1)$ takes account of the lateral repulsive interaction of the adsorbate and its specificity to the reactant. The results obtained for Zn^{2+} discharge inhibited by *n*-butanol fit this equation very well in a wide range of θ(0–0.89). The transfer coefficient is, in general, independent of θ over a relatively wide range showing that the mechanism of the electrode reaction is unchanged on adsorption although the rate of the reaction is considerably reduced. However, at limitingly high values of coverage there is a sharp increase in the value of the transfer coefficient (for the dis-

charge Cu^{2+} and Cd^{2+}) indicating a change in the nature of the rate-determining step of the electrode reaction under these conditions.

If eqn. (7) is verified for other cases, fast electrode reactions may, in principle, be studied also by classical d.c. polarography employing a suitable surfactant to retard the reactions sufficiently. The well-established theory of irreversible polarographic waves may then be used to calculate the kinetic parameters from constant coverage polarographic waves, the kinetic parameters (in particular, K_s) for the fast electrode reaction being obtained by extrapolation to $\theta = 0$ using the above equation. The results obtained in this work for the discharge of Cd^{2+} and Cu^{2+} are promising in this regard.

ACKNOWLEDGEMENTS

The author is grateful to T. V. PADMA for valuable assistance in the course of this work and in the numerous calculations, and to Prof. HIRA LAL for his keen interest in the work.

SUMMARY

The inhibition of the cathodic discharge of Cu^{2+}, Cd^{2+} and Zn^{2+} by adsorbed *n*-butanol has been studied by polarographic and differential capacity measurements under similar conditions of adsorption and inhibition. By a superposition of coverage and current data, new "polarographic waves at constant coverage" are derived. The latter are analysed with the theory of irreversible polarographic waves in order to calculate the standard rate constant ($K_{s,\theta}$) and the cathodic energy transfer coefficient as a function of the degree of coverage θ. For the Zn^{2+} discharge reaction, $K_{s,\theta}$ depends on θ linearly only for θ values less than 0.5. For higher values of θ, a lateral interaction term is necessary. The equation $K_{s,\theta} = K_{s,0}(1-\theta)^b$ where b is a constant (>1) is in quantitative agreement with the results for Zn^{2+} discharge inhibited by *n*-butanol over a wide range of coverage ($0 \leqslant \theta \leqslant 0.85$). The lateral interaction term b is also specific for the nature of the reducible ion. For the reactions of Cd^{2+}- and Cu^{2+}-discharge, when the experimental values of $K_{s,\theta}$ are extrapolated to $\theta = 0$ using the above equation, the standard rate constants in the absence of inhibition ($K_{s,0}$) that are obtained are of the correct order. It is concluded that the mechanism of retardation of the electrochemical reactions by adsorbed *n*-butanol may be due to a "crowding effect". The cathodic transfer coefficient is, in general, independent of θ except at limiting high values of the latter, indicating that the nature of the rate-determining step for the electrode reactions is changed only at coverages approaching that of a monolayer.

REFERENCES

1 H. W. NÜRNBERG AND M. VON STACKELBERG, *J. Electroanal. Chem.*, 4 (1962) 26–41.
2 C. N. REILLEY AND W. STUMM, *Progress in Polarography*, Vol. 1, edited by P. ZUMAN, Interscience Publishers, New York, 1962, p. 81.
3 W. H. REINMUTH, *Advances in Analytical Chemistry and Instrumentation*, Vol. 1, edited by CHARLES N. REILLEY, Interscience Publishers, New York, 1960, pp. 275–286.
4 R. PARSONS, *Advances in Electrochemistry and Electrochemical Engineering*, Vol. 1, edited by P. DELAHAY, Interscience Publishers, New York, 1961, pp. 54–58.

5 A. N. FRUMKIN, ibid., pp. 90–100.
6 A. N. FRUMKIN, *Electrochim. Acta*, 9 (1964) 465.
7 E. B. WERONSKII, *Zh. Fiz. Khim.*, 36 (1962) 816.
8 A. ARAMATA AND P. DELAHAY, *J. Phys. Chem.*, 68 (1964) 880.
9 H. A. LAITINEN, K. EDA AND M. NAKANISHI, *Talanta*, 11 (1964) 321.
10 P. SILVESTRONI AND L. RAMPAZZO, *J. Electroanal. Chem.*, 7 (1964) 73.
11 J. KUTA AND I. SMOLER, *Z. Elektrochem.*, 64 (1960) 285.
12 J. KUTA AND I. SMOLER, *Advances in Polarography*, Vol. 1, edited by I. S. LONGMUIR, Pergamon Press, New York, 1960, p. 350.
13 R. W. SCHMID AND C. N. REILLEY, *J. Am. Chem. Soc.*, 80 (1958) 2087.
14 P. DELAHAY AND I. TRACHTENBERG, *J. Am. Chem. Soc.*, 80 (1958) 2094.
15 J. WEBER, J. KOUTECKY AND J. KORYTA, *Advances in Polarography*, Vol. 2, edited by I. S. LONGMUIR, Pergamon Press, New York, 1960, p. 447.
16 L. GIERST, D. BERMANE AND P. CORBUSIER, *Ric. Sci.*, 29 Suppl. Contributi di Polarografia, (1959) p. 75.
17 J. M. HALE AND R. PARSONS, *Collection Czech. Chem. Commun.*, 27 (1962) 2444.
18 S. SATHYANARAYANA, *J. Electroanal. Chem.*, 7 (1964) 403.
19 J. M. HALE AND R. PARSONS, *J. Electroanal. Chem.*, 8 (1964) 247.
20 K. M. JOSHI, W. MEHL AND R. PARSONS, *Transactions of the Symposium on Electrode Processes*, edited by E. YEAGER, John Wiley and Sons, Inc., New York, 1961, p. 249.
21 R. PARSONS, ref. 4, p. 25.
22 D. C. GRAHAME, *J. Am. Chem. Soc.*, 68 (1946) 301.
23 B. B. DAMASKIN, *Zh. Fiz. Khim.*, 32 (1958) 2199.
24 S. SATHYANARAYANA, *Indian J. Chem.*, 2 (1964) 474.
25 J. J. BIKERMAN, *Surface Chemistry*, Academic Press, New York, 1958, pp. 447–448.
26 V. I. MELIK-GAIKAZYAN, *Zh. Fiz. Khim.*, 26 (1952) 1184.
27 R. TAMAMUSHI AND N. TANAKA, *Z. Physik. Chem.* Neue Folge, 39 (1963) 117.
28 J. HORUITI AND A. MATSUDA, *J. Res. Inst. Catalysis Hokkaido Univ.*, 7 (1959) 19.
29 P. DELAHAY, ref. 4, p. 236.
30 D. C. GRAHAME, *Chem. Rev.*, 41 (1947) 441.
31 N. TANAKA AND R. TAMAMUSHI, *Electrochim. Acta*, 9 (1964) 963.
32 K. J. VETTER, *Elektrochemische Kinetik*, Springer-Verlag, Berlin, 1961, pp. 528–530.
33 P. DELAHAY, *New Instrumental methods in Electrochemistry*, Interscience Publishers Inc., New York, 1954, p. 79.
34 J. E. B. RANDLES, ref. 2, p. 123.

THEORETICAL ELECTROMOTIVE FORCES FOR CELLS CONTAINING A SINGLE SOLID OR MOLTEN OXIDE

WALTER J. HAMER
Institute of Basic Standards, National Bureau of Standards, Washington, D. C. (U.S.A.)
(Received May 3rd, 1965)

Standard oxidation–reduction potentials are available for numerous electrochemical reactions in aqueous systems at 25°[1]. These potentials refer to potentials when all solid, liquid or dissolved substances taking part in the oxidation–reduction processes are at unit activity and all gases are at a fugacity of one atmosphere. When the potentials of the elements alone are arranged in series in decreasing or increasing order of magnitude, relative to the conventional hydrogen electrode as reference, the series is commonly known as "the electromotive force (or electrochemical) series of the elements." E.m.f.-temperature coefficients for the various oxidation–reduction reactions are also available[2,3].

In an earlier paper[4] an electromotive force (e.m.f.) series for solid and molten (or fused) chlorides was presented for temperatures ranging from 25°–1500°. This series, the first published for molten salts, differed fundamentally from the aqueous series, in that the series was for a complete cell, rather than a half cell, and was based on the Gibbs energy (free energy) of formation of the electrolytic phase. These values corresponded to the ideal decomposition voltages of molten salts, assuming the decomposition voltages as determined experimentally, contain no ohmic voltages and are free of effects of polarization and other factors that would lead to deviations of the electrolyte and the electrodes from their standard states.

The theoretical decomposition voltages of molten electrolytes correspond to the reversible e.m.f. of galvanic cells composed of the electrolyte and two electrodes, one of which is reversible to the anion and the other to the cation of the molten electrolyte, the electrolyte and the electrodes being in their standard states. This reversible e.m.f. is also related to the Gibbs energy of formation of the electrolyte through the relation, $E^\circ = -\Delta G_f^\circ/nF$, where ΔG_f° is the standard Gibbs energy, F the faraday, and n the number of faradays involved in the electrochemical reaction. Although experimentally-measured decomposition voltages do not usually agree with the theoretical values owing to several factors (including the chemical interaction of the electrodes with the electrolyte, the production of electrodes in a non-standard state, deviations from isothermal conditions, ohmic voltages, and electrode polarization), it is nevertheless of importance to know the theoretical values in order to elucidate mechanisms and interpret experimental data on galvanic cells containing molten electrolytes.

In this paper a theoretical e.m.f. series for solid and molten oxides is presented for a temperature range from 25°–3000°. In preparing this series it became obvious that a great many oxides melt with decomposition and, as a result, the series for the

molten range is not as satisfactory as is the series for molten chlorides. The e.m.f. of each oxide in the series corresponds to the e.m.f. of a cell of the type:

$$\text{metal} \mid \text{metallic oxide} \mid \text{oxygen gas}^* \tag{A}$$

and is related to the Gibbs energy change for the chemical reaction:

$$\text{metal} + \text{oxygen gas} = \text{metallic oxide}^{**}. \tag{B}$$

According to convention this energy change is the Gibbs energy of formation, ΔG_f°, of the oxide when the metal, oxide, and gas are in their standard states, and is related to the heat of formation, ΔH_f°, by the relation: $\Delta G_f^\circ = \Delta H_f^\circ - T\Delta S^\circ$, where ΔS° is the difference in the entropy of the products and the reactants of the reaction. Tables of thermodynamic data for ΔG_f° and ΔH_f° are available for 25°.

To obtain ΔG_f° at temperatures above 25° use is made of the equation

$$\frac{\mathrm{d}\left(\frac{\Delta G_f^\circ}{T}\right)}{\mathrm{d}T} = -\frac{\Delta H_f^\circ}{T^2} \tag{1}$$

However, ΔH_f° is a function of temperature and depends on the difference between the heat capacities of the products and reactants, as expressed by

$$\Delta H_f^\circ = \Delta H_o^\circ + \int_0^T \Delta C_p \mathrm{d}T \tag{2}$$

where ΔH_o°, the integration constant, is evaluated from the heat of formation at 25° (298.15°K) as shown below, and ΔC_p represents the sum of the heat capacities of the products of a reaction less the sum of the heat capacities of the reactants and is usually expressed as a function of temperature by an equation of the empirical form:

$$\Delta C_p = a + (\Delta b)T + \Delta c/T^2 \tag{3}$$

where a, b, and c are known numerical values. Substitution of eqn. (3) in eqn. (2) and integration gives

$$\Delta H_o^\circ = \Delta H_f^\circ - (\Delta a)T - (\Delta b)T^2/2 + \Delta c/T \tag{4}$$

Substitution then of eqn. (4) in eqn. (1) and integration gives

$$\Delta G_f^\circ = \Delta H_o^\circ - (\Delta a)T \ln T - (\Delta b)T^2/2 - \Delta c/2T + IT \tag{5}$$

which gives ΔG_f° as a function of temperature. If ΔG_f° and ΔH_f° (or ΔH_o°) are known at some temperature, usually 298.15°K, the integration constant I can be evaluated. Equation (5) is then valid for the calculation of values of ΔG_f° from 25° up to temperatures for the first change in state for the oxide or metal, *i.e.*, for the first transition, fusion, or vaporization of the products (metallic oxides) or reactants (metal and oxygen). At this point, the heat change for the transition, fusion, or vaporization must be added for products, subtracted for reactants, to the ΔH_f° at the temperature in question. Then, from this revised ΔH_f° and the new ΔC_p values resulting from the change in state, a new ΔH_o° and a new integration constant, I', must be calculated. This procedure is followed for each change in state of the products and reactants.

* It is assumed that oxygen gas is adsorbed on an inert electronic conductor.

** Each oxide taken as the simplest stoichiometric formula with oxygen arbitrarily assigned *a* valence of −2.

TABLE 1 *(pp. 142–148)*

STANDARD ELECTROMOTIVE FORCES FOR SINGLE SOLID OR MOLTEN OXIDES*

					E°					
Order 25°	*Metal ion*	*25° (aqueous)***	*25° (solid)*	*Uncertainty (25°)*	*100°*	*200°*	*300°*	*350°*	*400°*	*450°*	*500°*
1	Zr^{2+}	–	5.287G	±0.053	5.298	5.199	5.100	5.051	5.002	4.953	4.904
2	Ca^{2+}	3.418h	3.131	±0.002	3.090	3.037	2.984	2.957	2.931	2.905	2.881
3	La^{3+}	3.298h	3.085L	±0.13	3.027	2.979	2.933	2.909	2.886	2.863	2.840
4	Ac^{3+}	3.091i	3.079G	±0.031	3.048	3.005	2.964	2.943	2.922	2.902	2.882
5	Pr^{3+}	3.247h	3.058L	±0.06	3.022	2.975	2.930	2.906	2.884	2.861	2.838
6	Nd^{3+}	3.242h	3.040L	±0.06	3.009	2.964	2.921	2.899	2.878	2.858	2.836
7	Th^{4+}	2.880h	3.018L	±0.001	2.982	2.933	2.883	2.858	2.833	2.808	2.784
8	Be^{2+}	3.021i	3.014	±0.065	2.975	2.922	2.869	2.842	2.815	2.789	2.764
9	Th^{2+}	–	3.003G	±0.030	2.970	2.924	2.878	2.855	2.832	2.809	2.786
10	Ce^{3+}	3.275h	2.999G	±0.030	2.963	2.915	2.868	2.844	2.820	2.796	2.772
11	Ba^{1+}	–	2.970G	±0.030	2.931	2.865	2.802	2.771	2.731	2.700	2.669
12	Sm^{3+}	3.233h	2.963G	±0.030	2.928	2.881	2.833	2.809	2.785	2.762	2.738
13	Mg^{2+}	3.091h	2.952	±0.001	2.910	2.854	2.798	2.770	2.742	2.714	2.686
14	Li^{1+}	3.363h	2.903	±0.002	2.857	2.533	2.406	2.341	2.277	2.212	2.147
15	Am^{3+}	3.107h	2.902G	±0.029	2.868	2.824	2.779	2.757	2.735	2.714	2.692
16	Sr^{2+}	3.276h	2.901	±0.002	2.861	2.809	2.758	2.733	2.708	2.683	2.659
17	Y^{3+}	3.120h	2.894G	±0.029	2.859	2.813	2.767	2.744	2.721	2.699	2.677
18	Sc^{3+}	3.013h	2.826G	±0.028	2.792	2.744	2.697	2.673	2.650	2.626	2.602
19	Hf^{4+}	2.901oh	2.797L	±0.067	2.757	2.705	2.654	2.628	2.603	2.577	2.552
20	U^{4+}	2.582h	2.786	±0.12	2.793	2.704	2.659	2.636	2.613	2.591	2.568
21	Ba^{2+}	3.209h	2.738	±0.002	2.701	2.651	2.603	2.579	2.555	2.532	2.508
22	Al^{3+}	2.701h	2.723	±0.009	2.683	2.629	2.575	2.549	2.522	2.494	2.468
23	U^{3+}	–	2.667G	±0.027	2.632	2.588	2.544	2.522	2.500	2.478	2.456
24	Pu^{3+}	2.821h	2.666G	±0.027	2.633	2.590	2.548	2.527	2.507	2.486	2.466
25	Ra^{2+}	2.548o	2.548L	±0.12	2.507	2.458	2.409	2.385	2.361	2.338	2.314
26	Ti^{2+}	2.537o	2.537G	±0.025	2.497	2.447	2.397	2.372	2.347	2.323	2.299
27	Pu^{4+}	2.457h	2.537G	±0.025	2.500	2.457	2.413	2.392	2.371	2.349	2.328
28	Pa^{4+}	–	2.526G	±0.025	2.487	2.439	2.391	2.367	2.343	2.319	2.295
29	Np^{4+}	2.529h	2.526G	±0.025	2.494	2.448	2.404	2.381	2.359	2.338	2.316
30	Am^{4+}	2.533h	2.504L	±0.038	2.468	2.424	2.379	2.357	2.334	2.312	2.291
31	Ti^{3+}	2.501o	2.501	±0.026	2.463	2.413	2.366	2.342	2.318	2.295	2.272
32	Pu^{2+}	–	2.385G	±0.024	2.355	2.320	2.285	2.268	2.252	2.236	2.219
33	Pr^{4+}	2.385o	2.385L	±0.038	2.347	2.299	2.250	2.225	2.202	u	
34	Ce^{4+}	2.374o	2.374	±0.3	2.341	2.298	2.256	2.234	2.213	2.192	2.171
35	Ti^{4+}	2.091ho	2.219	±0.084	2.177	2.132	2.087	2.065	2.043	2.021	2.000
36	Si^{2+}	–	2.125G	±0.021	2.089	2.039	1.991	1.966	1.941	1.916	1.891
37	Si^{4+}	2.101i	2.083	±0.056	2.045	1.999	1.954	1.931	1.908	1.886	1.863
38	Np^{5+}	2.025oh	2.077G	±0.021	2.041	1.996	1.952	1.930	1.908	1.886	1.864
39	U^{6+}	2.045o	2.045	±0.07	2.011	1.967	1.921	1.899	1.877	1.855	1.832
40	B^{3+}	2.045o	2.045	±0.003	2.011	1.965	1.920	1.897	1.875	1.852	1.839
41	Ta^{5+}	2.041o	2.041	±0.06	2.005	1.957	1.909	1.886	1.862	1.838	1.815
42	Pa^{5+}	–	2.025G	±0.020	1.988	1.940	1.891	1.867	1.843	1.819	1.795
43	V^{2+}	–	2.016G	±0.033	1.992	1.944	1.898	1.875	1.852	1.830	1.807
44	Nb^{2+}	–	1.973G	±0.02	1.936	1.893	1.850	1.829	1.808	1.787	1.766
45	Nb^{4+}	–	1.964L	±0.05	1.932	1.886	1.840	1.817	1.796	1.773	1.750
46	V^{3+}	1.959o	1.959	±0.045	1.925	1.881	1.837	1.815	1.795	1.773	1.753
47	Na^{1+}	2.678h	1.951	±0.002	1.904	1.830	1.757	1.721	1.686	1.651	1.616
48	Mn^{2+}	1.951h	1.882	±0.002	1.854	1.816	1.779	1.760	1.742	1.723	1.705
49	Nb^{5+}	–	1.873L	±0.036	1.838	1.791	1.746	1.722	1.700	1.677	1.655
50	Cr^{3+}	1.883h	1.806	±0.005	1.669	1.598	1.527	1.491	1.455	1.419	1.383

550°	600°	800°	1000°	1500°	1750°	2000°	2250°	2500°	2750°	3000°
4.856	4.807	4.614	4.381	3.947	3.715	3.489	3.254	nd		
2.855	2.830	2.728	2.626	2.354	2.114	1.882	1.657	1.439	1.227 |	nd
2.817	2.794	2.703	2 550	2.317	2.204	2.091	1.982	nd		
2.862	2.843	2.766	2.687	2.503	2.422 |	2.350	nd			
2.815	2.793	2.702	2.608	2.370	2.254 |	2.139	2.027	1.917	1.808	1.701
2.816	2.796	2.717	2.642	2.334	2.214	2.095	1.979 |	1.970	u	
2.759	2.734	2.636	2.539	2.296	2.173	2.049	1.925	1.799	1.672	1.542
2.737	2.712	2.607	2.505	2.309	2.130	1.828	1.670 |	nd		
2.764	2.741	2.649	2.557	2.325	2.207 |	2.100	2.002	1.905	1.810	1.742 (2977V)
2.748	2.724	2.627	2.526	2.280 |	2.165	2.066	1.969	1.873	1.778	1.685
2.638	2.608 |	2.518 (767V)								
2.714	2.691	2.596	2.507	2.260	2.135	2.021	1.917 |	1.813	1.709	1.607
2.659	2.631	2.508	2.366	1.905	1.636	1.370	1.107	0.847	0.588 |	0.332
2.081	2.016	1.752	1.489	1.689 |	1.291	0.933	0.578	0.470 (2327V)		
2.670	2.648	2.563	2.477	2.262	2.161 |	2.069	nd			
2.634	2.610	2.513	2.409	2.105	1.871	1.642	1.416 |	nd		
2.654	2.632	2.545	2.459	2.250	2.141	2.036	1.934	nd		
2.579	2.555	2.461	2.367	2.127	2.002	1.878	1.755 |			
2.528	2.502	2.405	2.308	2.074	1.960	1.848	1.739	1.631	1.525 |	nd, u
2.546	2.523	2.434	2.342	2.110	1.995	1.881	u			
2.485	2.461	2.361	2.224	2.021	1.860 |	1.673	1.497	1.323	1.167 (2727V)	
2.441	2.414	2.301	2.188	1.909	1.772	1.637 |	nd			
2.434	2.411	2.313	2.213	1.963	1.831	1.699	1.568	nd		
2.446	2.426	2.336	2.253	2.061 |	1.986	1.917	1.850	1.785	1.722	1.663 (2977V)
2.291	2.267	2.173	2.077	1.788	1.559	1.335	1.112	0.893	u	
2.274	2.250	2.155	2.062	1.838	1.731 (1737D)	nd				
2.308	2.287	2.200	2.114	1.906	1.805	1.707 |	1.620	1.543	1.466	1.390
2.272	2.248	2.152	2.056	1.815	1.693	1.570	1.447 |	nd		
2.294	2.273	2.115	2.018	1.750	1.623	1.498	1.375 |	1.337	nd	
2.268	2.247	2.162	2.076	1.863	1.762	1.663	u			
2.249	2.226	2.136	2.046	1.828	1.725	1.614 |	1.509	1.418	1.329	1.241
2.203	2.187	2.115	2.043 |	1.931	1.878	1.826	1.815 (2052V)			
2.150	2.129	2.043	1.954	1.734	1.626	1.519	nd			
1.978	1.955	1.869	1.776	1.557	1.449 |	1.340	1.247	1.155	1.064	1.001 (2927D)
1.866	1.841	1.740	1.638	1.368	1.203	1.039	0.875 |	nd		
1.841	1.822	1.734	1.647	1.412 |	1.288	1.166 (1977D)				
1.842	1.820	1.809 (627D)								
1.810	1.789	1.766 (652D)	u							
1.820	1.801	1.727	1.655	1.476	1.387	1.297	1.207 (2247V)	u		
1.792	1.768	1.674	1.583	1.356	1.246 |	1.142	nd			
1.771	1.747	1.650	1.554	1.314	1.191 |	1.081	nd			
1.785	1.763	1.675	1.590	1.382	1.283	1.174 |	1.097	1.025	0.954	0.883
1.746	1.725	1.646	1.569	1.390	1.307	1.228	1.153 |	nd, u		
1.729	1.707	1.621	1.536	1.329	1.229	1.129 |	1.047	0.971	0.896	0.824
1.732	1.712	1.632	1.553	1.366	1.271 |	1.184	1.110	1.037	0.965	0.895
1.582	1.549	1.422 |	1.256	0.743 (1275S)						
1.686	1.668	1.591	1.515	1.305	1.190 |	1.103	nd, u			
1.632	1.610	1.522	1.439 |	1.245	1.169	1.096	1.023	0.950	0.878	0.827 (2927V)
1.346	1.310	1.165	1.019	0.651	0.465 |	u				

TABLE 1 *(continued)*

Order 25°	Metal ion	25° (aqueous)**	25° (solid)	Uncertainty (25°)	E° 100°	200°	300°	350°	400°	450°	500°
51	V^{4+}	–	1.724	±0.011	1.690	1.646	1.604	1.583	1.562	1.541	1.521
52	Ga^{3+}	1.647h	1.714L	±0.008	1.673	1.613	1.553	1.523	1.493	1.462	1.433
53	K^{1+}	2.651h	1.652L	±0.018	1.577	1.496	1.415	1.376	1.335	1.296	1.255
54	Zn^{2+}	1.646h	1.649	±0.001	1.610	1.558	1.507	1.482	1.456	1.431	1.403
55	Ga^{1+}	1 630o	1.630L	±0.009	1.582	1.518	1.453	1.420	1.389	1.357	1.325
56	Ca^{2+}	1.550o	1.550L	±0.013	1.516	1.473	1.440 (275D)				
57	Mn^{2+}	1.387h	1.534L	±0.010	1.500	1.456	1.412	1.390	1.368	1.346	1.324
58	Rb^{1+}	2.548h	1.507L	±0.006	1.455	1.381	1.306	1.270	1.232	1.194	1.157
59	Sr^{2+}	1.507h	1.507L	±0.007	1.469	1.418	1.410 (215D)				
60	Mg^{2+}	1.497o	1.497G	±0.015	1.511 (88D)						
61	V^{2+}	1.492o	1.492	±0.012	1.457	1.412	1.368	1.346	1.323	1.302	1.280
62	Ba^{2+}	1.472o	1.472L	±0.010	1.435	1.387	1.337	1.319	1.288	1.264	1.243
63	Li^{2+}	1.463o	1.463L	±0.004	1.453	1.380 (197D)					
64	In^{3+}	1.401h	1.449L	±0.002	1.411	1.358	1.304	1.277	1.250	1.223	1.196
65	Ge^{2+}	1.431o	1.431L	±0.25	1.389	1.331	1.276	1.249	1.221	1.194	1.166
66	Cs^{1+}	2.452h	1.422L	±0.04	1.350	1.250	1.150	1.101	1.051	1.001	0.953
67	P^{5+}	1.887i	1.420G	±0.014	1.384	1.333	u				
68	Cr^{4+}	–	1.388G	±0.014	1.356	1.310	1.265	1.242	1.220	1.208 (427D)	
69	Ge^{4+}	1.401i	1.377L	±0.13	1.334	1.278	1.222	1.195	1.167	1.139	1.111
70	W^{4+}	–	1.349L	±0.007	1.315	1.271	1.228	1.206	1.185	1.164	1.144
71	Sn^{4+}	1.237h	1.346	±0.003	1.307	1.254	1.200	1.173	1.145	1.118	1.090
72	Sn^{2+}	1.321h	1.333	±0.003	1.303	1.258	1.168	1.135	u		
73	W^{6+}	1.451i	1.321	±0.001	1.286	1.242	1.199	1.178	1.157	1.136	1.115
74	Fe^{3+}	1.170h	1.280	±0.001	1.245	1.199	1.154	1.132	1.110	1.088	1.066
75	Mo^{4+}	1.272o	1.272L	±0.008	1.235	1.191	1.148	1.127	1.106	1.084	1.064
76	Fe^{2+}	1.277h	1.266	±0.002	1.237	1.200	1.165	1.147	1.129	1.112	1.095
77	In^{2+}	–	1.258G	±0.013	1.220	1.167	1.113	1.086	1.059	1.032	1.005
78	H^{1+}	1.229h	1.229	±0.0002	1.169 (100V)						
79	Mn^{4+}	1.201o	1.208	±0.001	1.172	1.124	1.077	1.053	1.030	1.006	0.983
80	Cd^{2+}	1.209h	1.166	±0.030	1.127	1.078	1.028	1.004	0.976	0.949	0.922
81	Ni^{2+}	1.119h	1.121	±0.007	1.084	1.037	0.990	0.967	0.943	0.920	0.897
82	Na^{2+}	1.114o	1.114L	±0.047	1.075	1.018	0.962	0.933	0.905	0.876	0.849
83	Co^{2+}	1.134h	1.106	±0.002	1.069	1.024	0.980	0.957	0.935	0.912	0.898
84	K^{2+}	1.085o	1.085L	±0.026	1.043	0.984	0.927	0.897	0.869	0.840	0.813
85	Sb^{3+}	1.061i	1.077	±0.009	1.041	0.995	0.949	0.938	0.903	0.880	0.858
86	Te^{4+}	–	1.062G	±0.011	1.027	0.977	0.928	0.904	0.879	0.854	0.825
87	Sb^{4+}	–	1.019	±0.001	0.982	0.934	0.887	0.863	0.840	0.816	0.793
88	As^{3+}	1.081i	0.995	±0.005	0.959	0.913	0.871	0.857	0.841	0.826	0.824 (457V)
89	Tc^{4+}	–	0.985G	±0.010	0.948	0.901	0.854	0.830	0.807	0.783	0.760
90	Pb^{3+} red	0.952h	0.981	±0.001	0.944	0.893	0.844	0.820	0.794	0.768	0.742

550°	600°	800°	1000°	1500°	1750°	2000°	2250°	2500°	2750°	3000°
1.499	1.479	1.400	1.321	1.131 |	1.053	0.978	0.907	0.837	0.770	0.703
1.403	1.374	1.257	1.145	0.881 |	0.709	0.599	0.489	0.380	0.324 (2627V)	
1.215	1.176	1.071	0.805	0.347	0.131	−0.051	nd, u			
1.376	1.348	1.239	u							
1.294	1.262 |	1.201 (727V)								
1.302	1.281	1.197	1.111	0.892 (1347D)						
1.119	1.082 |	u								
1.259	1.238 |	1.164	1.054	0.931	0.852	0.773	0.757 (2052V)	u		
1.223	1.203	1.119	1.104 (837D)							
1.169	1.142	1.035	0.926	0.660 |	0.530	0.419	nd			
1.140	1.112	1.052 (710S)								
0.909	0.866	0.830 (642V)								
1.083	1.056	0.947	0.836 |	0.574	0.449	0.326	0.206	0.157	u	
1.122	1.102	1.022	0.946 |	0.781	0.715	0.689 (1852D)				
1.063	1.036	0.930	0.824	0.566 |	0.439	0.330	0.227	0.064	−0.097	−0.210 (2927V)
1.094	1.073	0.991	0.911 |	0.724	0.651	0.629 (1827V)				
1.045	1.024	0.939	0.855	0.645	nd, u					
1.043	1.021	0.939	0.859	0.662	0.568 |	0.497 (1977D)				
1.077	1.060	0.982	0.920 |	0.767	0.695	0.622	0.549	0.498 (2427V)		
0.979	0.952	0.846	0.742 |	0.516	0.418 (1727V)					
0.960	0.937	0.828	0.806 (847D)	u						
0.895	0.867	0.742	0.538	0.036	−0.022 (1559S)					
0.875	0.852	0.763	0.677	0.476	0.345 |	0.253	nd			
0.820	0.792	u								
0.876	0.854	0.765	0.676	0.448	0.316 |	0.223	0.131	0.041	−0.004 (2627V)	
0.789	0.766	0.662	0.497	0.099	0.078 (1527V)					
0.836	0.814 |	0.731	0.654	0.496 (1425V)						
0.795	0.764 |	0.650	0.559	0.261	0.259 (1502V)					
0.770	0.747	0.643	u							
0.737	0.714	0.622	0.532	0.314	0.211	0.110 |	0.021	−0.060	−0.139	−0.218
0.717	0.692	0.595	0.505	0.318 (1472V)						

TABLE 1 *(continued)*

Order 25°	Metal ion	25° (aqueous)**	25° (solid)	Uncertainty (25°)	100°	200°	300°	350°	E° 400°	450°	500°
91	Re^{4+}	0.977o	0.977L	±0.006	0.943	0.897	0.852	0.829	0.806	0.785	0.763
92	Bi^{2+}	–	0.943L	±0.011	0.908	0.859	0.809	0.780	0.751	0.720	0.691
93	Re^{6+}	0.946i	0.918G	±0.092	0.887	0.846	0.812	u			
94	Rb^{2+}	0.906o	0.906L	±0.02	0.860	0.799	0.738	0.708	0.678	0.647	0.617
95	Sb^{5+}	0.801i	0.869	±0.020	0.834	0.783	0.733	0.708	0.694 (380D)		
96	Cr^{6+}	0.867o	0.867G	±0.009	0.832 |	0.791	0.757	0.741	0.725	0.709	0.693
97	Bi^{3+}	0.858o	0.858	±0.002	0.823	0.777	0.731	0.705	0.679	0.654	0.628
98	Cs^{2+}	0.848o	0.848	±0.04	0.811	0.753	0.701	0.675	0.649	0.623	0.598
99	As^{4+}	–	0.810G	±0.008	0.775	0.726	0.678	0.654	0.630	0.606	0.581
100	Tc^{6+}	–	0.802G	±0.008	0.767	0.723	0.679	0.657	0.636	0.615	0.593
101	As^{5+}	1.097i	0.801	±0.001	0.765	0.716	0.668	0.644	0.620	0.596	0.572
102	Re^{7+}	0.985i	0.788G	±0.079	0.755	0.712 |	0.671	0.655	0.650 (363V)		
103	Cu^{3+}	0.759o	0.758	±0.010	0.729	0.690	0.652	0.634	0.614	0.596	0.578
104	K^{3+}	0.723o	0.723L	±0.09	0.689	0.642	0.596	0.573	0.550 |	0.529	0.510
105	Re^{8+}	–	0.720G	±0.072	0.691 |	0.658 (187V)					
106	Tl^{3+}	0.744h	0.718	±0.007	0.666	0.598	0.537 |	0.510	0.482	0.455	0.428
107	In^{3+}	–	0.716G	±0.007	0.669	0.618	0.559 |	0.533	0.512	0.491	0.470
108	Te^{4+}	0.971i	0.700	±0.001	0.517	0.471	0.425	0.401	0.379	0.358	0.332
109	Tc^{7+}	–	0.691G	±0.007	0.525	0.488 |	0.455	0.451 (311V)			
110	Rb^{3+}	0.668o	0.668L	±0.05	0.630	0.578	0.526	0.499	0.473	0.447 |	0.423
111	Cu^{2+}	0.620h	0.659	±0.004	0.626	0.578	0.531	0.508	0.485	0.462	0.439
112	Cs^{3+}	0.622o	0.622L	±0.040	0.587	0.541	0.497	0.475	0.453	0.432	0.411
113	Pb^{4+}	0.567o	0.567	±0.002	0.530	0.482	0.438 (290D)				
114	P^{4+}	–	0.553G	±0.006 |	0.513	0.478 (180S)					
115	K^{4+}	0.540o	0.540L	±0.08	0.513	0.479	0.445	0.429	u		
116	Rb^{4+}	0.513o	0.513L	±0.06	0.481	0.437	0.394	0.372	0.351 |	0.324	0.313
117	Na^{4+}	0.504o	0.504L	±0.06	0.481	0.449	0.417	0.401	0.385	0.369	0.354
118	Cs^{4+}	0.501o	0.501L	±0.16	0.467	0.422	0.378	0.355	0.334 |	0.322	0.304
119	Po^{4+}	0.901i	0.499	±0.012	0.463	0.416	0.368	0.343	0.317	0.292	0.267
120	Se^{4+}	0.767i	0.450L	±0.002	0.417	0.369	0.320	0.305 (330S)			
121	Ru^{4+}	0.441o	0.441L	±0.011	0.346	0.358	0.311	0.287	0.263	0.240	0.216
122	Rh^{4+}	0.414o	0.414L	±0.013	0.393	0.363	0.335	0.321	0.307	0.293	0.280
123	Os^{4+}	0.383o	0.383	±0.01	0.506	0.461	0.414	0.391	0.368	0.345	0.322
124	Os^{6+}	0.383o	0.383	±0.01 |	0.359	0.350 (130V)					
125	Rh^{3+}	0.361o	0.361L	±0.008	0.324	0.277	0.229	0.206	0.182	0.160	0.136
126	Rh^{2+}	0.347o	0.347L	±0.013	0.314	0.274	0.234	0.215	0.196	0.176	0.158
127	K^{5+}	0.316o	0.318G	±0.003 |	0.286	0.253	0.221	0.206	0.191	0.178 (442V)	
128	Pd^{2+}	0.332h	0.312L	±0.008	0.269	0.215	0.160	0.134	0.107	0.079	0.053
129	Ir^{3+}	0.304o	0.304L	±0.05	0.274	0.235	0.197	0.178	0.159	0.141	0.123
130	Ir^{4+}	0.304o	0.304L	±0.04	0.270	0.231	0.193	0.173	0.155	0.136	0.117
131	Hg^{2+}	0.303o,l	0.303l	±0.001	0.263	0.208	0.153	0.126	0.075	0.024	−0.026 (500D)

550°	600°	800°	1000°	1500°	1750°	2000°	2250°	2500°	2750°	3000°
0.741	0.719	0.634	0.550 |	0.377	0.306	0.236	0.171	0.106	0.044	−0.012 (2977V)
0.662	0.632	0.514 |	0.405	0.153	0.080 (1647V)					
0.588 |	0.560	0.416	0.241	−0.183	u					
0.677	0.662	0.619 (727V)								
0.603	0.579	0.479 |	nd							
0.573 |	0.549	0.528 (650D)								
0.557	0.533	0.416 |	0.311	0.080	nd					
0.572	0.551	0.467	nd							
0.549	0.525	0.421	0.407 (827D)							
0.560	0.541	0.469	0.400 |	0.229	0.212	0.202 (1800D)				
0.490	0.471	0.432 (702V)								
0.459 (527V)										
0.307	0.282 |	0.178	0.084	−0.176	−0.309	nd, u				
0.400	0.378	0.260	0.124	u						
0.416	0.393	0.303	0.215	0.078 (1336D)	u					
0.393	0.376	0.285	0.175	−0.091	−0.219	nd, u				
0.285	0.267	0.169	nd							
0.338 |	0.326	0.283	0.220	0.209 (1027V)						
0.287	0.274	0.173	0.072	−0.170	−0.287	−0.401	nd			
0.241 |	0.220	0.135	0.050	−0.251	−0.397	−0.539	nd			
0.193	0.169	0.076	−0.015	−0.074						
0.267	0.254	0.203	0.155	0.126	nd, u					
0.300	0.277	0.255 (650D)								
0.112	0.090	−0.008	−0.138	−0.197 (1115D)						
0.139	0.120	0.049	−0.019	−0.060 (1121D)						
0.027	0.001	−0.101	−0.138 (877D)	u						
0.105	0.086	0.015	−0.053 |	−0.204	−0.272	−0.336 (1977V)				
0.099	0.081	0.011	−0.057	−0.089 (1100D)						

TABLE 1 *(continued)*

Order 25°	Metal ion	25° (aqueous**)	25° (solid)	Uncertainty (25°)	E° 100°	200°	300°	350°	400°	450°	500°	550°
132	Ru^{3+}	0.287o	0.287G	±0.029 l	0.285	u						nd, u
133	Pt^{2+}	0.251h	0 239G	±0.024	0.198	0.153	0.109	0.088	0.066	0.045	0.024	
134	Pt^{4+}	0.226i	0.206G	±0.021	0.177	0.131	0.086	0.064	0.041 l	0.019	0.007 (477D)	
135	Ag^{1+}	0.057o	0.057	±0.001	−0.067	−0.097 (187D)						
136	Ag^{2+}	−0.028o	−0.028L	±0.05	−0.039 (100D)							
137	Au^{3+}	−0.228h	−0.282	±0.14	−0.355	−0.415 (160D)						

S = sublimation; V = vaporization; D = decomposition.
* Values listed at the sublimation, vaporization, or decomposition temps. apply to cells with the solid or molten electrolyte.
G - Glassner, Alvin
L - Latimer, Wendell M.
h - hydroxide
i - ionic; Ac^{3+}, $Be_2O_2^{2-}$, SiO_3^{2-}, PO_4^{3-}, $HGeO_3^-$, WO_4^{2-}, SbO_2^-, AsO_2^-, ReO_4^{2-}, $H_3SbO_4^{4-}$, AsO_4^{3-}, ReO_4^-, TeO_3^{2-}, PoO_3^{2-}, SeO_3^{2-}, $Pt(OH)_6^{2-}$
oh - $HfO(OH)_2$; $NpO_2(OH)$
o - oxide
ho - $TiO_2 \cdot H_2O$
u - uncertain
nd - no data
l - activity of liquid mercury is unity

Values of $\Delta G_f°$ at 25° were obtained from Circular 500 of the National Bureau of Standards[5] unless otherwise noted; the e.m.f. values at 25° followed by the letter L or the letter G were based on $\Delta G_f°$ values at 25° listed by LATIMER[1] and GLASSNER[6], respectively. The heat capacity data were obtained from KELLEY[7] or GLASSNER[6]. Heats of fusion, transition and vaporization were obtained from refs. 4, 5, or 6. In some cases the heat capacities had to be estimated using the method of SHOMATE[8] and employing values of heat content and heat capacity given by (i) the National Bureau of Standards[5] or (ii) using the rule of KELLEY[9] which gives 7.0, 8.0, 7.3, and 7.5 cal/°/mean g-atom, respectively, for the heat capacity of solid compounds, liquid compounds, solid metals, and liquid metals. These data are not listed here since they are readily available in refs. 1, 4, 5, and 6. Oxygen gas is common to all the systems and its heat capacity as a function of temperature is given by [6,10]:

$$C_p(O_2, \text{gas}) = 8.27 + 0.000258T - 187700/T^2 \qquad (6)$$

The electromotive forces thus calculated when the oxide is solid or molten are given in decreasing order in Table 1. A vertical line in the table indicates that the values to the left of the line are for solid oxides while those to the right are for molten (or fused) oxides. The other notations given in the table are defined in the foot-notes. A comparison with the aqueous series at 25° is also given; in some cases the comparison is with the oxide, in other cases with the hydroxide, depending on which is the more stable form. For this oxide series, as for the previously published chloride series, the higher the e.m.f. the greater is the reducing power of the metal in an oxide system. For example, if thorium were placed in molten stannic oxide at 2000° it would displace tin with the formation of thorium oxide, *i.e.*, stannic ions are reduced, thus:

$$Th + SnO_2(\text{molten}) = Sn + ThO_2(\text{molten}) \qquad (C)$$

This follows from the simple fact that the Gibbs energies of formation may be added

or subtracted, hence at 2000°, for example:

$$Th + O_2 = ThO_2 \qquad \Delta G_{ThO_2}^\circ = -189{,}000 \text{ cal} \qquad E_{ThO_2}^\circ = 2.049 \text{ V} \tag{7}$$

$$Sn + O_2 = SnO_2 \qquad \Delta G_{SnO_2}^\circ = -30{,}440 \text{ cal} \qquad E_{SnO_2}^\circ = 0.330 \text{ V} \tag{8}$$

Then, subtracting (8) from (7) one has reaction (C) for which $E^\circ = 1.719$ V and $\Delta G^\circ = -158{,}560$ cal and reaction (C) would be a spontaneous one. The equilibrium constant for reaction (C), using the data above, is 1.8×10^{15} and accordingly, reaction (C) goes to completion.

For Gibbs energy changes when the reactants and the products are not in their standard states, thermodynamics give:

$$\Delta G_{ThO_2} = \Delta G_{ThO_2}^\circ + RT \ln \frac{a_{ThO_2}}{a_{Th}\, a_{O_2}} \tag{9}$$

$$\Delta G_{SnO_2} = \Delta G_{SnO_2}^\circ + RT \ln \frac{a_{SnO_2}}{a_{Sn}\, a_{O_2}} \tag{10}$$

and $\Delta G = \Delta G^\circ$ only when the a's are unity (the standard state). When one is dealing with the pure fused salt and the pure electrode phases, the activities are all unity and the last terms in eqns. (9) and (10) are zero. However, when reaction (C) proceeds, the stannic oxide originally present as a pure phase becomes diluted with thorium oxide as it forms during the chemical reaction, and the molten electrolyte and each electrode may or may not be mutually soluble in each other; now the activities of the molten phases (or phase) can no longer be taken as unity. After reaction (C) attains equilibrium, each phase (electrode and electrolyte) could be analyzed. The activity of each component in each phase would be given by:

$$a_{Th} = N_{Th} f_{Th};\ a_{Sn} = N_{Sn} f_{Sn};\ a_{ThO_2} = N_{ThO_2} f_{ThO_2};\ a_{SnO_2} = N_{SnO_2} f_{SnO_2}$$

where N represents mole fraction and f the activity coefficient. Analysis will give N but not f, but the latter is obtained from the expression:

$$\frac{f_{Sn} f_{ThO_2}}{f_{Th} f_{SnO_2}} = K \frac{N_{Th} N_{SnO_2}}{N_{Sn} N_{ThO_2}} \tag{11}$$

To obtain values of each activity coefficient separately would be extremely involved and would entail information on each phase separately. If thorium and tin did not dissolve in the molten phase, or the molten phase dissolve in them, their activities would be unity and eqn. (11) would reduce to

$$\frac{f_{ThO_2}}{f_{SnO_2}} = K \frac{N_{SnO_2}}{N_{ThO_2}} \tag{12}$$

involving only the fused phase. Since the term on the right-hand side of this equation is known, the ratio of the activity coefficients could be evaluated. However, for the present case we are concerned only with the relative positions of the oxides in a series and the added refinement of determining the activity coefficient is unnecessary.

Owing to the slowness of diffusion in the solid state the usefulness of the data for the oxides in the solid state is necessarily limited. Even so, these data can serve a useful purpose in the consideration of those cases where two or more electrolytic phases are present and one is molten.

Finally, it must be stressed that the e.m.f. values given in the table are for

complete cells. The values may also be taken to represent the potentials of the metals (anodes) if the potential of the oxygen electrode (pressure of oxygen is one atmosphere) is arbitrarily assumed to be zero for all pure oxides at all temperatures. A similiar procedure could also have been followed for the chloride series, previously published[4], by taking the potential of the chlorine electrode (pressure of chlorine is one atmosphere) as zero for all chlorides at all temperatures; in fact, this is the convention followed by LAITY[11]. However, for practical purposes it is unnecessary to divide the e.m.f. values into separate anodic and cathodic potentials as interpretations can be based on the Gibbs energy of formation of the electrolytic phase whether it be an oxide, a chloride, or other type of electrolyte. In any case, the potentials assigned to any molten-salt half cell should relate back to the thermodynamic data of the molten salt.

REFERENCES

1 W. M. LATIMER, *The Oxidation States of the Elements and Their Potentials in Aqueous Solutions*, Prentice-Hall, Inc., New York, 2nd ed., 1952.
2 A. J. DEBETHUNE, T. S. LICHT AND N. SWENDEMAN, *J. Electrochem. Soc.*, 106 (1959) 616.
3 G. R. SALVI AND A. J. DEBETHUNE, *J. Electrochem. Soc.*, 108 (1961) 672.
4 W. J. HAMER, M. S. MALMBERG AND B. RUBIN, *J. Electrochem. Soc.*, 103 (1956) 8.
5 F. D. ROSSINI, D. D. WAGMAN, W. H. EVANS, S. LEVINE AND I. JAFFE, *Selected Values of Chemical Thermodynamic Properties*, National Bureau of Standards, Circular 500, 1952; *also* Series III, 1948–53.
6 ALVIN GLASSNER, *The Thermodynamic Properties of the Oxides, Fluorides, and Chlorides to 2500°K*, Argonne National Laboratory, Report ANL-5750, U.S. Government Printing Office: 1959-0-490339.
7 K. K. KELLEY, Bulletin 476, U.S. Dept. of the Interior, 1949; also Bulletins 383, 1935 and 393, 1936.
8 C. H. SHOMATE, *J. Am. Chem. Soc.*, 66 (1944) 928.
9 Ref. 7, p. 206.
10 O. KUBACHEWSKI AND E. EVANS, *Metallurgical Thermochemistry*, Academic Press, New York, N.Y., 1951, chap. III; R. R. WENNER, *Thermochemical Calculations*, McGraw-Hill, New York, N.Y., 1941, chap. VIII; W. M. LATIMER, *J. Am. Chem. Soc.*, 73 (1951) 1480; E. T. TURKDOGAN, *J. Appl. Chem. London*, 5 (1955) 101.
11 R. W. LAITY, *Reference Electrodes*, edited by D. J. G. IVES and G. J. JANZ, Academic Press, New York, N.Y. 1961, chap. 12.

CATHODIC REDUCTION OF FOUR-VALENT GERMANIUM*

B. LOVREČEK AND LJ. DUIĆ
Institute of Electrochemistry and Electrochemical Technology, Faculty of Technology, University of Zagreb (Yugoslavia)
(Received March 30th, 1965)

It has been reported in previous work[1-11] that Ge(IV) in aqueous solution takes part in cathodic reactions. According to the conditions, the following phenomena are on record:

(a) lowering of hydrogen overvoltage;
(b) reduction of Ge(IV) to Ge(II);
(c) deposition of a thin layer of germanium.

Ge(IV) can be present in aqueous solutions in different forms (as a monomer, polymer and anions)[12-14].

In the present work, an attempt has been made to define the regions in which each of the above reactions takes place, and to determine their dependence on the form in which germanium is present in the solution.

EXPERIMENTAL

Polarographic and galvanostatic single pulse methods have been used in these investigations. For the polarographic measurements, the usual manual apparatus was used; the potential of the dropping mercury electrode was measured independently *vs.* S.C.E.

The apparatus used for the galvanostatic measurements allowed the electrode to be polarized cathodically and anodically with impulses having current densities from 1.2×10^{-4}–3.0×10^{-2} A/cm^2. The time bases were in a relatively slow range, from 0.1–15 sec for 10 cm of the C.R.O. screen. The $\eta_t - t$ plots were recorded using two time bases, 0.58 and 6.7 cm/sec. The working electrode for the galvanostatic measurements was a hanging mercury drop of a defined surface.

As it was possible to achieve a previous partial electrochemical reduction, solutions containing Ge(IV) only, and solutions in which Ge(IV) was reduced to a lower valency, could be examined by polarographic and galvanostatic methods.

The supporting electrolyte for the solutions containing Ge(IV) only was Sørensen's phosphate buffer mixture**. The pH values of the solutions examined polarographically were in the range 1.7–12.6. For the galvanostatic measurements, solutions of different pH were used: acid, approximately neutral, and alkaline, respectively.

* Presented at the 15th Meeting of C.I.T.C.E., London and Cambridge, September, 1964.
** The pH range was somewhat extended by adding H_3PO_4 and NaOH, respectively.

The solutions containing partially-reduced germanium were prepared in the following manner. A solution 0.1 N with respect to NaOH and containing GeO_2 in a dissolved state, was subjected for a definite time to cathodic reduction on a mercury electrode, with fixed current density. After partial reduction, the pH was adjusted to the required value by the addition of phosphoric acid. Partially-reduced solutions obtained in this way were examined polarographically at pH values ranging from 1.5–11.3. Three of these solutions, having pH values in acid, approximately neutral and alkaline ranges, respectively, were subjected to galvanostatic examination. The solutions examined and the methods applied are listed in Table 1.

TABLE 1

Method of investigation	*Solutions*
Polarography	Sørensen's buffer mixture + $7 \cdot 10^{-4}$ M GeO_2; pH range, 1.7–12.6
Galvanostatic single pulse method	Sørensen's buffer mixture + $7 \cdot 10^{-4}$ M GeO_2; pH = 3.1, 6.5 and 11.4
Galvanostatic single pulse method	Sørensen's buffer mixture + 1.8×10^{-2} M GeO_2; pH = 3.1, 6.5 and 11.4
Polarography	0.1 N NaOH + H_3PO_4 + $7 \cdot 10^{-4}$ M GeO_2 (partly reduced); pH range, 1.5–12.2
Galvanostatic single pulse method	0.1 N NaOH + H_3PO_4 + $7 \cdot 10^{-4}$ M GeO_2 (partly reduced); pH = 2.3, 6.7 and 11.7
Galvanostatic single pulse method	0.1 N NaOH + H_3PO_4 + 1.8×10^{-2} M GeO_2 (partly reduced); pH = 2.3, 6.7 and 11.0

All measurements were carried out in atmosphere of pure nitrogen gas and at a fixed temperature: 20 and 25° for the polarographic measurements and 25° for the galvanostatic measurements*.

RESULTS

Investigations of solutions containing Ge(IV) only

An inspection of the results obtained with solutions containing Ge(IV) only, shows that two characteristic regions can generally be distinguished:

(1) a region in which only a lowering of the hydrogen overvoltage has been detected, but no polarographic reduction wave, nor a corresponding galvanostatic step, and

(2) a region in which one or several reduction waves have been recorded polarographically and the corresponding steps, galvanostatically.

Region (1). The systems examined having pH values below 3.1 yield polaro-

* A detailed description of the apparatus used and experimental techniques can be found in the thesis of LJ. DUIĆ: *Studies on the mechanism of the electrochemical reduction of tetravalent germanium.*

grams and η_t–t plots without a reduction wave or corresponding step. A characteristic plot of reduction potential against pH is shown in Fig. 1 for the entire pH range investigated. A comparison with the results of measurements on the pure supporting electrolyte shows that the reduction potential, or the potential of the steady state achieved (at fixed current densities) is shifted towards more positive values when the solution contains Ge(IV). It has also been observed polarographically that in this region the reduction potential depends on the pH changes in the solution, the potential being shifted towards more negative values when the pH is increased. It has been possible to record by galvanostatic technique, a step at a high concentration of GeO_2 using current densities $i_c = 1.6 \times 10^{-2}$A/cm^2. However, no significant relation has been found between the reduction potential and the drop time, t, or the height of the mercury column, h.

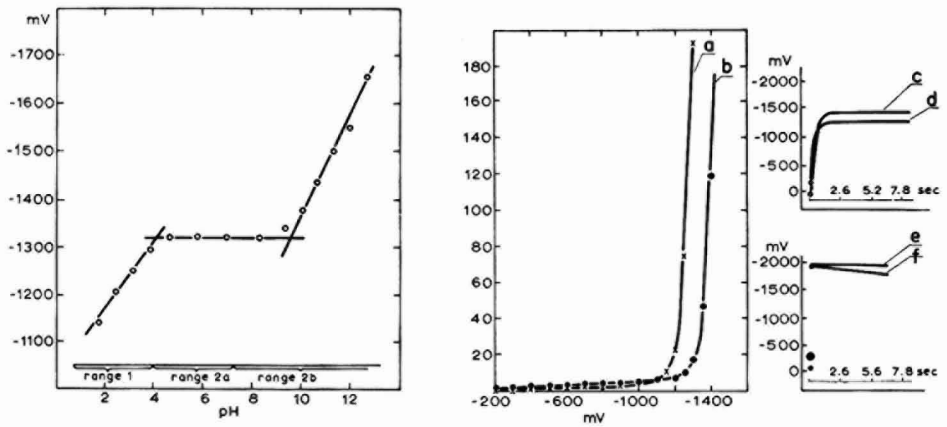

Fig. 1. The dependence of reduction potential on pH: $c_{GeO_2} = 7 \cdot 10^{-4}$ M, temp. = 25°, h = 407 mm.

Fig. 2. Typical polarograms and η_t–t plots for the first region: (a), $c_{GeO_2} = 7 \cdot 10^{-4}$ M, pH = 1.8, temp. = 25°, h = 407 mm; (b), $c_{GeO_2} = 0$, pH = 1.9, temp. = 25°, h = 407 mm; (c), $c_{GeO_2} = 0$, pH = 3.1, $i_c = 1.2 \times 10^{-4}$ A/cm^2; (d), $c_{GeO_2} = 7 \cdot 10^{-4}$ M, pH and i_c, as (c); (e), $c_{GeO_2} = 0$, pH = 3.1, $i_c = 1.4 \times 10^{-2}$ A/cm^2; (f), $c_{GeO_2} = 7 \cdot 10^{-4}$ M, pH and i_c as (e).

A phenomenon which is particularly characteristic in galvanostatic measurements at higher current densities is the gradual lowering of the working electrode potential with the duration of an impulse when the current is kept constant.

Typical polarograms and η_t–t plots for the first region are given in Fig. 2.

Region (2). Systems having a pH value of 3.75 or more, yield polarograms showing one or more waves; the η_t–t plots show corresponding steps at definite current densities. In this region the following sub-regions can be distinguished:

(a) below pH 6.9, the sum of both waves is approximately constant, and the temperature coefficient of the first wave is, in most instances, between +1 and +2%. The second wave which makes its appearance at pH 4.6 is not always equally well-developed and within this pH range the temperature coefficient is clearly positive and varies between +5 and +10% per degree.

The relation between the wave height and the height of the mercury column is

neither clearly linear nor does it follow the square-root law. It has also been observed that in this region the reduction potential of the first wave (or its half-wave potential) does not depend on the pH of the solution, but remains constant. The irreversibility of the first wave increases with the pH value.

In a series of galvanostatic measurements in this region, a double step has been recorded in the lower GeO_2 concentration range at a current density of 2×10^{-2} A/cm^2 and in the higher concentration range at $i_c = 1.4 \times 10^{-2}$ A/cm^2.

(b) At pH values equal to or above 8.2 the temperature coefficient of the first wave is, in most instances, about $+1.5\%$, and the temperature coefficient becomes strongly negative, attaining values as low as -10% per degree and lower. When the pH is increased, the first and second waves gradually merge into each other, while their sum decreases. Above pH 10.6 only a single wave is recorded. In this region the reduction potential of the first wave again becomes dependent on pH change in the solution, the potentials being shifted towards higher values when the pH is increased (Fig. 1).

The galvanostatic measurements within narrow limits of current densities and

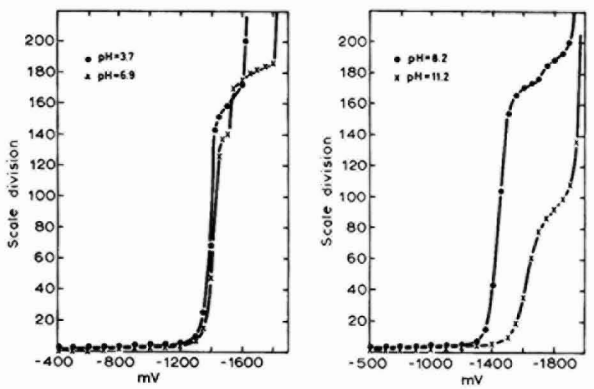

Fig. 3. Typical polarograms for the second region: $c_{GeO_2} = 7 \cdot 10^{-4}$ M, temp. = 25°, h = 407 mm.

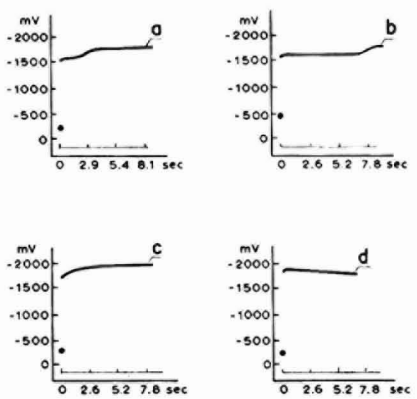

Fig. 4. Typical cathodic η_t–t plots: (a), $c_{GeO_2} = 7 \cdot 10^{-4}$ M, pH = 6.5, $i_c = 2.0 \times 10^{-3}$ A/cm^2; (b), $c_{GeO_2} = 1.8 \times 10^{-2}$ M, pH = 6.5, $i_c = 1.2 \times 10^{-2}$ A/cm^2; (c), $c_{GeO_2} = 7 \cdot 10^{-4}$ M, pH = 11.4, $i_c = 1.5 \times 10^{-3}$ A/cm^2; (d), $c_{GeO_2} = 1.8 \times 10^{-2}$ M, pH = 11.4, $i_c = 2.2 \times 10^{-2}$ A/cm^2.

in the lower GeO_2 concentration range revealed a feebly-developed step. In the higher GeO_2 concentration range above $i_c = 4 \times 10^{-3}$ A/cm², a potential drop has been recorded at the working electrode within the duration of an impulse. Typical polarograms for the second region are shown in Fig. 3, and typical η_t–t plots for the same range in Fig. 4.

Investigation of partially-reduced solutions

Measurements on partially-reduced solutions yielded an anodic wave in the entire region explored. According to the shape of the anodic curve, this region can be subdivided as follows.

(1) Below pH 4.4, measurements yielded a single anodic wave the height of which decreases with increasing pH, while deviations from polarographic reversibility increase with pH. In the cathodic part of the polarogram a cathodic wave has been recorded the height of which is equal to the anodic wave and which has no analogue in the polarograms obtained on solutions of Ge(IV) only.

The anodic and the cathodic waves show, approximately, the features of diffusion-controlled waves, the temperature dependence of both waves being about +2% per degree. The relation between the ratios of wave height changes and mercury column height ratios follow the square-root law. In the more acid pH range polarographic criteria show that the electrode reaction is nearly reversible.

The galvanostatic measurements yielded η_t–t plots showing in the anodic part a step which corresponds to the anodic wave of the polarogram. With appropriate current densities, a step has also been recorded in the cathodic part of the η_t–t plots, corresponding to the cathodic wave of the polarogram. Typical polarograms and η_t–t plots are shown in Fig. 5.

(2) At and above pH 5.4 a double anodic wave appears as the pH is increased. The total wave height increases with the pH, but the fraction of the originally-recorded wave in the total wave height, decreases. With increasing pH the new anodic wave approaches polarographic reversibility.

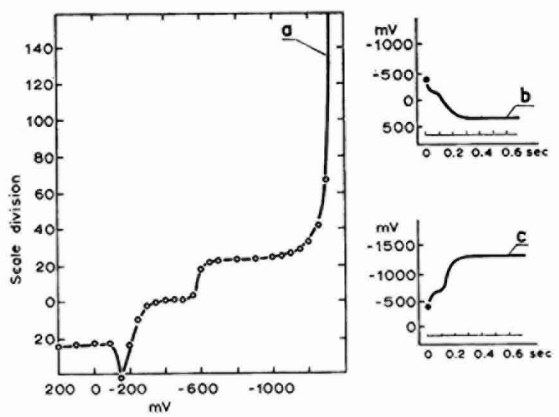

Fig. 5. Polarogram and η_t–t plots for partially-reduced solutions with $c_{GeO_2} = 7 \cdot 10^{-4}$ M: (a) pH = 1.6, temp. = 25°, h = 407 mm; (b), anodic η_t–t plot, $i_a = 2.0 \times 10^{-4}$ A/cm², pH = 2.6; (c), cathodic η_t–t plot, $i_c = 2.0 \times 10^{-4}$ A/cm², pH = 2.6.

Because of the poor definition of the first wave, it is difficult to determine the temperature coefficient accurately, but it can be estimated to vary in most cases between -2 and -5% per degree. The temperature coefficient of the second anodic wave in this region is a maximum at $+6\%$ per degree; and with increasing pH drops gradually to about $+1.5\%$ per degree.

The cathodic waves recorded in this pH range are analogous to the waves obtained in the preceding series of measurements (on solutions containing Ge(IV) only).

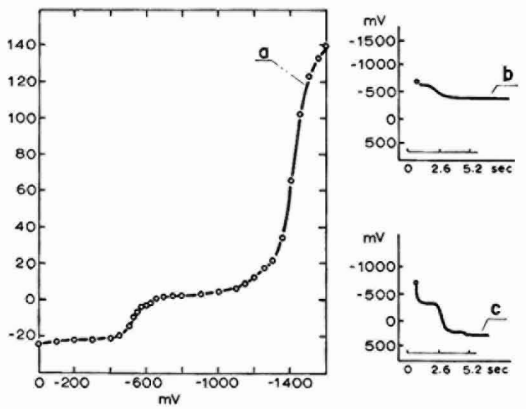

Fig. 6. Polarogram and η_t–t plot for partially-reduced solutions: (a), $c_{GeO_2} = 7 \cdot 10^{-4}$ M, pH = 7.3, temp. = 25°, h = 407 mm; (b), $c_{GeO_2} = 1.8 \times 10^{-2}$ M, pH = 6.7, $i_a = 2.0 \times 10^{-4}$ A/cm²; (c), $c_{GeO_2} = 1.8 \times 10^{-2}$ M, pH = 6.7, $i_a = 2.0 \times 10^{-3}$ A/cm².

The galvanostatic measurements, in agreement with the polarographic measurements, yield (when an appropriate current density is used) an analogous anodic step at all GeO_2 concentrations. Typical polarograms and η_t–t plots are shown in Fig. 6.

DISCUSSION

Solutions containing tetravalent germanium only

The results of the investigations reported in this work indicate that different processes can occur on the electrodes, depending on the pH of the electrolyte. Moreover, it is evident that the most important factor in determining the kind of process occurring is the form in which germanium is present; this, in its turn, depends on the pH of the solution. According to reports in the literature[12–14], corroborated by our own observations, germanium can exist in solution as monomer, pentamer, or as the corresponding anions, according to the pH of the solution. Special consideration must be given to the possibility of the existence of germanium pentamer.

The results reported above will be discussed under the same headings as in the experimental part of the present paper.

Region 1 (low pH values). In this region, although the reduction potential is shifted to more positive values than in solutions without GeO_2, no polarographic wave has been recorded contrary to expectation based on an evaluation of the

diffusion current at this GeO_2 concentration. However, since there is a shift of the reduction potential, the reduction wave of germanium must be masked by the process of catalytic discharge of hydrogen. The information obtained by polarographic measurements is supported by the method of single galvanostatic impulses. These results confirm that the hydrogen overvoltage is lowered by the presence of germanium. Galvanostatic techniques allow a better insight into the process causing the lowering of the hydrogen overvoltage, *i.e.*, it has been observed that in some instances a lowering of the potential on the working electrode occurs within the duration of an impulse. This indicates that in the course of the current impulse some unstable intermediate product is accumulated which is active in the catalytic discharge of hydrogen. The existence of intermediate products instrumental in the catalytic discharge of hydrogen has been assumed by some authors[15-16] for other systems. According to these authors, in organic systems the unstable product acts as an intermediary in the transfer of protons, causing a drop of the hydrogen overvoltage on the mercury. It has been suggested that the transfer of protons occurs through the OH groups in organic molecules. The assumption of a similar process in the present instance is supported by the fact that, in this region, Ge(IV) is thought to be present in the form of a pentamer, which involves the saturation of germanium atoms with OH-groups. The possibility of the existence of the pentamer and its structure will be discussed later in more detail.

In the galvanostatic investigations of more concentrated solutions of GeO_2 at higher current densities, two steps have been observed, the first representing the catalytic, the second the normal discharge of hydrogen. The step corresponding to the catalytic discharge of hydrogen may be limited in this instance by the rate of proton acceptance by the intermediate product.

Region 2a and 2b. In this region the appearance of polarographic waves can be explained on the basis of any of the following assumptions:

(a) the two waves correspond to the two steps of the reduction of Ge(IV) to Ge(O);

(b) the first wave is the reduction wave of germanium, the second an adsorption post wave;

(c) the first wave is the reduction wave of germanium, the second the hydrogen catalytic wave;

(d) the two waves represent the reduction of two different modifications of Ge(IV) (including monomer, polymer, undissociated and dissociated forms).

The first three assumptions are not supported by the characteristic features of the respective waves (height of the waves, temperature dependence, variation of wave height with height of the mercury column).

Before discussing the nature of the processes occurring in this pH range, it must be emphasized that although the pattern of the polarographic plot in the entire region 2 shows some common features (for instance, the occurrence of a double wave), in view of the differences in the behaviour of the reduction potential with variation in pH and temperature dependence, the existence of different electrode processes must be assumed.

According to an older conception, elaborated by PUGH[12], germanium can be present in aqueous solutions in three different forms, depending on the pH: below pH 7 almost all the germanic acid is present in its undissociated form; above pH 7 the

concentration of the first anion increases, and above pH 10.6 the second anion appears, and the concentration of the undissociated acid drops to zero.

The more recent papers of CARPÉNI[13] and EVEREST AND SALMON[14], report that additional forms of germanium can be distinguished in this pH range. CARPÉNI concludes that germanium is present in the solutions as a pentamer in the lower pH range, and as a monomer and its anions, in the higher range. Although none of these authors discussed the structure of the pentamer, it can be deduced from the electron configuration of germanium and by analogy with the polymerization of silicic acid. The assumption of six co-ordinating OH-groups surrounding Si^{4+} is supported by the existence of the ion SiF_6^{-2}. Since germanium also forms a stable compound, GeF_6^{-2} (sp^3d^2 hybridization), it may be deduced by analogy that in the formation of germanium polymers the same or similar steps are involved. The established process of polymerization of silicic acid and the assumed analogy with germanic acid are shown schematically in Fig. 7.

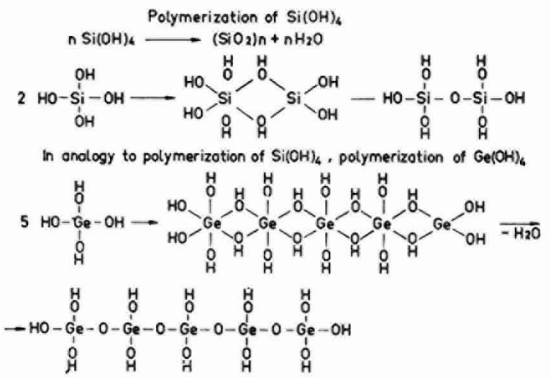

Fig. 7. The established process of polymerization of silicic acid and the assumed analogy with germanic acid.

By applying this reasoning to our results we are led to the conclusion that in the acid region the intermediate product of the reduction of pentagermanic acid is responsible for the catalytic discharge of hydrogen and that in a part of the second region the recorded wave represents the reduction of pentagermanic acid. In order to explain the formation and characteristics of the second wave, it should be noted that, according to EVEREST AND SALMON[14], some monomer is formed at pH values as low as 4–5. The assumption that the second wave represents the reduction of the monomer is borne out by the temperature dependence, *i.e.*, while the first wave is nearly independent of temperature, the temperature coefficient of the second wave in this region varies between +10 and +5% per degree, which is in agreement with the fact that on degradation, molecular concentration increases.

The galvanostatic measurements in the region about pH 6.5 yielded a plot with two steps, which corresponds to the two-wave polarographic plot. As the potential of the second step is inferior to the potential of hydrogen discharge, it can be deduced that the two steps represent the penta- and mono-modification of germanium in the solution, with limited rate of equilibrium establishment between them. At this pH value and higher GeO_2 concentration, a plot with two steps was also ob-

tained, but only at higher current densities, which is in agreement with the foregoing assumption and with the fact that at higher concentrations the fraction of pentamer in the solution is increased.

A comparison of the ratio of lengths of the first step with the ratio of current densities applied (at higher concentration) shows that these ratios are within the expected limits for the predominant concentration polarization control.

When the pH values of the systems are increased, the temperature dependence of the polarographic waves undergoes a marked change. That the mechanism of reduction undergoes some change may be inferred already from the polarogram obtained on a solution at pH 6.9. The first and the second wave merge and a new wave appears at more negative values. According to the above-mentioned authors, the concentration of the undissociated pentagermanic acid decreases and the concentration of the monomer and a number of the possible modifications of its anions, increases when the solution becomes more alkaline. It is likely that above this pH value the reduction of monogermanic acid and its anion is predominant. In agreement with the results of BRDIČKA[17] and BRDIČKA AND WIESNER[18], who have studied the polarographic reduction of an acid with an undissociated form which is reduced at more positive potential than its anion, two waves have been recorded in this region. The second wave recorded for our system has a pronouncedly negative temperature coefficient. In a system of this kind, the second wave might be expected to be higher at more elevated temperatures, since the degree of dissociation is increased when the temperature increases. However, if the reaction $HA \rightleftharpoons H^+ + A^-$ is considered, it must be assumed that an increase of temperature would also increase the rate of the reaction from right to left, when the undissociated acid HA is removed by the electrode reaction, which is the case at a potential more positive than the reduction potential of the anion. The limiting current for such mixed diffusion-reaction waves is given by the equation: $i_+ = (i_d)_{HA} + i_k$, where $(i_d)_{HA}$ is the diffusion current of the undissociated form, and i_k the reaction current proportional to the reaction rate constant. Consequently, it must be assumed that the drop in $(i_d)_{HA}$ caused by increase of temperature is lower than the simultaneous rise of i_k. Since the sum $C_{HA} + C_{A^-}$ is constant, it is obvious that the height of the second wave must decrease.

Polarograms obtained on systems in more alkaline pH ranges show a constant decrease of the sum of the waves. This is expected, since the concentration of the undissociated acid is gradually decreasing (above pH 10.6 it vanishes) and a second anion, GeO_3^{-2}, makes its appearance beside the first anion, $HGeO_3^-$. The wave representing the second anion at higher pH values has not been detected, probably owing to the discharge of hydrogen, this anion being more difficult to reduce.

The galvanostatic measurements in this region revealed a poorly-developed step, analogous to the polarographic wave. However, it is interesting to note that at higher GeO_2 concentrations and greater current densities, a gradual potential lowering of the working electrode was observed within the interval of an impulse, as in the acid region. This indicates that in this case, too, an intermediate product may be instrumental in lowering the hydrogen overvoltage, but this reaction is evidently slower in alkaline solution and at lower concentrations of GeO_2 it has not been observed at all. It may be inferred that the intermediate product formed in the alkaline region is relatively stable; this is borne out by previous investigations[19], which in-

dicated that when the reduction proceeded at a fixed potential, the intermediate product of the reduction of Ge(IV) was accumulated only in solutions when the pH exceeded 9.8.

The different forms and reactions in the investigated range of pH values is

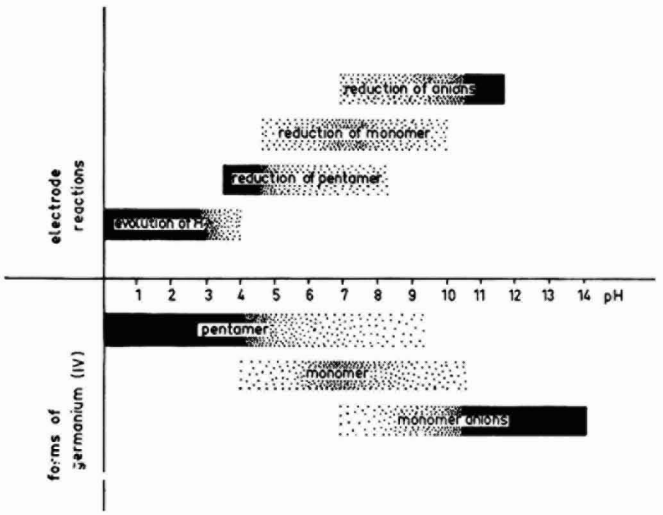

Fig. 8. The different forms of Ge and reactions in the investigated systems and their dependence on pH.

shown schematically in Fig. 8. The limits of the areas of existence of the different forms of Ge(IV) and the boundaries of the different types of reactions occurring are not well-defined.

Partially reduced solutions

From the results obtained on systems where the pH was adjusted to definite values after a partial cathodic reduction it is evident that in the entire range investigated an intermediary product of lower valency is present. The shape of the polarograms and $\eta_t - t$ plots obtained experimentally, points to the conclusion that the form in which lower-valent germanium is present varies with the pH of the solution. The discussion of the form in which bivalent germanium is present is constrained by the fact that data on Ge(II) are even scarcer than those on Ge(IV). However, in view of the results of the present investigation and by analogy with Ge(IV), it can be strongly inferred that Ge(II) is amphoteric in character and that both the undissociated acid (even different forms of it) and the acid anion can exist.* Even for the lower pH range, where only one wave is recorded, polarographic characteristics point to the

* It is also of interest that the form in which Ge(II) is present in these systems after acidification is apparently not identical with the form obtained by reduction of the Ge(IV) on the mercury drop in the same pH ranges. In the series of experiments discussed above, this Ge(II) was obviously responsible for the catalytic discharge of hydrogen in strongly acid solutions. Mention should also be made of a previous work[19] in which Ge(IV) was cathodically reduced at defined pH values of the solution, and lower-valent germanium was not recorded unless the pH exceeded 9.8. Further, according to CARPÉNI[13], and EVEREST AND SALMON[14], above pH 9.8 no pentamer, which we suppose is essential for catalytic hydrogen evolution, is present in the solution.

possibility of existence of two forms of Ge(II); but since only one wave is recorded below pH 4 it may be deduced that the equilibrium between the two forms, A and B, of lower-valent germanium is established very rapidly, so that only one polarographic wave can develop. In order to explain the decrease in height of this wave with increasing pH, it seems logical to assume that forms A and B are the monomer and a polymer, respectively, or two polymers of different degrees of polymerization. The assumption that the equilibrium between monomer (or lower polymer) and (higher) polymer is rapidly established at lower pH values, rationalizes the observed decrease in height of the anodic wave, if the fraction of higher polymer increases with the pH. Since, within a narrow pH range, an increase of pH shifts the equilibrium in the direction of formation of polymers, the molecular concentration of Ge(II) decreases with the increase of pH, and so do both the diffusion coefficient and the wave height.

The appearance of another wave above pH 5.75 must obviously be attributed either to a decrease in the rate of transformation of one form into the other, or even to the appearance of a new form (for instance, an anion), which is oxidized at different potentials. The slopes $\Delta E_{\frac{1}{2}}$–pH are not identical for both waves,—rather, their half-wave potentials are seen to move farther apart as the pH decreases (Fig. 9).

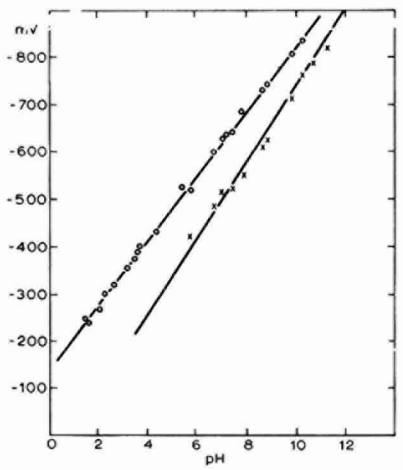

Fig. 9. The dependence of half-wave potentials on pH: (o), first anodic wave; (x), second anodic wave; temp. = 25°, h = 407 mm.

The assumption that one of these waves at lower pH could not be detected because oxidation took place at so positive a potential that this process was masked by the anodic dissolution of mercury—is merely qualitative and probably not valid, because the values obtained by extrapolation into the acid region do not warrant such a conclusion. It is more likely that this second form of Ge(II) is formed only at higher pH values and is then also oxidized. The assumption that this new form is the product of the polymer degradation with formation of monomer anion at higher pH values (which is supported by the fact that the height of the wave increases with the pH) accounts for the temperature dependence of the new wave, which is definitely positive, while for the original anodic wave it has now become negative.

The wave recorded in the cathodic region probably represents the reduction of Ge(II) to Ge(O). That the form involved in this reduction is identical with the one oxidized in the cathodic region, may be inferred from the characteristic features of the wave, which agree with the features of the anodic wave in the same region (the heights are equal, the temperature dependence is identical, the change of height with the height of the mercury column obeys in both cases the square-root law, the deviations from polarographic reversibility for both waves increase with pH). Moreover, this wave can be detected only when a certain amount of Ge(II) has previously accumulated in the solution.

The measurements by the method of single galvanostatic impulses confirm the polarographic results. Thus, in the acid region a corresponding anodic step has been recorded, confirming the conclusion, drawn from the polarographic observations, that the solutions prepared in this way contain a relatively stable form of germanium on a lower-valency level. This is borne out by the results of the examination of solutions containing germanium in higher concentration. In the cathodic area, a step has been recorded which is analogous to the polarographic wave representing the reduction of a bivalent modification of germanium to Ge(O).

In solutions of pH 6.7, a plot with two steps, corresponding to the two-wave polarographic plot has been recorded. Where this step is well-developed, it meets the criterion of concentration polarization with galvanostatic conditions, thus confirming the conclusion that two forms of lower-valent germanium are present, which change from one to another at a limited rate.

Investigations of alkaline solutions containing low concentrations of GeO_2 reveal only a slight step; with higher concentrations a very pronounced step was obtained at the same potentials at which an anodic wave was recorded polarographically.

ABSTRACT

An investigation of solutions containing germanium established that in all the systems explored and under all the conditions applied, germanium takes part in electrode reactions. In cathodic reactions an important part is played by (i) the different forms in which Ge(IV) is present in the solution (pentamer, monomer, anions), (ii) the equilibria between them and (iii) the rate of transition from one form to the other. When a decrease of hydrogen overvoltage was observed, some special features of the mechanism of this phenomenon have been noted. It has been firmly established that in all systems examined, cathodic reduction gives rise to a more-or-less stable intermediate product. Its form, as a rule, increasingly approaches the defined Ge(II) when the alkalinity of solution is increased. Bivalent germanium, prepared by reduction of Ge(IV) in alkaline medium, is relatively stable even when the solution is made acid. Evidence has also been adduced that with germanium thus prepared, the form in which it is present in the solution plays an important part.

REFERENCES

1 N. DE ZOUBOV, E. DELTOMBE AND M. POURBAIX, CEBELCOR *Rapp. Tech.*, 27 (1955).
2 C. G. FINK AND V. M. DOKRAS, *J. Electrochem. Soc.*, 95 (1949) 80.
3 M. GREEN AND P. H. ROBINSON, *J. Electrochem. Soc.*, 106 (1959) 253.

4 D. A. EVEREST AND H. TERREY, *J. Chem. Soc.*, (1950) 2282.
5 A. K. GUPTA AND N. NAIR, *Anal. Chim. Acta*, 9 (1953) 287.
6 P. VALENTA AND P. ZUMAN, *Chem. Listy*, 46 (1952) 478.
7 S. K. DHAR, *Anal. Chim. Acta*, 15 (1956) 91.
8 M. N. PLATONOVA, *Zh. Neorgan. Khim.*, 3 (1958) 1002.
9 T. ØSTERUD AND M. PRYTZ, *Arch. Math. Naturvidenskab.*, 47 (1943) 73.
10 F. PANETH AND RABINOWITSCH, *Ber.*, 58 (1925) 1138.
11 A. G. PECHERSKAYA AND V. V. STENDER, *Zh. Fiz. Khim.*, 24 (1950) 856.
12 W. PUGH, *J. Chem. Soc.*, (1929) 1537, 1994.
13 G. CARPÉNI, *Bull. Soc. Chim. France*, 15 (1948) 725.
14 D. A. EVEREST AND J. E. SALMON, *J. Chem. Soc.*, (1954) 2438.
15 K. J. VETTER, *Elektrochemische Kinetik*, Springer Verlag, Berlin, Göttingen and Heidelberg, 1961, p. 461.
16 A. N. FRUMKIN, *Advances in Electrochemistry and Electrochemical Engineering*, Vol. 1, edited by P. DELAHAY, Interscience Publishers, Inc., New York and London, 1961, chap. 2: *Hydrogen Overvoltage in Adsorption Phenomena*; Part 1: *Mercury*, p. 100.
17 R. BRDIČKA, *Chem. Listy*, 10 (1946) 232.
18 R. BRDIČKA AND K. WIESNER, *Chem. Listy*, 4 (1946) 66.
19 B. LOVREČEK AND LJ. DUIĆ, unpublished results.

REPORT

GORDON RESEARCH CONFERENCE ON ELECTROCHEMISTRY, SANTA BARBARA, CALIFORNIA

The second Gordon Research Conference on Electrode Processes was held in Santa Barbara during the week of January 25th–29th, 1965. The quality of the conference, as well as the weather and the scenery, was all that the newcomers had been led to expect; many a discussion was continued in the relaxed atmosphere in and around the swimming pool. The smooth running of the mechanics of the conference paid tribute to the excellent organisation of the Director, Dr. W. G. PARKS and his staff and the Conference Chairman, Dr. R. P. BUCK.

Dr. R. PARSONS discussed the characterisation of adsorption at the electrode–solution interphase in terms of adsorption isotherms. He considered various methods of interpreting experimental results and illustrated these with some new results on mixed electrolyte adsorption and on non-electrolyte adsorption in non-aqueous systems. Dr. D. M. MOHILNER developed the thermodynamic treatment of curved interphases and predicted that the effects would be scarcely noticeable with a capillary electrometer but may be important on solid electrodes. Dr. J. N. BUTLER presented some new results on the double layer at amalgam electrodes and their application to the evolution of hydrogen on these electrodes.

Professor J. O'M. BOCKRIS reviewed a wide range of studies of the anodic oxidation of organic compounds. He emphasized the advantage of steady-state methods and made some provocative criticisms of sweep methods. Dr. E. GILEADI described results obtained, particularly by radio-tracer techniques, for the adsorption of uncharged molecules on solid metals. These were interpreted in terms of the molecular nature of the adsorbate and its replacement of solvent molecules.

Professor A. STREITWIESER Jr. discussed the correlation of spectroscopically-determined energy levels with polarographic half-wave potentials, particularly for

hydrocarbons and alkyl halides. Professor P. W. SELWOOD began by remarking that the amenities of Santa Barbara provided a strong temptation to leave the research laboratory; it was clear that he had resisted and he described some elegant experiments on *o–p* hydrogen conversion using ruby powder obtained from laser material.

Dr. J. KORYTA gave a very comprehensive review of the analysis of polarographic currents controlled by the rate of chemical reactions in the bulk of the solution. He also described a variety of effects due to the adsorption of reacting species which may find an interpretation in terms of the Butler–Frumkin theory of adsorption of non-polar substances. Professor I. SHAIN emphasized the value of voltage-scan techniques for diagnosing types of reaction schemes involving coupled chemical reaction. He then described some potentiostatic experiments on the reduction of azobenzene. Professor R. N. ADAMS described results for the rates of homogenous electron transfers between organic ions and radicals obtained from EPR line broadening. These were compared with the heterogeneous rates for the same systems obtained using the rotating disc electrode.

Professor W. B. SCHAAP illustrated the technique of electrochemical measurement in non-aqueous solvents with examples from the ethylene diamine system. He also described the problems in the determination of polarograms in poorly-conducting media using a radio-chemical method. Professor R. IWAMOTO discussed the effect of difunctional solvents on the electrode potentials of ion–metal and redox couples.

Dr. R. MUELLER surveyed the application of optical techniques to electrochemical problems, showing an unusually beautiful film of schlieren effects in colour. Professor R. N. O'BRIEN made the use of a laser for interference studies sound easy and showed a film of a rotating disc electrode and a dropping-mercury electrode taken with this technique. Dr. A. K. REDDY gave a clear account of the use of ellipsometry to solve electrochemical problems, emphasizing its promise for the future.

On the final morning of the Conference, Professor P. VAN RYSSELBERGHE introduced a discussion on the fundamental derivation of the rate equation in electrochemical kinetics. He was especially critical of the usual way in which the *psi*-effect is formulated. His remarks stimulated a particularly vigorous discussion in which opposing views were freely ventilated. In the course of this Dr. D. B. MATTHEWS presented a modified theory of the hydrogen-ion discharge reaction.

A third conference will be held in the winter at the same location (there was little support for any change during the discussion of future plans) with Professor E. YEAGER as Chairman and Dr. R. OSTERYOUNG as Co-Chairman.

Department of Physical Chemistry,
University of Bristol (England)

ROGER PARSONS

CONTENTS

The electrochemical reduction of the tetraphenylstibonium ion
M. D. MORRIS, P. S. MCKINNEY AND E. C. WOODBURY (Cambridge, Mass., U.S.A.) . . 85

Electrochemical studies of organic compounds dissolved in carbon-paste electrodes
F. A. SCHULTZ AND T. KUWANA (Riverside, Calif., U.S.A.) 95

Electroluminescence in non-aqueous solutions
J. M. BADER AND T. KUWANA (Riverside, Calif., U.S.A.) 104

Reduction from a pre-enriched solution of amalgam-forming metals: A new electroanalytical method
CH. YARNITSKY AND M. ARIEL (Haifa, Israel). 110

The retardation of electrochemical reactions by adsorbed organic molecules; a quantitative treatment involving the theory of irreversible polarographic waves
S. SATHYANARAYANA (Bombay, India) 119

Theoretical electromotive forces for cells containing a single solid or molten oxide
W. J. HAMER (Washington, D.C., U.S.A.) 140

Cathodic reduction of four-valent germanium
B. LOVREČEK AND L. DUIĆ (Zagreb, Yugoslavia) 151

Report
Gordon Research Conference on Electrochemistry, Santa Barbara, California 163

RODD'S CHEMISTRY OF CARBON COMPOUNDS

Second Edition

edited by S. COFFEY, M.Sc. (London), D.Sc. (Leyden). Formerly of I.C.I. Dyestuffs Division, Blackley, Manchester. Assisted by an Advisory Board of prominent scientists.

This completely revised edition of this standard work has been undertaken to take into account the important advances in theoretical and experimental organic chemistry recorded since the appearance of the first edition.
The treatment has remained largely unchanged although the sheer extent of new material has made it necessary to create further subdivision in order to reduce publication delay.

VOLUME IA - GENERAL INTRODUCTION, HYDROCARBONS, HALOGEN DERIVATIVES
General Introduction
1. The saturated or paraffin hydrocarbons. Alkanes. 2. Unsaturated acyclic hydrocarbons. 3. Halogen derivatives of the aliphatic hydrocarbons.
6 × 9″ xx + 569 pages, 1964, subscription price £7.0.0.
non-subscription price £8.0.0.

VOLUME IB - MONOHYDRIC ALCOHOLS, THEIR ETHERS AND ESTERS, SULPHUR ANALOGUES; NITROGEN DERIVATIVES; ORGANOMETALLIC COMPOUNDS
4. Monohydric alcohols, their ethers and esters. 5. Sulphur analogues of the alcohols and their derivatives. 6. Nitrogen derivatives of the aliphatic hydrocarbons. 7. Aliphatic organometallic and organometalloidal compounds.
6 × 9″ xvi + 313 pages, 16 tables, 1964, subscription price £4.8.0.
non-subscription price £5.0.0.

VOLUME IC - MONOCARBONYL DERIVATIVES OF ALIPHATIC HYDROCARBONS; THEIR ANALOGUES AND DERIVATIVES
8. Aldehydes and ketones. 9. Monobasic carboxylic acids. 10. Carbon monoxide, isocyanides and fulminic acid. 11. Carbonic acid and its derivatives.
6 × 9″ xvi + 432 pages, 17 tables, April 1965, subscription price £6.0.0.
non-subscription price £7.10.0.

VOLUME ID - DIHYDRIC ALCOHOLS, THEIR OXIDATION PRODUCTS AND DERIVATIVES
12. Dihydric alcohols or glycols and their derivatives. 13. Hydroxyaldehydes and ketones and related compounds; dicarbonyl compounds. 14. Aliphatic hydroxycarboxylic acids and related compounds. 15. Nitro- and amino-acids and their derivatives. 16. Aldehydic and ketonic carboxylic acids and related compounds. 17. Dicarboxylic acids.
6 × 9″ xvi + 352 pages + index, 29 tables, 1965

VOLUME IE - TRI- AND TETRA-HYDRIC ALCOHOLS, THEIR OXIDATION PRODUCTS AND DERIVATIVES
18. Trihydric alcohols and their oxidation products. 19. Phospholipids and glycolipids. 20. Dihydroxycarboxylic and tricarboxylic acids and their derivatives. 21. Tetrahydric alcohols and their oxidation products.

VOLUME IF - PENTA-, HEXA- AND HIGHER POLYHYDRIC ALCOHOLS, THEIR OXIDATION PRODUCTS AND DERIVATIVES; SACCHARIDES
22. Penta-, hexa- and higher polyhydric alcohols. 23. Monosaccharides. 24. Oligosaccharides and polysaccharides.

VOLUME IG - ENZYMES; MACROMOLECULES; CUMULATIVE INDEX TO VOLUME I A-G
25. Enzymes. 26. Synthetic macromolecules. 27. Rubber.
To follow
Volume II Alicyclic Compounds; Volume III Aromatic Compounds; Volume IV Heterocyclic Compounds; Volume V Miscellaneous; General Index

Multi-volume works such as Rodd's Chemistry of Carbon Compounds represent a considerable outlay for the purchaser. In order to alleviate this to a certain extent, the publishers offer a discount of 15% on the publication price. Subscribers to the complete series will thus be able to acquire the work for only 26s. (approx.) per 100 pages.

ELSEVIER PUBLISHING COMPANY
AMSTERDAM LONDON NEW YORK